SRM VALLIAMMAI ENGINEERING COLLEGE

(An Autonomous Institution)

SRM Nagar, Kattankulathur

DEPARTMENT OF ELECTRICAL & ELECTRONICS ENGINEERING

LAB MANUAL / OBSERVATION

PS3167- POWER SYSTEM SIMULATION LABORATORY - II
LAB MANUAL
M.E. (POWER SYSTEMS ENGINEERIGNG)
SEMESTER I

Aademic Year 2026-2027 odd

Regulation 2023

Prepared by

Ms.R.V.Preetha, AP(Sr.G)/EEE

PS3167- POWER SYSTEM SIMULATION LABORATORY - II

SYLLABUS

1. To analysis harmonics and design the filters for mitigation of harmonics.

2. Small-signal stability analysis of multi-machine configuration with classical machine model.

3. Induction motor starting analysis.

4. Transient analysis of two-bus system with STATCOM.

5. Available Transfer Capability calculation using an existing load flow program.

6. Study of variable speed wind energy conversion system- DFIG.

7. Study of variable speed wind energy conversion system- PMSG.

8. Computation of harmonic indices generated by a rectifier feeding a R-L load.

9. Design of active filter for mitigating harmonic.

10. Testing of Low impedance biased Current Differential protection with Simulation of excitation failure of generator by PSCAD/EMTDC.

PS3167- POWER SYSTEM SIMULATION LABORATORY - II

CYCLE I

1. To analysis harmonics and design the filters for mitigation of harmonics.

2. Small-signal stability analysis of multi-machine configuration with classical machine model.

3. Induction motor starting analysis.

4. Transient analysis of two-bus system with STATCOM.

5. Available Transfer Capability calculation using an existing load flow program.

CYCLE – II

6. Study of variable speed wind energy conversion system- DFIG.

7. Study of variable speed wind energy conversion system- PMSG.

8. Computation of harmonic indices generated by a rectifier feeding a R-L load.

9. Design of active filter for mitigating harmonic.

10. Testing of Low impedance biased Current Differential protection with Simulation of excitation failure of generator by PSCAD/EMTDC.

ADDITIONAL EXPERIMENTS

1. Transient stability analysis SMIB using classical model
2. Small signal stability analysis of a single machine infinite bus system with field circuit, exciter and power system stabilizer

INDEX

S.No	Date of Experiment.	Name of the experiment	Date of submission.	Staff Sign
1.				
2.				
3.				
4.				
5.				
6.				
7.				
8.				
9.				
10.				
11.				
12.				

EXP NO:1 **DATE:**

TO ANALYSIS HARMONICS AND DESIGN THE FILTERS FOR MITIGATION OF HARMONICS

Aim:

To understand the concept of harmonics and conduct basic harmonic analysis using an oscilloscope and a function generator.

Apparatus required :

- Oscilloscope
- Function generator
- Resistive loads (e.g., resistors)
- Passive low-pass filter (optional)
- Cables and connectors
- MATLAB or other data analysis software (for post-processing)

Theory:

Setup:

Connect the function generator to the oscilloscope. Ensure proper grounding. Set up a resistive load. You can use resistors of various values to represent different loads in your system. Optionally, insert a passive low-pass filter (RC filter) between the function generator and the load to reduce harmonics generated by thefunction generator itself.

Generating a Signal:

Configure the function generator to output a sinusoidal waveform with a specific frequency, amplitude, and DC offset. This will serve as your fundamental frequency component.

Harmonic Analysis:

Use the oscilloscope to measure and capture the waveform. Make sure to capture a few cycles of the signal. Use the FFT (Fast Fourier Transform) function of the oscilloscope or transfer the captured waveform to MATLAB for analysis. Analyze the FFT results to identify the harmonic components present in the signal. You can observe the magnitudes and frequencies of harmonics.

Load Variation:

Change the load resistance to introduce non-linearity and observe the effect on harmonic content. Note any changes in the harmonics generated by the system.

Filter Design (Optional):

If you want to experiment with harmonic mitigation, design and insert a simple passive low-pass filter into the circuit to attenuate higher harmonics.

Repeat Analysis:

Re-capture the waveform and analyze the harmonic content with the filter in place. Compare the results with and without the filter to observe its effectiveness in reducing harmonics.

Data Visualization:

Plot and visualize the harmonic spectrum using MATLAB or other data analysis software.

Observations and Analysis:

Record your observations related to harmonics and the impact of load variation on harmonic content. Assess the effectiveness of the passive low-pass filter in mitigating higher harmonics.

MATLAB CODE

```
% Sample data - Replace with your actual harmonic data
time = 0:0.0001:1; % Time vector
fundamental_frequency = 50; % Fundamental frequency (Hz)
amplitude = 1; % Amplitude of the fundamental component
harmonic_freq = 150; % Frequency of the 3rd harmonic
harmonic_amplitude = 0.1; % Amplitude of the 3rd harmonic component
total_harmonics = 5; % Total number of harmonics to simulate
% Generate a signal with harmonics
signal = amplitude * sin(2 * pi * fundamental_frequency * time);
for n = 1:total_harmonics
    signal = signal + harmonic_amplitude * sin(2 * pi * harmonic_freq
* n * time);
end
% Perform FFT to analyze the spectrum
Fs = 1 / (time(2) - time(1)); % Sampling frequency
N = length(signal); % Number of data points
f = (0:(N/2)) * Fs / N; % Frequency vector
Y = fft(signal);
P2 = abs(Y / N);
P1 = P2(1:N/2+1);
P1(2:end-1) = 2 * P1(2:end-1);
% Plot the spectrum
figure;
subplot(2,1,1);
plot(time, signal);
title('Signal with Harmonics');
xlabel('Time (s)');
ylabel('Amplitude');
subplot(2,1,2);
plot(f, P1);
title('Harmonic Spectrum');
xlabel('Frequency (Hz)');
ylabel('Amplitude');
% Calculate Total Harmonic Distortion (THD)
harmonic_magnitudes = P1(2:total_harmonics + 1);
THD = sqrt(sum(harmonic_magnitudes.^2)) / P1(1) * 100;
fprintf('Total Harmonic Distortion (THD): %.2f%%\n', THD);
```

Result:

EXP NO: 2 **DATE:**

SMALL SIGNAL STABILITY ANALYSIS OF MULTI-MACHINE CONFIGURATION WITH CLASSICAL MACHINE MODEL

AIM:

To write a MATLAB program to analyze the small signal stability of a multi-machine power system.

THEORY:

To analyze the small signal stability of the multi machine power system it is necessary to reduce the original network to the size of the generators and to derive the equations for multi-machine system that represent the dynamics of the machine and the controllers, in the state-space form. The state variables for the machine are $\Delta\delta$, $\Delta\omega$ and possibly $\Delta E_q'$ and $\Delta E_d'$. The controllers of the synchronous machine and the network will throw in additional state variables. The synchronous machines are represented by constant voltage sources in series with their transient reactances.

Analysis methodology:

Step-1: Equations in network coordinates:

$$\begin{bmatrix} \hat{Y}_{1i,1i} & 0 & \hat{Y}_{1i,1} & 0 & 0 & .... \\ 0 & \hat{Y}_{2i,2i} & 0 & \hat{Y}_{2i,2} & 0 & .... \\ \hat{Y}_{1,1i} & 0 & \hat{Y}_{11} & \hat{Y}_{12} & .... & .... \\ 0 & \hat{Y}_{2,2i} & \hat{Y}_{21} & \hat{Y}_{22} & .... & .... \\ 0 & 0 & .... & .... & .... & .... \\ .... & .... & .... & .... & .... & .... \\ .... & .... & .... & .... & .... & .... \end{bmatrix} \begin{bmatrix} \hat{E}_1' \\ \hat{E}_2' \\ \hat{V}_1 \\ \hat{V}_2 \\ . \\ . \\ . \end{bmatrix} = \begin{bmatrix} \hat{I}_1 \\ \hat{I}_2 \\ 0 \\ 0 \\ . \\ . \\ . \end{bmatrix} \qquad (1)$$

In the above equation $\hat{E}_1'$ and $\hat{E}_2'$ are interval voltage phasors and $\hat{I}_1'$ and $\hat{I}_2'$ are the stator currents.

$$\begin{bmatrix} Y_{GG} & Y_{G,NG} \\ Y_{NG,G} & Y_{NG,NG} \end{bmatrix} \begin{bmatrix} \hat{E}_G' \\ \hat{V}_{NG} \end{bmatrix} = \begin{bmatrix} \hat{I}_G \\ 0 \end{bmatrix} \qquad (2)$$

Where

G – Generator, NG – Non-generator.

(a) Representation

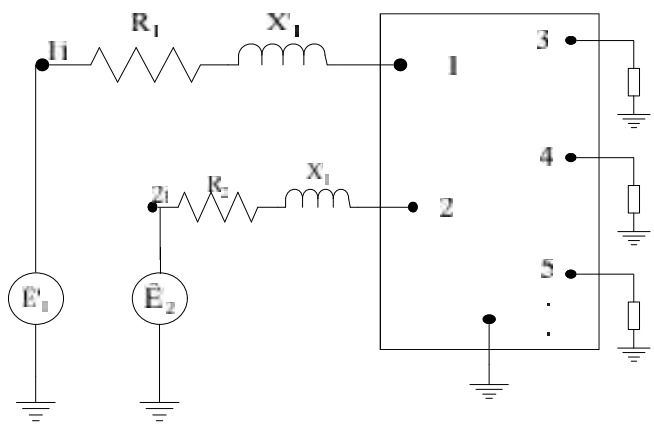

(a) With generators and loads replaced by their equivalents

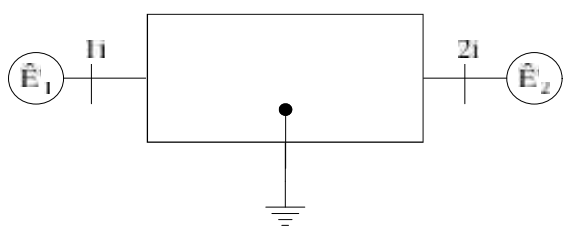

(b) All nodes except generator internal nodes eliminated

Fig1. Two machine n-bus system

$$Y_{GG} = \begin{bmatrix} \hat{Y}_{1i,1i} & 0 \\ 0 & \hat{Y}_{2i,2i} \end{bmatrix};$$

$$Y_{G,NG} = \begin{bmatrix} \hat{Y}_{1i,1} & 0 & 0 & 0 & .... \\ 0 & \hat{Y}_{2i,2} & 0 & 0 & .... \end{bmatrix};$$

$$Y_{NG,G} = Y^{T}{}_{G,NG};\ \text{Dimension: (n-2)×2}$$

$$Y_{NG,NG} = \begin{bmatrix} Y_{11} & Y_{12} & Y_{13} & .... & .... \\ Y_{21} & Y_{22} & Y_{23} & .... & .... \\ Y_{31} & Y_{32} & Y_{33} & .... & .... \\ .... & .... & .... & .... & .... \\ .... & .... & .... & .... & .... \end{bmatrix};\ \text{Dimension: (n-2) × (n-2)}$$

Step-2: Reduction of network equations:

Eliminate the non-generator nodes.

From Eq. (2), we get

$$V_{NG} = -Y^{-1}_{NG.NG}\{Y_{NG,G}E'_G\} \tag{3}$$

Substituting Eq. (3) in Eq. (2), we get

$$Y^{red}_{GG}E'_G = I_G \tag{4}$$

Where

$$Y^{red}_{GG} = Y_{GG} - Y_{G,NG}Y^{-1}_{NG,NG}Y_{NG,G} \tag{5}$$

With Eq. (4) step-2 is completed.

Step-3: Transformation of reduced equations:

Let E'_{1r} and E'_{2r} and I_{1r} and I_{2r} be the internal voltage and stator current phasors in individual machine q-d coordinates. The corresponding quantities in network coordinates are E'_1, E'_2 and I_1, I_2.

$$\begin{aligned} E'_1 &= E'_{1r}e^{j\delta_1};\ E'_2 = E'_{2r}e^{j\delta_2}; \\ I_1 &= I_{1r}e^{j\delta_1};\ I_2 = I_{2r}e^{j\delta_1}; \end{aligned} \tag{6}$$

Relative displacements of q-axis of the machine with respect to the network Q_{REF}

The above relationships between the quantities in network and individual machine rotor coordinates can be expressed as

$$E'_G = TE'_{Gr};\ I_G = TI_{Gr} \tag{7}$$

Where T is the transformation matrix given by

$$T = \begin{bmatrix} e^{j\delta_1} & 0 \\ 0 & e^{j\delta 2} \end{bmatrix} \tag{8}$$

and the subscript r denotes individual machine rotor coordinates.

The inverse transformation is given by

$$T^{-1} = \begin{bmatrix} e^{-j\delta_1} & 0 \\ 0 & e^{-j\delta 2} \end{bmatrix} \tag{9}$$

$$I_{Gr} = M E_{Gr} \tag{10}$$

$$M = T^{-1} Y_{GG}^{red} T \tag{11}$$

$$M = \begin{bmatrix} Y_{11} e^{j\theta_{11}} & Y_{12} e^{j(\theta_{12} - \delta_{12})} \\ Y_{12} e^{j(\theta_{12} + \delta_{12})} & Y_{22} e^{j\theta_{22}} \end{bmatrix} \tag{12}$$

Step-4: Linearization of reduced network equations in individual machine rotor coordinates:
Let us denote the relative displacements of individual machine q-axis with respect to network reference as

$$\delta_1 = \delta_{10} + \Delta\delta_1; \delta_2 = \delta_{20} + \Delta\delta_2; \tag{13}$$

Let these incremental changes cause incremental changes in other quantities as follows:

$$I = I_0 + \Delta I \tag{14}$$

$$E' = E'_0 + \Delta E' \tag{15}$$

$$M = M_0 + \Delta M \tag{16}$$

$$T = T_0 + \Delta T \tag{17}$$

$$I_0 + \Delta I = M_0 E'_0 + M_0 \Delta E' + \Delta M E'_0 + \Delta M \Delta E' \tag{18}$$

$$\Delta I = M_0 \Delta E' + \Delta M E'_0 \tag{19}$$

Equation (19) represents the linearised reduced network equations in individual machine rotor coordinates.

$$\Delta I = M_0 \Delta E' - j\{\Delta\delta M_0 - M_0 \Delta\delta\} E'_0 \tag{20}$$

$$M_0 = \begin{bmatrix} Y_{11} e^{j\theta_{11}} & Y_{12} e^{j(\theta_{12} - \delta_{12,0})} \\ Y_{12} e^{j(\theta_{12} + \delta_{12}, 0)} & Y_{22} e^{j\theta_{22}} \end{bmatrix} \tag{21}$$

$$\Delta I = \begin{bmatrix} Y_{11} E'_{q1} + Y_{12} e^{-j_{12,0}} \Delta E'_{q2} + Y_{13} e^{-j\delta_{13,0}} \Delta E'_{q3} - jY_{12} e^{-j\delta_{12,0}} E'_{q20} \Delta\delta_{12} - jY_{13} e^{-j\delta_{13},0} E'_{q30} \Delta\delta_{13} \\ Y_{12} e^{j\delta_{12,0}} \Delta E'_{q1} + Y_{22} \Delta E'_{q2} + Y_{23} e^{-j\delta_{23,0}} \Delta E'_{q3} + jY_{12} e^{j\delta_{12,0}} E'_{q10} \Delta\delta_{12} - jY_{23} e^{-j\delta_{23,0}} E'_{q30} \Delta\delta_{23} \\ Y_{13} e^{j\delta_{13,0}} \Delta E'_{q1} + Y_{23} e^{j\delta_{23,0}} \Delta E'_{q2} + Y_{33} \Delta E'_{q3} + jY_{13} e^{j\delta_{13,0}} E'_{q10} \Delta\delta_{13} + jY_{23} e^{j\delta_{23,0}} E'_{q20} \Delta\delta_{23} \end{bmatrix} \tag{22}$$

We can separate out the real and imaginary parts and obtain the q and d components.
Step-4 is now completed.

Step-5: Linearization of differential equations:
The acceleration equation for the i_{th} machine given below:

$$2H_i \frac{d(\Delta\bar{\omega}_i)}{dt} = \Delta\bar{T}_{mi} - \Delta\bar{T}_{ei} - K_D(\Delta\bar{\omega}_i), i = 1, 2 \tag{23}$$

The above equation involves $\Delta\bar{T}_e$. We can easily shown that $\bar{T}_e$ is a function of V_d, I_d, V_q and I_q.
Assuming a 2-pole machine, the electrical power output in p.u. is given by

$$\bar{P}_e = \mathrm{Re}\left\{\hat{V}\hat{I}^*\right\}$$

In the individual machine q-d coordinates

$$\overline{P}_e = \mathrm{Re}\left\{\left(V_q + jV_d\right)\left(I_q - jI_d\right)\right\} = V_d I_d + V_q I_q = \overline{T}_e \tag{24}$$

Assuming type 1B machine

$$\begin{aligned}\overline{T}_e &= \left(-X_q I_q\right) I_d + \left(X'_d I_d + E'_q\right) I_q \\ &= \left(X'_d - X_q\right) I_q I_d + E'_q I_q\end{aligned} \tag{25}$$

Linearising Eq. (25),

$$\Delta\overline{T}_e = \left(X'_d - X_q\right)\left[I_{q0}\Delta I_d + I_{d0}\Delta I_q\right] + E'_{q0}\Delta I_q + I_{q0}\Delta E'_q \tag{26}$$

i.e.

$$\Delta\overline{T}_e = \left[E'_{q0} + \left(X'_d - X_q\right) I_{d0}\right]\Delta I_q + \left(X'_d - X_q\right) I_{q0}\Delta I_d + I_{q0}\Delta E'_q \tag{27}$$

Equation (26) holds good for machine 1 or machine 2.
Hence,

$$\Delta\overline{T}_{e1} = \left[E'_{q10} + \left(X'_{d1} - X_{q1}\right) I_{d10}\right]\Delta I_{q1} + \left(X'_{d1} - X_{q1}\right) I_{q10}\Delta I_{d1} + I_{q10}\Delta E'_{q1} \tag{27}$$

and

$$\Delta\overline{T}_{e2} = \left[E'_{q20} + \left(X'_{d2} - X_{q2}\right) I_{d20}\right]\Delta I_{q2} + \left(X'_{d2} - X_{q2}\right) I_{q20}\Delta I_{d2} + I_{q20}\Delta E'_{q2} \tag{28}$$

Linearization of swing equation is straight forward. Linearization yields,

$$\frac{d\left(\Delta\delta_i\right)}{dt} = \overline{\omega}_s \Delta\overline{\omega}_i, i = 1, 2 \tag{29}$$

Linearising the differential equation for the voltage behind the transient reactance of machine-1 is given by

$$p\Delta E'_{q1} = -\frac{1}{T'_{d01}}\left[\Delta E'_{q1} - \left(X_{d1} - X'_{d1}\right)\Delta I_{d1} - \Delta E_{FD1}\right] \tag{30}$$

Similarly, for the second machine we have

$$p\Delta E'_{q2} = -\frac{1}{T'_{d02}}\left[\Delta E'_{q2} - \left(X_{d2} - X'_{d2}\right)\Delta I_{d2} - \Delta E_{FD2}\right] \tag{31}$$

Equations (23) taken together with Eqs. (29), (30) and (31) are the linearised differential equations required for small signal stability analysis. This completes step-5.

Step-6: Elimination of the incremental changes in algebraic variables from the linearised differential equations:

$$\Delta\overline{T}_{e1} = T_{11}\Delta E'_{q1} + T_{12}\Delta E'_{q2} + T_{13}\Delta\delta_{12} \tag{32}$$

$$\Delta\overline{T}_{e2} = T_{21}\Delta E'_{q1} + T_{22}\Delta E'_{q2} + T_{23}\Delta\delta_{12} \tag{33}$$

The only equations that are to be expressed in the standard state variable form are the equations for the incremental changes in the generator internal voltages.

$$p\Delta E'_{q1} = E_{11}\Delta E'_{q1} + E_{12}\Delta E'_{q2} + E_{13}\Delta\delta_{12} + \frac{1}{T'_{d01}}\Delta E_{FD} \tag{34}$$

Where

$$E_{11} = -\frac{1}{T'_{d01}}\left[1 - B_{11}\left(X_{d1} - X'_{d1}\right)\right] \tag{35}$$

$$E_{12} = \frac{1}{T'_{d01}}\left(X_{d1} - X'_{d1}\right)\left(B_{12}\cos\delta_{12,0} - G_{12}\sin\delta_{12,0}\right) \tag{36}$$

$$E_{13} = -\frac{1}{T'_{d01}}\left(X_{d1} - X'_{d1}\right)\left(G_{12}\cos\delta_{12,0} + B_{12}\sin\delta_{12,0}\right)E'_{q20} \tag{37}$$

Similarly for the second generator, we can show that

$$p\Delta E'_{q2} = E_{21}\Delta E'_{q1} + E_{22}\Delta E'_{q2} + E_{23}\delta_{12} + \frac{1}{T'_{d02}}\Delta E_{FD2} \tag{38}$$

Where

$$E_{21} = \frac{1}{T'_{d02}}\left(X_{d2} - X'_{d2}\right)\left(B_{12}\cos\delta_{12,0} + G_{12}\sin\delta_{12,0}\right) \tag{39}$$

$$E_{22} = -\frac{1}{T'_{d01}}\left[1 - B_{22}\left(X_{d2} - X'_{d2}\right)\right] \tag{40}$$

$$E_{23} = -\frac{1}{T'_{d02}}\left(X_{d2} - X'_{d2}\right)\left(G_{12}\cos\delta_{12,0} - B_{12}\sin\delta_{12,0}\right)E'_{q10} \tag{41}$$

$$\begin{bmatrix} p\Delta\bar{\omega}_{12} \\ p\Delta\delta_{12} \\ p\Delta E'_{q1} \\ p\Delta E'_{q2} \end{bmatrix} = \begin{bmatrix} -\frac{K_D}{2H} & \left(\frac{T_{13}}{2H_1} - \frac{T_{23}}{2H_3}\right) & -\left(\frac{T_{11}}{2H_1} - \frac{T_{21}}{2H_2}\right) & -\left(\frac{T_{12}}{2H_1} - \frac{T_{22}}{2H_2}\right) \\ \omega_s & 0 & 0 & 0 \\ 0 & E_{13} & E_{11} & E_{12} \\ 0 & E_{23} & E_{21} & E_{22} \end{bmatrix} \begin{bmatrix} \Delta\bar{\omega}_{12} \\ \Delta\delta_{12} \\ \Delta E'_{q1} \\ \Delta E'_{q2} \end{bmatrix} + \begin{bmatrix} \frac{\Delta\bar{T}_{m1}}{2H_1} - \frac{\Delta\bar{T}_{m2}}{2H_2} \\ 0 \\ \frac{1}{T'_{d01}}\Delta E_{FD1} \\ \frac{1}{T'_{d02}}\Delta E_{FD2} \end{bmatrix}$$

We completed step-6

We can now apply eigenvalue analysis to the computed state space model.

Simplifications for classical machines:

Let us assume machine-1&2 are classical (Type 0). Note the following:

i. E'_{q1} & E'_{q2} are constant. $\Delta E'_{q}$ will be absent in the equation. Set all the terms containing $\Delta E'_{q}$ to zero. Equation (27) for the incremental electrical torque becomes

$$\Delta T_{e1} = T_{12}\Delta E'_{q2} + T_{13}\Delta\delta_{12} \tag{42}$$

ii. Set $X'_{d1} = X_{q1}$

iii. The state variables are $\Delta\bar{\omega}_{12}$, $\Delta\delta_{12}$. Hence, only the equations for these variables are to be considered.

Two identical machine feed a common load, the impedance between each machine terminal 0+j0.8p.u on the total rated MVA, the terminal voltages of each machine is 1p.u assume classical moadel for machine.

Generator data: Both generators are identical rating of each is 80MVA. Reactance parameters X_d=3.4p.u X_d=0.49p.u Xq=3.28p.u T_{do}=6 sec. Total kinetic energy stored at synchrouns speed both machine 3979.2 MJ rated frequency=60Hz.

Load data: Both generators are identically loaded active power output of each machine is 0.5p.u on totoal MVA power factor=0.851.Choose base MVA as 160

(i) Determine the network equations in the individual machine stator dq coordinates of small signal stability analysis

(ii) Lineraised network equations in the individual machine rotor equation

(iii)Numerical expression for electrical torque

(iv)Eigen value and natural frequency

(i) $E_{q1}'$and $E_{q2'}$ are constant. $\Delta Eq'$ will be absent in the equation, Set all the terms containing $E_{q1}'$to zero. The incremental electrical torque becomes

$\Delta T_{e1}=T_{12}\Delta Eq_2'+T_{13}\Delta\delta_{12}$

(ii) Set $X_{d1'}=X_{q1}'$

(iii) The state variables are $\Delta\omega_{12}$. ΔE_{12}Hence only the equations for these variable are to be considered.

To obtain the state matrix equations for this case ignore the third row and the third column of the state matrix. If both machines are classical, then the state matrix obtained by ignoring the third and fourth rows and third and fourth columns of the state matrix.

PROGRAM:

```
%program for multimachine
clc;
clear all;
%program for multimachine
Et=1.0;
xd=3.4;
xdp=.49;
xq=3.28;
Td0p=6.0;
f=60;
rating=80;
kenergy=379.2;
xt=0.8;
%generator dataa
ngen=2;
%loading data
p1=0.5;
%0n total rated mva
p2=.5;
pf=.85;
basemva=160;
%initial loading conditions
b=acos(pf);
q1=p1*tan(b);
q2=q1;
s=p1+q1*i;
I1=s'/Et;
%stator current
I2=I1;
%voltage behind transient reactance
Eq1p=Et+(xdp*i)*(I1);
Eq2p=Eq1p;
delt10=angle(Eq1p);
delt20=angle(Eq2p);
%load current
IL=I1+I2;
%load voltage
vL=Et-xt*i*I1;
%load admittance
yL=IL/vL;
zL=1/yL;
a=real(zL);
b=imag(zL);
d=xdp+xt;
linedata=[1 3 0 d 0
        3 2 0 d 0
```

```
   0 3 a b 0];
i=sqrt(-1);
nl=linedata(:,1);
nr=linedata(:,2);
R=linedata(:,3);
X=linedata(:,4);
Bc=j*linedata(:,5);
nbr=length(linedata(:,1));
nbus=max(max(nl),max(nr));
Z=R+j*X;
y=ones(nbr,1)./Z;
%branch admittance
Ybus=zeros(nbus,nbus);
%initialize Ybus to Zero
%formation of the off diagonal elements
for k=1:nbr
   if nl(k)>0 & nr(k)>0
      Ybus(nl(k),nr(k))=Ybus(nl(k),nr(k))-y(k);
      Ybus(nr(k),nl(k))=Ybus(nl(k),nr(k));
   end
end
%formation of the diagonal elements
for n=1:nbus
   for k=1:nbr
      if nl(k)==n | nr(k)==n
         Ybus(n,n)=Ybus(n,n)+y(k)+Bc(k);
      end
   end
end
Ybus
%COMPUTATION OF REDUCED Y BUS
ygg=Ybus(1:ngen,1:ngen);
ygl=Ybus(1:ngen,ngen+1:nbus);
ylg=Ybus(ngen+1:nbus,1:ngen);
yll=Ybus(ngen+1:nbus,ngen+1:nbus);
YBUS=ygg-ygl*inv(yll)*ylg;
%reduced Y bus
%network equations in individual machine qd coordinates
m=[0 1;1 0];
M=m.*YBUS;
Ep=[abs(Eq1p);abs(Eq2p)];
M0=M*Ep;
dI=[-1*i;1*i].*M0;
%numerical exp for elec torque
Eq10p=abs(Eq1p);
Eq20p=abs(Eq2p);
B12=imag(YBUS(1,2));d120=0;
```

```
T13=B12*cos(d120)*Eq10p*Eq20p
T23=-T13;
H1=kenergy/(2*80*2);
H2=H1;
a11=0;
a12=-((T13/(2*H1))-(T23/(2*H2)))
a21=2*pi*f;
a22=0;
A=[a11 a12;
   a21 a22]
eig(A)
wn=sqrt(det(A))
fn=wn/(2*pi)
```

EIGEN VALUE ANALYSIS:

For P = 0.9; Q = 0.3; K_D =0

FOR CLASSICAL MODEL:

EIGEN VALUES	±9.7333i
DAMPING RATIO	0
FREQUENCY (HZ)	1.5491

INFERENCE:

From the damping ratio (ζ=0) of the swing mode it can be observed that the system is small signal unstable**.**

RESULT:

A MATLAB program was written to analyze the small-signal stability of a multi-machine power system.

EXP NO: 3 **DATE**:

INDUCTION MOTOR STARTING ANALYSIS

AIM:

To analyse the study of motor starting

THEORY:

The purpose of the motor starting is to determine the initial voltage depressions on the distribution buses serving the motors and to calculate the approximate acceleration times of the selected motors during starting-up. This information is used in determining if satisfactory motor starting and acceleration will occur, if the protective devices are properly applied, and if the voltage dips during starting will result in loss of adjacent loading due to contactor drop out.

A motor starting study should be made if the motor horse power exceeds approximately 30% of supply transformer(s) base KVA rating, if no generators are present. If generation is present and no other sources are involved, a study should be considered whenever the motor horse power exceeds 10-15% of the generator KVA rating

System modeling:

A simplified model of the distribution system is adapted. It contains the motor bus, the associated main (typically 6.6 kV) bus and the main upstream higher voltage bus (typically 33 kV) as shown in the single line diagram.

Equations:

Assume a base power for the system and that all the impedances shown are converted to the base power. Let S_{sys} be the system base power.

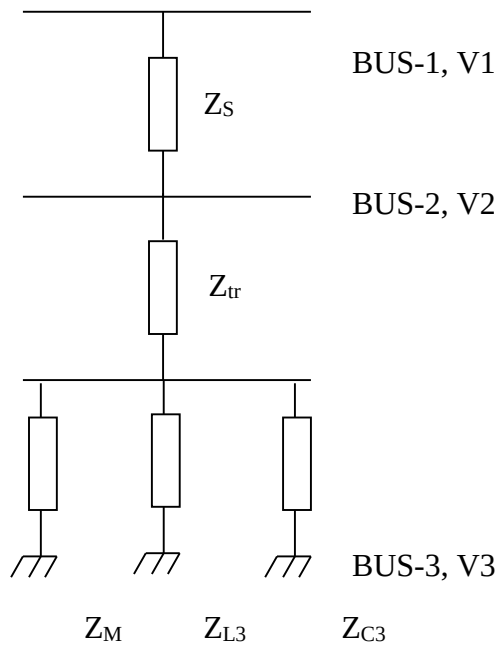

Equivalent circuit diagram

$$Z_S = \frac{1}{\left(\frac{S_{3\phi}}{S_{sys}}\right)} \text{p.u} \qquad (1)$$

Where, $S_{3\phi}$ = 3-phase fault level at bus-2.

$Z_2 = Z_{tr}$ – transformer impedance converted to $S_{sys.}$

$$Z_{L_3} = \frac{|V_3|^2}{P_{L_3} - jQ_{L_3}} \text{p.u} \qquad (2)$$

Where, Z_{L3} = Impedance of constant impedance loads in p.u

V_3 = Voltage of bus-3 in p.u

P_{L3} = Active power consumed by the load in p.u on S_{sys}

Q_{L3} = Reactive power consumed by the load in p.u on S_{sys} (+ve i/p)

Z_{C3} = Impedance of capacitor, computed from reactive power injected at nominal voltage.

$$Z_{C_3} = \frac{|V_3|^2}{-jQ_{C_3}} \text{p.u} \qquad (3)$$

Where, Q_{C3} = Reactive power consumed by the capacitor in p.u on $S_{sys.}$ (-ve i/p)

Z_M = Impedance presented by the motor to the bus. At the instant of starting, it is equal to locked rotor impedance of motor-Z_{LR}. It is a function of speed (and time) indirectly since motor current, voltage and power factor are functions of speed (and time) during acceleration.

$$Z_{LR} = \frac{1}{\left(I_{LR}/I_{FL}\right)} e^{j\phi_{st}} \tag{4}$$

Z_{LR} = Locked rotor impedance of motor in p.u on motor base.
Where,

I_{LR} = Locked rotor current in amp at rated voltage
I_{FL} = Full load current
ϕ_{st} = Starting power factor

$$Z_3 = Z_M // Z_{L_3} // Z_{C_3} \tag{5}$$

$$T = I_0 \alpha \tag{6}$$

$$I_0 = \frac{WK^2}{2g} lb - ft - s^2 \tag{7}$$

$$\omega^2 = \omega_0^2 + 2\alpha(\theta - \theta_0) rev/s \tag{8}$$

$$\Delta\theta = \omega_0 t + \frac{1}{2}\alpha t^2 rev \tag{9}$$

$$\alpha = \frac{T_n 2g}{WK^2} rev/s^2 \tag{10}$$

A simplified approximation for starting time,

$$t(s) = \frac{WK^2(rpm_1 - rpm_2)2\pi}{60gT_n} \tag{11}$$

Where, T – Average motor shaft output torque

v – Motor terminal voltage

I_0 – Moment of inertia

g – Acceleration due to gravity

ω – Angular velocity

α – Angular acceleration

t – Time in seconds to accelerate

T_n – Net average or accelerating torque between rpm-1 and rpm-2

θ – Electrical angle in degrees

WK^2 – Inertia

Alternatively, if moment of inertia J is given in kg-m^2,

$$J\frac{\Delta\omega}{\Delta t} = T_{acc}$$

$$\Delta t = J\frac{\Delta\omega}{T_{acc}} \qquad (12)$$

Δt will be in seconds if $\Delta\omega$ is in rad /sec

$$T_{acc} = T_{motor} - T_{load}$$

Instantaneous torque,

$$T = \frac{q_1 V^2 (r_2/s)}{\omega_s[(r_1 + (r_2/s))^2 + (x_1 + x_2)^2]} \qquad (13)$$

Where,

q_1 – Number of phases

ω_s – Angular velocity at synchronous speed

v – Motor terminal voltage

r_1, x_1 – Stator resistance and reactance

r_2, x_2 – Rotor resistance and reactance

s – Slip

In metric system, following are the consistent set of units for various quantities.

T, T_n – Newton-meter

J – kg-m^2 replaces $WK^2/2g = I_0$

ω – Radians /sec

$\Delta\theta$, θ – radians

Algorithm for advancing simulation to cover a speed interval:

Consider k-th interval

1) Read the value of I_{inrush}/I_{FL} from speed vs. current curve and ϕ_k from speed vs. power factor curve. Calculate Z_M.

$$Z_M = \frac{1}{(I_{inrush}/I_{FL})} e^{j\phi_k}$$

2) Compute impedances and current

$$Z_{L_3} = \frac{|V_3|^2}{P_{L_3} - jQ_{L_3}} \text{ p.u}$$

$$Z_{C_3} = \frac{|V_3|^2}{-jQ_{C_3}} \text{ p.u}$$

$$Z_3 = Z_M // Z_{L_3} // Z_{C_3}$$

$$Z_2 = Z_{tr}$$

$$Z_S = \frac{1}{\left(\frac{S_{3\phi}}{S_{sys}}\right)} \text{ p.u}$$

$$Z = Z_S + Z_2 + Z_3$$

$$I = \frac{V_1}{Z}$$

$$\omega_s = \frac{2\pi n_s}{60}$$

$$n_s = \frac{120f}{p}$$

3) Compute voltages

$$V_3 = IZ_3$$

$$V_3 = I(Z_2 + Z_3)$$

4) Compute motor torque

$$T_{motor} = \frac{q_1 V_3^2 (r_2/s)}{\omega_s[(r_1 + (r_2/s))^2 + (x_1 + x_2)^2]}$$

Where,

s = (100 – percent speed for which acceleration time was just computed) /100

5) Compute accelerating torque

$$T_{acc} = T_{motor} - T_{load}$$

6) Compute time for this interval

$$\Delta t = J\frac{\Delta\omega}{T_{acc}}$$

Repeat above steps till 98.5% speed is reached.

$$t_{acc}(1) = \Delta t_1$$

$$t_{acc}(k) = T_{acc}(k-1) + \Delta t_k$$

PROGRAM:

```
clc;
clear all;
KW=1678.5;
KV=2.3;
RPM=1800;
J=63.87;
FLA=526.675;
f=60;
Np=4;
q=3;
tstart(1)=.5;
V1=1.026+0.0i;
V2=1.026+0.0i;
V3=1.026+0.0i;
S3p=125;
Ssys=10;
PL3=0.0;
QL3=0.0;
QC3=0.0;
Ztr=0.0001+0.0001i;
r1=0.0029;
r2=0.022;
x1=0.226;
x2=0.226;
n=input('Enter the number of values');
for j=1:n
   N(j)=input('Enter the %of speed:');
   K(j)=input('Enter the K value:');
   PF(j)=input('Enter the power factor%:');
   LT(j)=input('Enter the load torque %:');
end
flw=(2*pi*RPM)/60
flt=(KW*1000)/flw
Ns=(120*f)/Np
Ws=(2*pi*Ns)/60
MKVA=1.732*KV*FLA
Zsy=1/(S3p/Ssys);
Zs=0+(i*Zsy)
for j=2:n
   PF1(j)=PF(j)/100;
   PK(j)=acos(PF1(j));
   Zm(j)=(1/K(j))*(cos(PK(j))+(i*sin(PK(j))))*(Ssys/MKVA)*1000
   Z3(j)=Zm(j);
   Z(j)=Zs+Ztr+Z3(j);
   I(j)=V1/Z(j)
```

```
    V3(j)=I(j)*Z3(j);
    V2(j)=I(j)*(Ztr+Z3(j));
    S(j)=(100-N(j))/100
    num(j)=q*(((real(V3(j))*KV*1000)/sqrt(3))^2)*(r2/S(j));
    den(j)=Ws*((r1+(r2/S(j)))^2+(x1+x2)^2);
    tmotor(j)=num(j)/den(j) ;
    tload(j)=(LT(j)*flt)/100;
    tacc(j)=tmotor(j)-tload(j);
    delt1(j)=(J*0.1*flw)/tacc(j);
    tstart(j)=tstart(j-1)+delt1(j)
    Istart(j)=FLA*K(j)
end
figure(1);
plot(tstart,tmotor)
Xlabel('time');Ylabel('motor torque');
figure(2);
plot(tstart,Istart)
Xlabel('time');Ylabel('starting current');
figure(3);
plot(S,tmotor)
Xlabel('slip');Ylabel('motor torque')
```

OUTPUT:

1) **Starting current vs. time:**

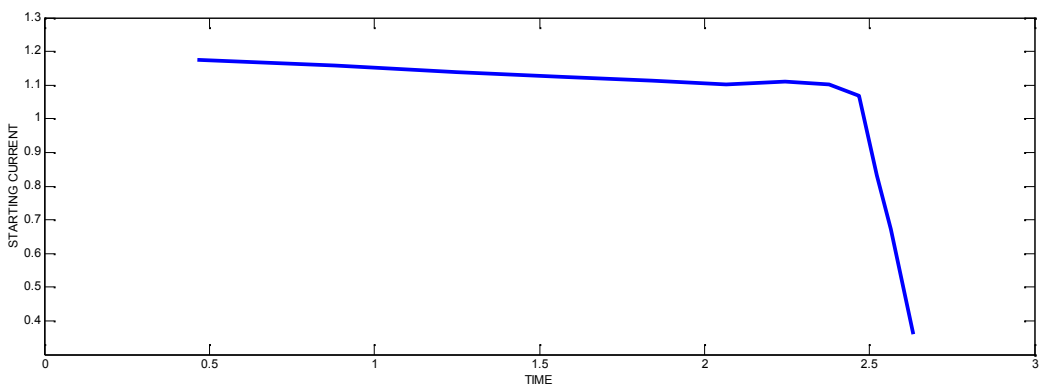

2) **Torque vs. time:**

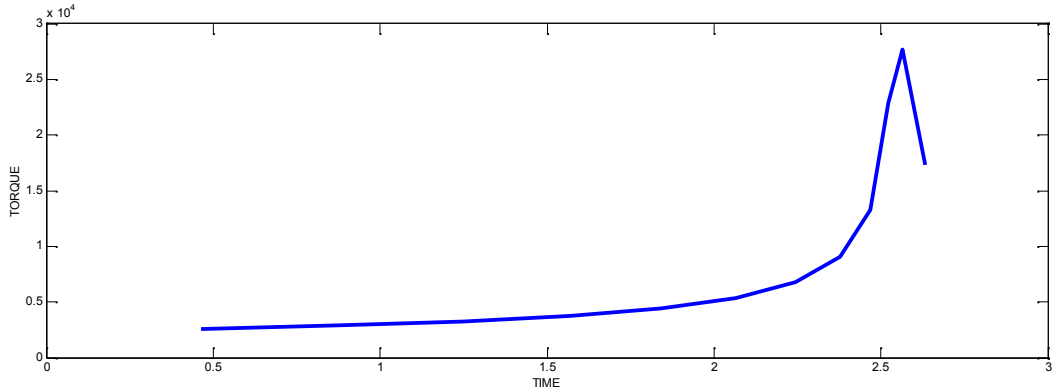

3) Torque vs. slip:

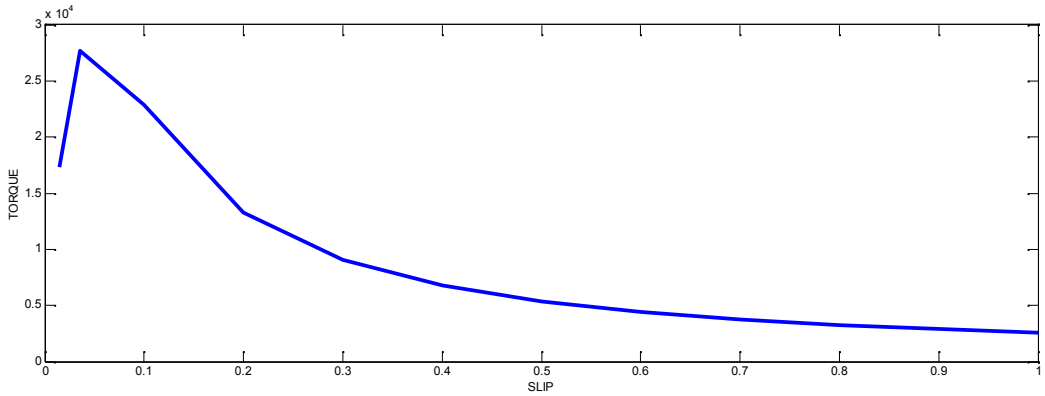

RESULT:

A MATLAB program was written to analyze the study of motor starting and the response of the induction motor starting current, torque Vs slip curves were plotted.

EXP NO:4 **DATE:**

TRANSIENT ANALYSIS OF TWO BUS SYSTEM WITH STATCOM M

AIM:

To calculate the compensated voltage and angle in the two bus system using STATCOM as the compensator

SOFTWARE REQUIRED:

Power system module of MATLAB

THEORY:

The STATCOM (or SSC) is a shunt-connected reactive-power compensation device that is capable of generating and /or absorbing reactive power and in which the output can be varied to control the specific parameters of an electric power system. It is in general a solid-state switching converter capable of generating or absorbing independently controllable real and reactive power at its output terminals when it is fed from an energy source or energy-storage device at its input terminals. Specifically, the STATCOM considered in this chapter is a voltage-source converter that, from a given input of dc voltage, produces a set of 3-phase ac-output voltages, each in phase with and coupled to the corresponding ac system voltage through a relatively small reactance (which is provided by either an interface reactor or the leakage inductance of a coupling transformer). The dc voltage is provided by an energy-storage capacitor. A STATCOM can improve power-system performance in such areas as the following:

1. The dynamic voltage control in transmission and distribution systems;
2. The power-oscillation damping in power-transmission systems;
3. The transient stability;
4. The voltage flicker control; and
5. The control of not only reactive power but also (if needed) active power in the connected line, requiring a dc energy source.

Furthermore, a STATCOM does the following:

1. It occupies a small footprint, for it replaces passive banks of circuit elements by compact electronic converters;
2. It offers modular, factory-built equipment, thereby reducing site work and commissioning time; and

3. It uses encapsulated electronic converters, thereby minimizing its environmental impact.

A STATCOM is analogous to an ideal synchronous machine, which generates a balanced set of three sinusoidal voltages at the fundamental frequency with controllable amplitude and phase angle. This ideal machine has no inertia, is practically instantaneous, does not significantly alter the existing system impedance, and can internally generate reactive (both capacitive and inductive) power.

The Tennessee Valley Authority (TVA) installed the first 100-MVA STATCOM in 1995 at its Sullivan substation. The application of this STATCOM is expected to reduce the TVA's need for load tap changers, thereby achieving savings by minimizing the potential for transformer failure. This STATCOM aids in resolving the off-peak dilemma of over voltages in the Sullivan substation area while avoiding the more labor- and space-intensive installation of an additional transformer bank. Also, this STATCOM provides instantaneous control and therefore increased capacity of transmission voltage, providing the TVA with greater flexibility in bulk-power transactions, and it also increases the system reliability by damping grids of major oscillations in this grid.

EXERCISE:

Rs=0.01; Xs=0.1;Rp=200;K+=0.9

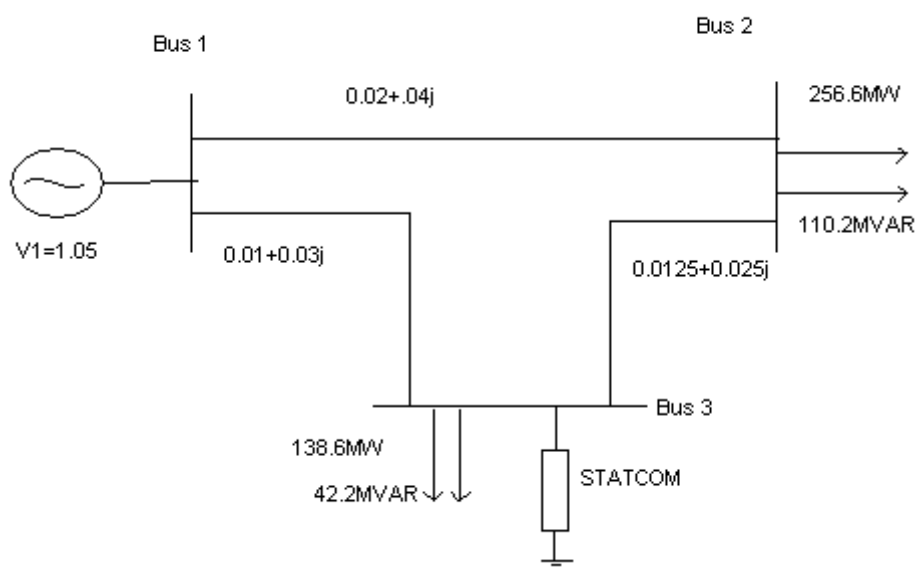

BUS DATA OF 3 BUS SYSTEM:

Bus no.	Bus code	V p.u.	angle	load		gen	
				MW	MVAR	MW	MVAR
1	1	1	0	0	0	0	0
2	0	1	0	256.6	110.2	0	0
3	0	1	0	138.6	45.2	0	0

LINE DATA:

Bus		R pu	X pu	B pu
From	To			
1	2	0.02	0.04	0.05
1	3	0.01	0.03	0.03
2	3	0.0125	0.025	0.06

PROGRAM:

```
clc;
clear all;
n=3;
pd=[0 2.562 1.102];
qd=[0 1.386 0.452];
qg=[0 0 0];
pg=[0 0 0];
vs=[1.05 1 1];
theta=[0 0 0];
con=0.1;
yb=[20-50j -10+20j -10+30j;
   -10+20j 26-52j -16+32j;
   -10+30j -16+32j 26-62j];
zs=0.01+0.1j;
beta=angle(zs);
rp=200;
k=0.9;
m=1;
cont=0.1;
vdc=1;
alpha=0;
b=imag(yb);
g=real(yb);
an=angle(yb);
my=abs(yb);
iter=1;
while(cont>0.01 && iter<4)
```

```
iter
vc=(k*k)*(m)*(vdc);
pg(3)=((vc*vs(3)*cos(theta(3)-alpha+beta))-(vs(3)*vs(3)*cos(beta)))/abs(zs);
qg(3)=((vc*vs(3)*sin(theta(3)-alpha+beta))-(vs(3)*vs(3)*sin(beta)))/abs(zs);
pac=((vc^2*cos(beta))-(vs(3)*vc*cos(beta+alpha-theta(3))))/abs(zs);
p=pg-pd;
q=qg-qd;
for o=1:n
   pp(o)=0;
   qq(o)=0;
   for l=1:n
      pe(o)=vs(o)*vs(1)*my(o,1)*cos(an(o,1)-theta(o)+theta(1))+pp(o);
      pp(o)=pe(o);
      qe(o)=-vs(o)*vs(1)*my(o,1)*sin(an(o,1)-theta(o)+theta(1))+qq(o);
      qq(o)=qe(o);
   end
end
pp;
qq;
pchang(1:2)=p(2:3)-pp(2:3);
qchang(1:2)=q(2:3)-qq(2:3);
pdc=(vdc^2)/rp;
pext=pac-pdc;
del=[0 0 0 0 0 ];
del=[pchang qchang pext];
%calculation of jacobian
for k=2:n
for l=1:n
   if k~=1
      H(k,l)=vs(k)*vs(l)*my(k,l)*sin(an(k,l)+theta(l)-theta(k));
      N(k,l)=vs(k)*vs(l)*my(k,l)*cos(an(k,l)+theta(l)-theta(k));
      J(k,l)=-vs(k)*vs(l)*my(k,l)*cos(an(k,l)+theta(l)-theta(k));
      L(k,l)=-vs(k)*vs(l)*my(k,l)*sin(an(k,l)+theta(l)-theta(k));
   else
      H(k,l)=-qq(k)-vs(k)*vs(k)*b(k,k);
      N(k,l)=pp(k)+vs(k)*vs(k)*g(k,k);
      J(k,l)=pp(k)-vs(k)*vs(k)*g(k,k);
      L(k,l)=qq(k)-vs(k)*vs(k)*b(k,k);
   end
end
end
H11(1:2,1:2)=H(2:3,2:3);
N12(1:2,1:2)=N(2:3,2:3);
J21(1:2,1:2)=J(2:3,2:3);
L22(1:2,1:2)=L(2:3,2:3);
jac=zeros(5,5);
jac=[H11 N12;J21 L22];
```

```
    jac(1,4)=0;
    jac(2,2)=(vs(3)*vc*sin(theta(3)-alpha+beta)/abs(zs))-(qq(k)-vs(k)*vs(k)*b(k,k));
    jac(2,4)=-(k*vdc*cos(theta(3)-alpha+beta))/abs(zs);
    jac(2,5)=-(k*m*vdc*sin(theta(3)-alpha+beta))/abs(zs);
    jac(3,4)=0;
    jac(4,2)=-((vs(3)*vc*cos(theta(3)-alpha+beta))/abs(zs))-(pp(k)-vs(k)*vs(k)*g(k,k));
    jac(4,4)=(k*vdc*vs(3)*sin(theta(3)-alpha+beta))/abs(zs);
    jac(4,5)=-(k*vdc*vs(3)*cos(theta(3)-alpha+beta))/abs(zs);
    jac(5,2)=-(k*vdc*m*vs(3)*sin(alpha-theta(3)+beta))/abs(zs);
    jac(5,4)=(k*m*vs(3)*vdc*sin(alpha-theta(3)+beta))/abs(zs);
    jac(5,5)=-((vdc*k*vs(3)*cos(alpha-theta(3)+beta))-(2*k*k*m*vdc^2*cos(beta)))/abs(zs);
    jac;
    delta=(jac)\del';
    dtheta(2:3)=delta(1:2);
    theta=theta+dtheta
    dv=[0 0 0];
    dv(2:2)=delta(3:3);
    vs=vs+dv
    con=max(abs(dv));
    iter=iter+1;
    m=m+delta(4);
    alpha=alpha+delta(5);
end
```

OUTPUT:

```
iter =     1
theta =     0   -0.0262    0.0033
vs =    1.0500    0.9778    1.0000
iter =     2
theta =     0   -0.1781   -0.2471
vs =    1.0500    0.9770    1.0000
iter =     3
theta =       0   -0.5447   -0.8483
vs =  1.0500    0.9305    1.0000
```

RESULT:

Thus the compensated voltage and angle in the given system is calculated by using STATCOM as the compensator

EXNO:5 **DATE :**

AVAILABLE TRANSFER CAPABILITY CALCULATION USING AN EXISTING LOAD FLOW PROGRAM

AIM:

To calculate the value of Available Transfer Capability using Fast decoupled load flow method.

SOFTWARE REQUIRED:

Power system module of MATLAB.

THEORY:

All over the world, power systems are being deregulated, restructured and privatized with an objective to introduce competition and to improve the efficiency and economy of operation. Single utility is divided into different independent organizations such as Gencos, Transcos and Discos.

Gencos and Discos are given open access to transmission grid. An Independent System Operator (ISO) regulates and maintain the grid sale of power (MW) between these Gencos and Discos is encouraged and these transactions are called bilateral transactions.

The market participants, gencos and discos, need to know the "Available Transfer Capacity (ATC)" between various source nodes (Genco buses) , and sink nodes (Disco buses) of the gird tomorrow in order to finalize these bilateral transactions. ATC between a source node **'k'** and a sink node **'m'** is defined as the difference between the "Total Transfer Capacity (TTC)" of MW power between nodes **k** and **m** and the base case MW flow (BCMW) between **k** and **m.**
ATCkm = TTCkm – BCMWkm

The TTCkm is the maximum MW power that can be transferred in the system between the source node k and the sink node **m** without violating the line flow and bus voltage operating limits.

ATCkm can be determined by conducting repeated Load Flow analysis on the system starting with the base case load and increasing the generation at the **k**th bus and demand at the **m**th bus by certain percentage until any of the line flow or bus voltage constraints is just violated. The increased generation/load over the base case is the ATCkm.

EXERCISE:

Using a text editor create an input data file in the sequence given below for load flow solution of the 6-bus system. Run the program and print the output file. Check the results obtained using the available software.

Single-Line Diagram

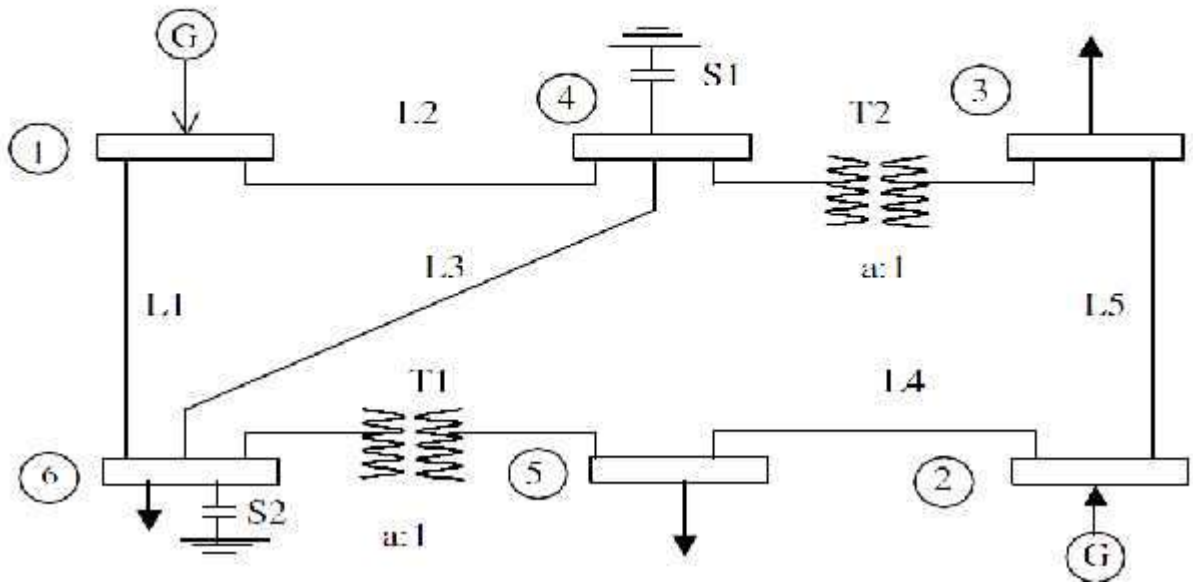

(i)Consider the optimal operating state for the base case loading of the 6 bus system. Determine the ATC between the "source bus" 1 and "sink bus"5 for base case operating state. Limit on bus voltage magnitude:0.9≤V≤1.05 p.u.

Bus Data:

Bus ID NO.	BUS Code	Voltage Magnitude p.u.	Angle degrees	Load		generation			
				MW	MVAR	MW	MVAR	Q min	Q MAX
1	1	1.05	0	0	0	0	0	-50	100
2	2	1.05	0	0	0	50	0	-25	50
3	0	1	0	55	13	0	0	0	0
4	0	1	0	0	0	0	0	0	0
5	0	1	0	30	18	0	0	0	0
6	0	1	0	50	5	0	0	0	0

Transmission Line Data:

Line ID No.	Send bus No.	Received Bus No.	Resistance p.u.	Reactance p.u.	Half line Charging Susceptance p.u.	Rating MVA
1	1	6	0.123	0.518	0	65
	1	4	0.08	0.37	0	75
2	4	6	0.087	0.407	0	30
3	5	2	0.282	0.64	0	40
4	2	3	0.723	1.05	0	65
5	6	5	0	0.300	0	70
6	4	3	0	0.133	0	30

Transformer Data:

Transformer ID no.	Send bus no.	Receive bus no.	Tap ratio
1	6	5	0.956
2	4	3	0.981

Shunt element data:

Shunt id no.	Bus id no.	Rated capacity MVAR
1	4	5
2	6	5.5

PROGRAM:

```
clear all;
clc;
r1=input('enter the reactance b/w 1 & 2');
r2=input('enter the reactance b/w 2 & 3');
r3=input('enter the reactance b/w 1 & 3');
temp=[(r1+r2) r1 r3;r1 (r1+r2) r2;r3 r2 (r3+r2)];
mw1=input('enter max mw limit b/w 1 and 2');
mw2=input('enter max mw limit b/w 2 and 3');
mw3=input('enter max mw limit b/w 1 and 3');
bo=[((1/r1)+(1/r2)) -(1/r2);-(1/r2) (1/r3)+(1/r2)]
xo=inv(bo)
disp('====ptdf cal b/w 1&3====')
ptdf1=xo(1,2)/r1
ptdf2=xo(2,2)/r3
ptdf3=(-xo(1,2)+xo(2,2))/r2
disp('====ptdf cal b/w 1&2====')
ptdf4=(-xo(1,1)+xo(1,2))/r1
ptdf5=(-xo(2,1)+xo(2,2))/r3
```

```
ptdf6=(xo(1,1)-xo(2,1)-xo(1,2)+xo(2,2))/r2
disp('====power flow due to transactions===')
a=[ptdf1 ptdf4;ptdf2 ptdf5;ptdf3 ptdf6]
b=[mw2;mw3]
p=[a]*[b]
disp('power flow due to transactions b/w 1&3 and 2&3:');
disp(p);
p1=p(1,1);
p2=p(2,1);
p3=p(3,1);
disp('===atc cal b/w 1&3===')
pmax12=(mw1-p1)/ptdf1
pmax13=-(mw2-p2)/ptdf2
pmax23=(mw3-p3)/ptdf3
disp('===atc cal b/w 2&3===')
pmax12=(mw1-p1)/ptdf4
pmax13=-(mw2-p2)/ptdf5
pmax23=(mw3-p3)/ptdf6
```

OUTPUT

```
enter the reactance b/w 1 & 20.1
enter the reactance b/w 2 & 30.066
enter the reactance b/w 1 & 30.05
enter max mw limit b/w 1 and 2600
enter max mw limit b/w 2 and 3200
enter max mw limit b/w 1 and 3600

bo =25.1515  -15.1515
     -15.1515   35.1515

xo = 0.0537    0.0231
       0.0231    0.0384
====ptdf cal b/w 1&3====

ptdf1 = 0.2315
ptdf2 =0.7685
ptdf3 =0.2315

====ptdf cal b/w 1&2====

ptdf4 =-0.3056
ptdf5 = 0.3056
ptdf6 =0.6944

====power flow due to transactions===

a =0.2315   -0.3056
    0.7685    0.3056
```

```
    0.2315    0.6944
b = 200
      600
p =-137.0370
      337.0370
      462.9630
power flow due to transactions b/w 1&3 and 2&3:
 -137.0370
  337.0370
  462.9630

===atc cal b/w 1&3===

pmax12 =3.1840e+003
pmax13 =178.3133
pmax23 = 592.0000

===atc cal b/w 2&3===

pmax12 = -2.4121e+003
pmax13 = 448.4848
pmax23 =  197.3333
```

OUTPUT FOR INCREMENT OF 10 MW AT SINK BUS:

Increment of steps (MW)	Voltage magnitude at load buses			
	3	4	5	6
5	0.925	0.929	0.903	0.904
10	0.923	0.925	**0.896**	**0.897**

ATC = 10MW

INFERENCE:

Therefore an increment by 10MW with the base case values it has been found that the voltage profile of buses 5 & 6 reaching below 0.9. Therefore it is a **voltage limited case**

(ii)Consider the optimal operating state for the base case loading of the 6 bus system. Determine the ATC between the "source bus" 1 and "sink bus"3 for base case operating state. Limit on bus voltage magnitude:0.9≤V≤1.05 p.u

OUTPUT FOR INCREMENT OF 15 MW AT SINK BUS:

Increment of steps (MW)	Voltage magnitude tn load buses			
	3	4	5	6

5	0.919	0.905	0.907	0.906
10	0.912	0.918	0.905	0.902
15	0.904	0.910	0.903	**0.898**

ATC = 15 MW

INFERENCE:

Therefore an increment by 15 MW with the base case values it has been found that the voltage profile of the bus 6 reaching below 0.9. Therefore it is a **voltage limited case.**

RESULT:

Thus the value of ATC (Available Transfer Capability) between buses 1 & 5 and buses 1 & 3 are calculated using Fast Decoupled load flow method.

EXPNO:6 **DATE:**

STUDY OF VARIABLE SPEED WIND ENERGY CONVERSATION SYSTEM

AIM:

To study of doubly fed induction generator based wind energy conversation system

THEORY:

FUNDAMENTALS OF WIND TURBINES.

The power extracted from the wind can be calculated by the given formula:

$$P_w = 0.5\rho\pi R^2 V^3 C_p(\lambda,\beta)$$

P_w = extracted power from the wind,

ρ = air density, (approximately 1.225 kg/m^3 at 20^0 C at sea level)

R = blade radius (in m), (it varies between 40-60 m)

V_w = wind velocity (m/s) (velocity can be controlled between 3 to 30 m/s)

C_p = the power coefficient which is a function of both tip speed ratio (λ), and blade pitch angle, (β) (Degrees)

Power coefficient (C_p) is defined as the ratio of the output power produced to the power available in the wind.

Betz Limit:

No wind turbine could convert more than **59.3%** of the kinetic energy of the wind into Mechanical energy turning a rotor. This is known as the Betz Limit, and is the theoretical Maximum coefficient of power for any wind turbine. The maximum value of $\mathbf{C_p}$ according to Betz limit is 59.3%. For good turbines it is in the range of 35-45%.

The wind turbine power curves shown in figure illustrate how the mechanical power that can be extracted from the wind depends on the rotor speed. For each wind speed there is an optimum turbine speed at which the extracted wind power at the shaft reaches its maximum. Such a family of Wind turbine power curves can be represented by a single dimensionless characteristic curve namely the C_p- λ curve, as in the figure, where the power coefficient is plotted against the TSR. For a given turbine, the power coefficient depends not only on the TSR but also on the blade pitch angle. Figure shows the typical variation of the power coefficient with respect to the TSR λ with the blade pitch control. The mechanical power transmitted to the shaft is

$$P_m - \frac{1}{2}\rho C_p A V_\infty^3$$

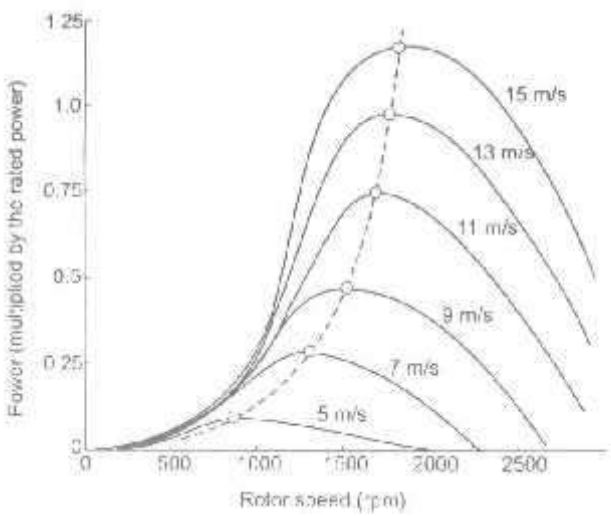

Figure 2.6 Power Speed Characteristics of Wind Turbine

Torque speed characteristics

Studying the torque versus rotational speed characteristics of any prime mover is very important for properly matching the load and ensuring stable operation of the electrical generator. The typical torque speed characteristics of the two – blade propeller- type wind turbine, the Darrieus

rotor, and the Savonius rotor are shown in figure. The profiles of the Torque-speed curves shown in the figure follow from the power curves, since torque and power are related as follows

$$T_m = P_m / w$$

From the equation, at optimum operating point ($C_{p,pot}, \lambda_{opt}$), the relation between the aerodynamic torque and rotational speed is,

$$T_m = 0.5\, \rho\, C_{p,opt}\, \pi\, (R^5/\lambda_{opt}^3)\, \omega^3.$$

It is seen that at the optimum operating point on the C_p- λ curve, the torque is quadratically related to the rotational speed.

The torque speed characteristic curve shows that for the propeller turbine and the darrieus rotor, for any wind speed, the torque reaches a maximum value at a specific rotational speed, and this maximum shaft torque varies approximately as the square of the rotational speed. In case of electricity production, the load torque depends on the electrical loading, and by properly choosing the load (or power electronics interface), the torque can be made to vary as the square of the rotational speed.

The choice of constant of proportionality of the load is very important. At the optimal value, the Load curve follows the maximum shaft power. But a higher value, the load torque may exceed the turbine torque for most speeds.

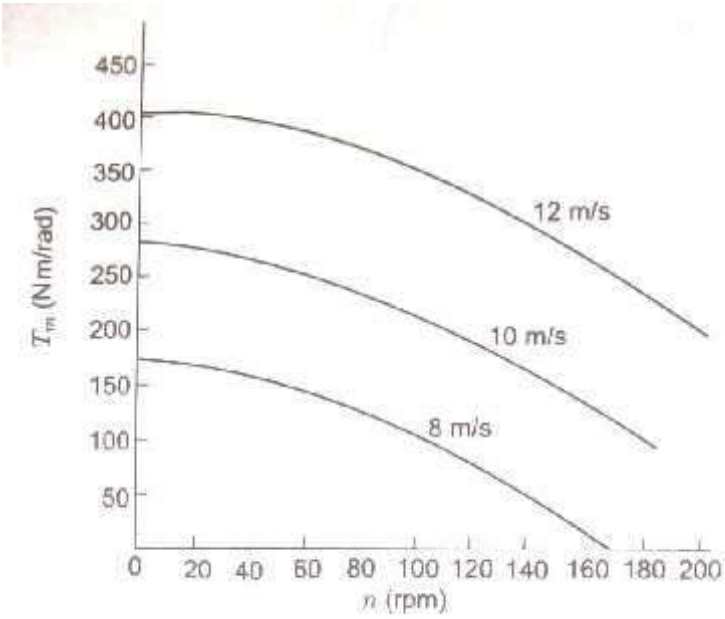
450
400
350
300
250
200
150
100
50
T_m (N m/rad)
12 m/s
10 m/s
8 m/s
0 20 40 60 80 100 120 140 160 180 200
n (rpm)

(a)

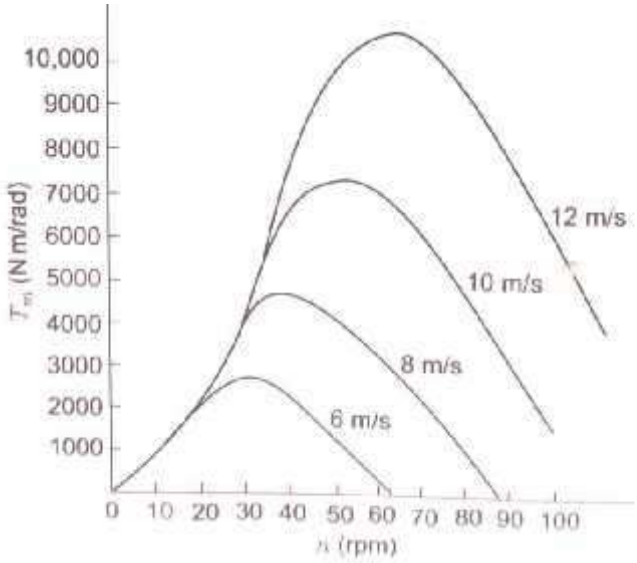
10,000
9000
8000
7000
6000
5000
4000
3000
2000
1000
T_m (N m/rad)
12 m/s
10 m/s
8 m/s
6 m/s
0 10 20 30 40 50 60 70 80 90 100
n (rpm)

(b)

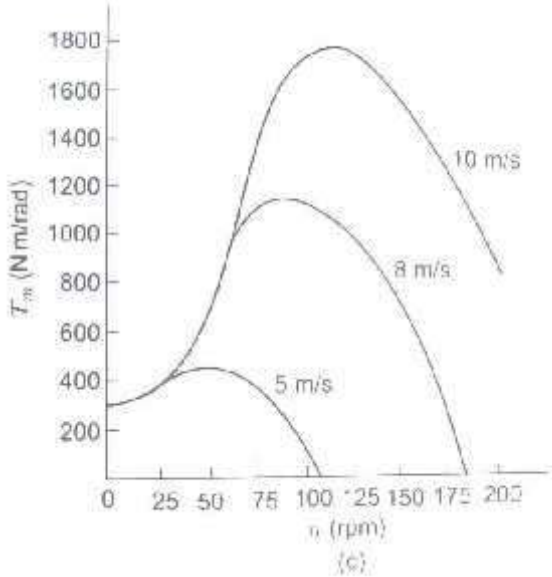

The Torque Speed Characteristics of Various Wind Machines: a. savonious rotor; b. Darrieus rotor; c. two-blade propeller-type

Wind Turbine Control Systems

Pitch Angle Control:

The system changes the pitch angle of the blades according to the variation of wind speed. As discussed earlier, with pitch control, it is possible to achieve a high efficiency by continuously aligning the blade in the direction of the relative wind.

On a pitch controlled machine, as the wind speed exceeds its rated speed, the blades are gradually turned about the longitudinal axis and out of the wind to increase the pitch angle. This reduces the aerodynamic efficiency of the rotor, and the rotor output power decreases. When the wind speed exceeds the safe limit for the system, the pitch angle is so changed that the power output reduces to zero and the machine shifts to the „stall" mode. After the gust passes, the pitch angle is reset to the normal position and the turbine is restarted. At normal wind speeds, the blade pitch angle should ideally settle to a value at which the output power equals the rated power. The input variable to the pitch controller is the error signal arising from the difference between the output electrical power and the reference power. The pitch controller operates the blade actuator to alter the pitch angle. During operation below the rated speed, the control system endeavours to the pitch the blade at an angle that maximises the rotor efficiency. The

generator must be able to absorb the mechanical power output and deliver to the load. Hence, the generator output power needs to be simultaneously adjusted.

StallControl

Passive stall control:

Generally, stall control to limit the power output at high winds is applied to constant-pitch turbines driving induction generators connected to the network. The rotor speed is fixed by the network, allowing only 1-4% variation. As the wind speed increases, the angle of attack also increases for a blade running at a near constant speed. Beyond a particular angle of attack, the lift force decreases, causing the rotor efficiency to drop. This lift force can be further reduced to restrict the power output at high winds by properly shaping the rotor blade profile to create turbulence on the rotor blade side not facing the wind.

Active stall control:

In this method of control, at high wind speeds, the blade is rotated by a few degrees in the direction opposite to that in a pitch controlled machine. This increases the angle of attack, which can be controlled to keep the output power at its rated value at all high wind speeds below the furling speed. A passive controlled machine shows a drop in power at high winds. The action of active stall control is sometimes called *deep stall*. Owing to economic reasons, active pitch control is generally used only with high- capacity machines.

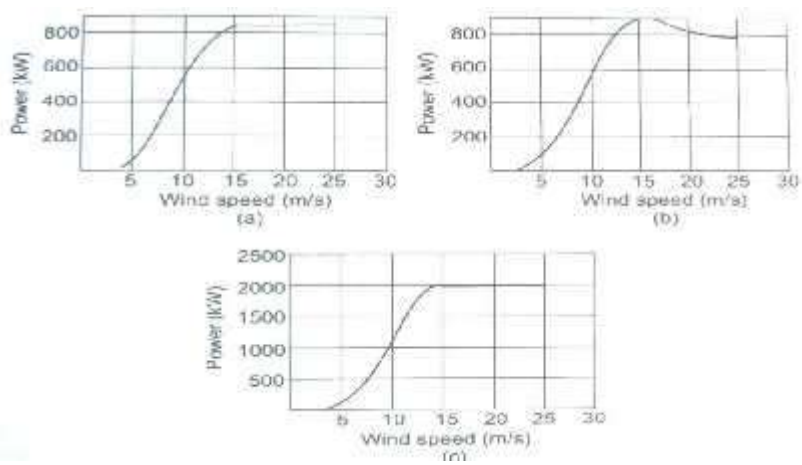

Figure 3.1 - Typical power profiles a.) pitch control b.) passive stall control c.) Active stall control

Control Strategy:

Different speed control strategies are required for the five different ranges of wind speed.

- Power is not generated by the machine below a cut-in speed. Rotation of the machine may start in this speed range if there is sufficient starting torque. But no power is generated and rotor rotates freely
- Maximum power is extracted from the wind at normal wind speeds. This is achieved at a particular TSR value. Hence, for tracking maximum power point, rotational speed is changed continuously proportional to the wind speed.
- At high wind speeds, rotor speed is limited to a maximum value which depends on the design of the mechanical components. Here C_p is lower than the maximum value. Power output is not proportional to the cube of the wind speed.
- At even higher wind speeds, output power is kept constant at the maximum value allowed by the electrical components.
- At cut-out or furling wind speed, the power generation is shut down and the rotation is stopped in order to protect the system components.

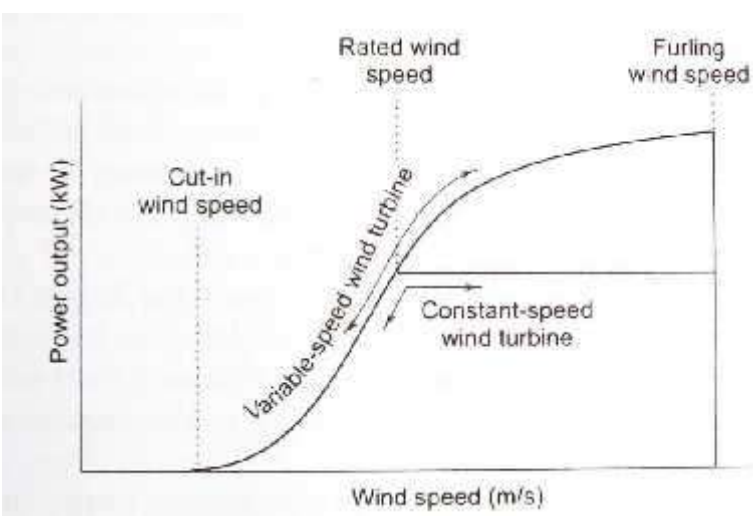

Figure 3.2 – Power versus wind speed characteristics of variable speed wind turbines

In the intermediate speed-range, the control strategy depends on the type of electrical power generating system used,

and can be divided into two basic categories:

a) Constant speed generation scheme, and b)

Variable-speed generation scheme.

If the electrical system involves a grid-connected synchronous generator, the constant generation scheme is necessary. In the case of grid-connected squirrel cage induction generators, the allowable range of speed variation is very small, requiring an almost constant rotational speed.

But the constant-speed generation systems cannot maximise the power extraction from wind. Power coefficient reaches a maximum specific value of TSR for every type of wind turbine. Hence for the extraction of maximum power from wind, the turbine should operate at a constant TSR, which means the rotational speed should be proportional to the wind speed. So maximum power extraction requires a variable-speed generation system with the speed control for keeping a constant TSR.

Such systems can yield 20-30% more power than constant-speed generation systems. With the development of induction generators and power electronic converters, variable-speed generation systems are favoured.

The constant-TSR region is achieved by regulating the mechanical power input through pitch control or the electrical power output by the power electronic control. In many cases a combination of both is employed.

The control scheme can have two possible forms. In the first case, the value of the TSR for maximum C_p is stored in a microprocessor. The operating TSR is obtained from the measured values of the wind speed and rotational speed. An error signal is generated whenever the operating TSR deviates from the optimum TSR. If the current value of the TSR is greater than the optimum TSR, the power electronic converter increases the power output so that the rotational speed is reduced to the desired value. The opposite action is performed if the optimal value exceeds the current TSR

This scheme has a few disadvantages. First, the wind speed measured in the neighbourhood of a wind turbine (or a wind farm) is not reliable indicator of V because of the shadowing effects. Also it is difficult to determine the value of TSR for maximum C_p. This value changes during the lifetime of a wind turbine due to the changes in the reference setting.

A second control scheme is devised to continuously track the maximum power point (MPP) using the property that the C_p versus TSR curve has a single smooth maximum point. This means that if operate at the maximum power point, small fluctuations in the rotational speed do not significantly change the power output. To implement this scheme, the speed is varied in small steps, the power output is measured and, and $\Delta P/\Delta\omega$ is evaluated. If this ratio is positive, more mechanical power can be obtained by increasing the speed. Hence the electrical power output is decreased temporarily by the power electronic control so that the speed increases. This increases the mechanical power, and can be obtained by increasing the speed. Hence the electrical power output is decreased temporarily by power electronic

control so that the speed increases. This increases the mechanical power, and the electrical power, and the electrical power output is decreased temporarily by the power electronic control so that the speed increases. This increases the mechanical power, and the electrical power is again raised to a higher value. The process continues until the optimum speed is reached, when the mechanical power becomes intensive to speed fluctuations. When the wind speed changes, this mechanism readjusts the speed at the optimum value.

While controlling the rotational speed, it should be remembered that a large difference between mechanical power and electrical power results in a large torque and, hence, a large stress on the rotor components. It is necessary to limit the acceleration and deceleration rates to values dictated by the structural strength of mechanical parts.

DOUBLY FED INDUCTION GENERATOR

1. In a doubly fed induction machine, two windings participate in energy conversion process. They can work at double the synchronous speed for constant torque, similar to synchronous machine but in synchronous machine only one winding participate in energy conversion DFIM (doubly fed induction machine) is to operate in narrow speed ranges.

.

2. CONSTRUCTION

1. Wound Rotor DFIM.
2. Brushless wound rotor:
   a. Brushless DF Induction electric machine.
   b. Brushless wound rotor DF electric machine.

Wound rotor DFIM uses the two windings of same power rating. One is winding on stator and the other on rotor. Stator supply is Normal 3 phase supply. Rotor supply is from power frequency converter. Slip ring assembly used to transfer Power to rotor winding. In a brushless DFIM **t**wo windings are adjacent to each the other on stator. Windings are excited separately. Brushless wound rotor DFIM **is s**imilar to wound rotor DFIM but slip ring assembly is not used. It has a large efficiency and less cost but instability is more.

WORKING:

Field can be from rotor or stator or from both. Both active power (for torque) and reactive power (for flux) have to be fed to rotor**.** Multi-phase supply with frequency f is given to stator. Control Frequency converter converts power from supply frequency to slip frequency.

ADVANTAGES:

- Theoretically system cost is half of other machines with same rating.
- Higher efficiency can be achieved due to less loss.
- Rotor core is effectively utilized hence power density is large.
- Active and reactive power to grid can be controlled using electronic converters

- DFIG can work in variable speed range around synchronous speed

Wound rotor DFIM found commercial success in very large applications with limited speed range. For a low cost, highly efficient and reliable electronic controlled DFIM is kept under study

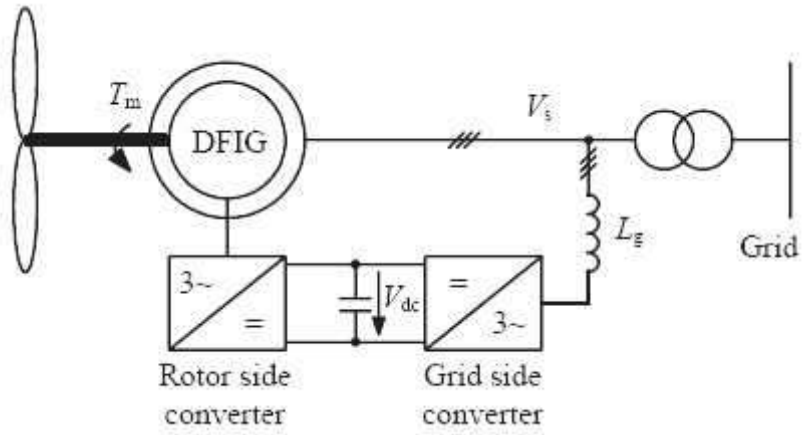

Figure 4.4 – DFIG Connected to the Grid

1. Pitch Control – analysis by MATLAB

Explanation:

$$P_m = 0.5\ C_p\ (\lambda, \beta)\ \rho A V_w^3$$

Equation 5.1

Where

P_m is the Mechanical output power of the wind turbine;

C_p (λ,α) is the performance coefficient of the turbine;

ρ is the density of air in kg/m^3;

A is the turbine swept area in m^2;

V_w is the speed of wind (m/s);

λ is the tip speed ratio;

β blade pitch angle (degrees)

A generic equation is used to model C_p (λ,β) :

$$C_p(\lambda,\beta) = C_1\left(\frac{C_2}{\lambda} - C_3\beta - C_4\right)e^{\frac{-C_5}{\beta}} + C_6\lambda$$

Equation 5.2

Where

$$\frac{1}{\lambda_i} = \frac{1}{\lambda + 0.08\beta} - \frac{0.035}{\beta^2 + 1}$$

Equation 5.3

The coefficients c_1 to c_6 are: $c_1 = 0.5176$, $c_2 = 116$, $c_3 = 0.4$, $c_4 = 5$, $c_5 = 21$ and $c_6 = 0.0068$. The C_p λ characteristics, for different values of the pitch angle β, are illustrated below. The maximum value of C_p ($C_{pmax} = 0.48$) is achieved for β = 0 degree and for λ = 8.1. This particular value of λ is defined as the nominal value (λ_{nom})

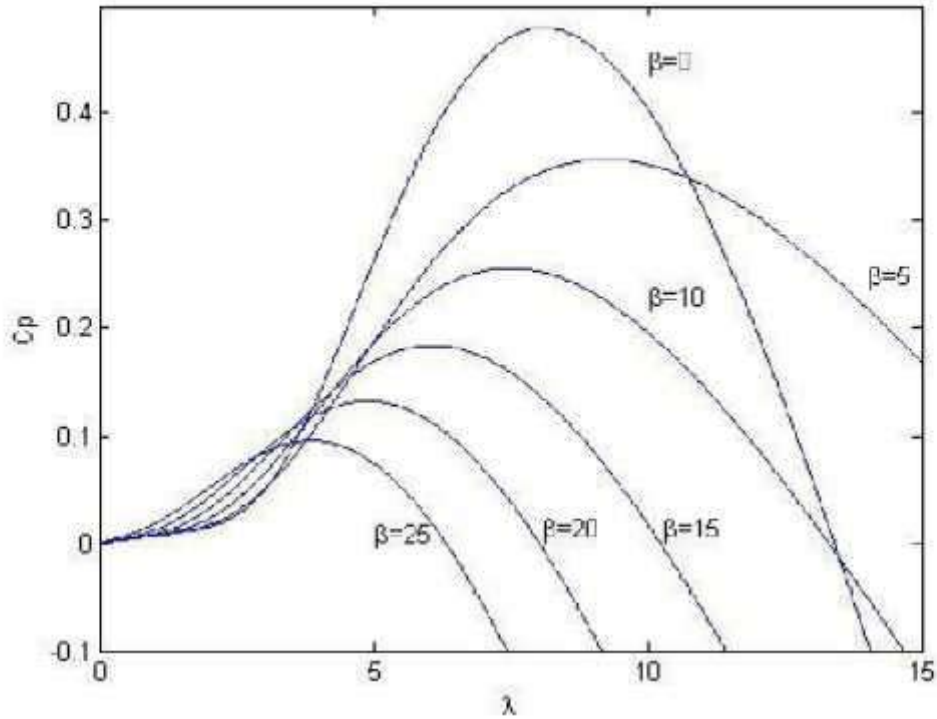

Figure 5.1 Power coefficient versus tip speed ratio

From the above graph we can see that we can obtain a maximum value of cp for a particular value of TSR. Based on this idea, the following algorithm was developed which calculates the value of pitch angle for getting the maximum value of C_p for a particular TSR.

We calculate TSR (tip speed ratio) in a case where the blade tip speed is almost constant in the case of a fixed speed turbine. And a C_p- **λ** graph is calculated for different values of beta (pitch angle)

TSR = tip of blade/ wind speed

OR

$$\lambda = 2\pi RN / V_\infty$$

MATLAB CODE:

```
%meshgrid(tsr,pitch);
Cp=0;
c1=0.5176;
c2=116;
c3=0.4;
c4=5;
c5=21;
c6=0.0068;
n=size(tsr);
for i=1:6
for j=1:n(2)
tsr_i=(1/(tsr(j)+0.08*pitch(i))-0.035/(pitch(i)^3+1))^(-1);
Cp(j)=c1*(c2/tsr_i-c3*pitch(i)-c4)*exp(-c5/tsr_i)+c6*tsr(j);
end
plot(tsr,Cp);
hold on;
end
axis ([0 15 -0.1 0.5 ]);
xlabel('\lambda'),ylabel('Cp');
```

2. Turbine Characteristics :analysis by MATLAB

Both horizontal and vertical axis wind turbines are used in wind generation systems. The vertical darrieus (egg beater) type has the advantages that it is located on the ground, can accept wind from any direction without any special yaw mechanism and, therefore, it is preferred for high power output. The disadvantages are that the turbine is not self-starting and there is a large pulsating torque which depends on wind velocity, turbine speed, and other factors related to the design of the turbine. The aerodynamic torque of a vertical turbine is given by the equation

$$T_m = C_p(\lambda) \cdot [0.5 \frac{\rho \pi R_w^5}{\eta_{gear}}] \cdot V_w^2$$

Equation 5.5

Where

C_p= power coefficient

λ = tip speed ratio (TSR)

ρ = air density

R_W , = turbine radius

η_{gear}= speed-up gear ratio v, = wind velocity

V_w= turbine angular speed

W_w=turbine angular speed

The power coefficient (C,) is the figure of-merit and is defined as the ratio of actual power delivered to the free stream power flowing through a similar but uninterrupted area, and tip speed ratio (TSR) is the ratio of turbine speed at the tip of a blade to the free stream wind speed. The oscillatory torque of the turbine is more dominant at the first, second, and fourth harmonics of fundamental turbine angular velocity and is given by the expression

$$T_{osc} = T_m \cdot [A\cos(\acute{\omega}_w) + B\cos(\acute{\omega}_w) + C\cos(\acute{\omega}_w)]$$

Equation 5.6

Where A, B, and C are constants. **Fig. 3** shows the block diagram of the turbine model with oscillatory torque. A typical family of turbine torque speed curves at different wind velocities is shown in Figure

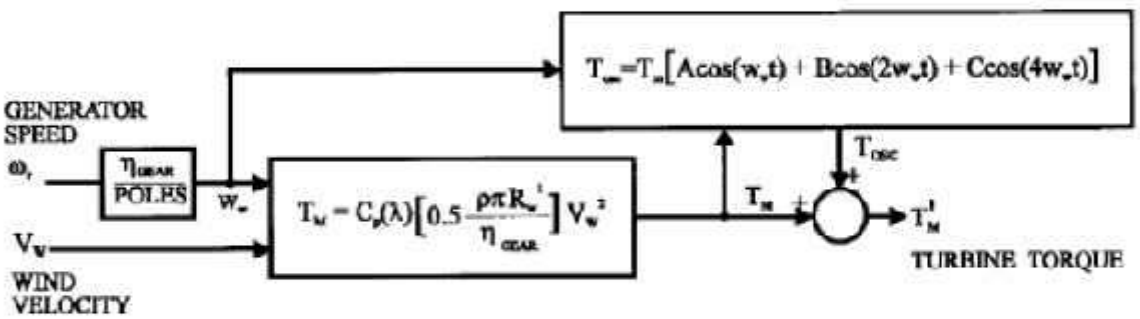

Figure 5.2 – Model of a wind turbine with oscillatory torque

```
%torque speed characteristic of a wind turbine

density=2.25;

Rw=20;

Gear_ratio=5;

Cp=0.25;

Vw=[6 6.5 7];


for i=1:3
```

```
Tm(i)=Cp*((0.5*density*pi*Rw^3)/(Gear_ratio))*Vw(i)^2;
end

%computed the aerodynamic torque of the vertical turbine

A=0.015;
B=0.03;
C=0.015;

t=1;

rotor_speed=linspace(-4,-2,100);
Tosc=Tm(1)*(A*cos(rotor_speed*t)+B*cos(2*rotor_speed*t)+C*cos(4*rotor_speed*t));
%computed the oscillatory torque
Tm1=Tosc-Tm(1);
plot(rotor_speed,Tm1);
hold on;

rotor_speed=linspace(-1,1,100);
Tosc=Tm(2)*(A*cos(rotor_speed*t)+B*cos(2*rotor_speed*t)+C*cos(4*rotor_speed*t));
%computed the oscillatory torque
Tm1=Tosc-Tm(2);
plot(rotor_speed,Tm1);
```

```
hold on;

rotor_speed=linspace(2.2,4.2,100);

Tosc=Tm(3)*(A*cos(rotor_speed*t)+B*cos(2*rotor_speed*t)+C*cos(4*rotor_speed*t));

%computed the oscillatory torque.

Tm1=Tosc+Tm(3);

plot(rotor_speed,Tm1);
```

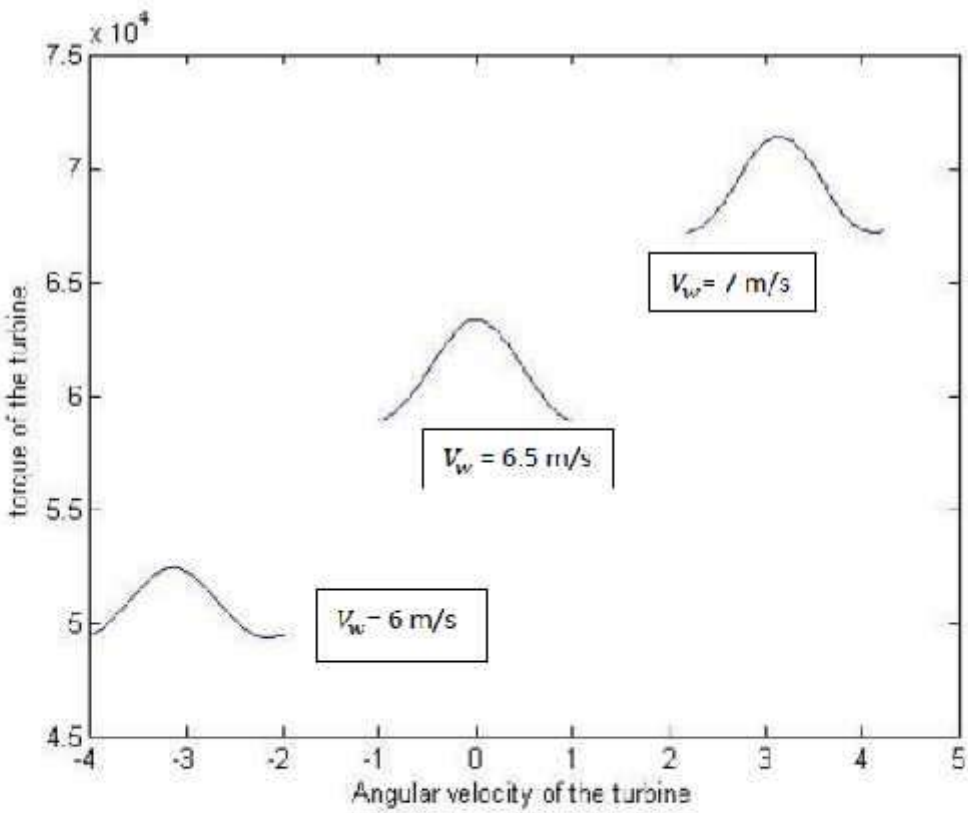

Figure 5.3 Torque-speed characteristics of wind turbine at different wind speeds.

control so that the speed increases. This increases the mechanical power, and the electrical power, and the electrical power output is decreased temporarily by the power electronic control so that the speed increases. This increases the mechanical power, and the electrical power is again raised to a higher value. The process continues until the optimum speed is reached, when the mechanical power becomes intensive to speed fluctuations. When the wind speed changes, this mechanism readjusts the speed at the optimum value.

While controlling the rotational speed, it should be remembered that a large difference between mechanical power and electrical power results in a large torque and, hence, a large stress on the rotor components. It is necessary to limit the acceleration and deceleration rates to values dictated by the structural strength of mechanical parts.

WIND FARM - DFIG DETAILED MODEL

SIMULATION:

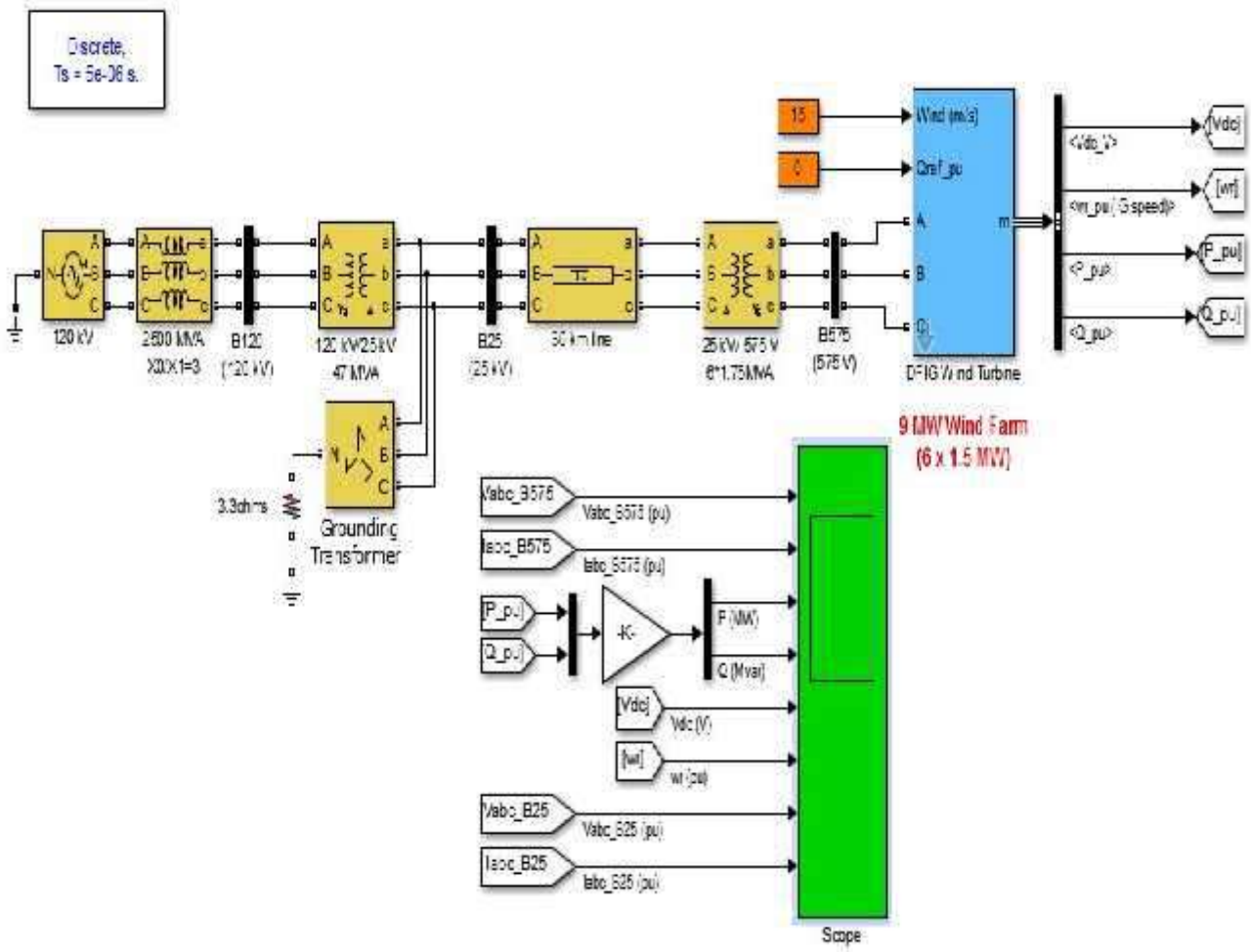

Wind Farm - DFIG Detailed Model

OUTPUT:

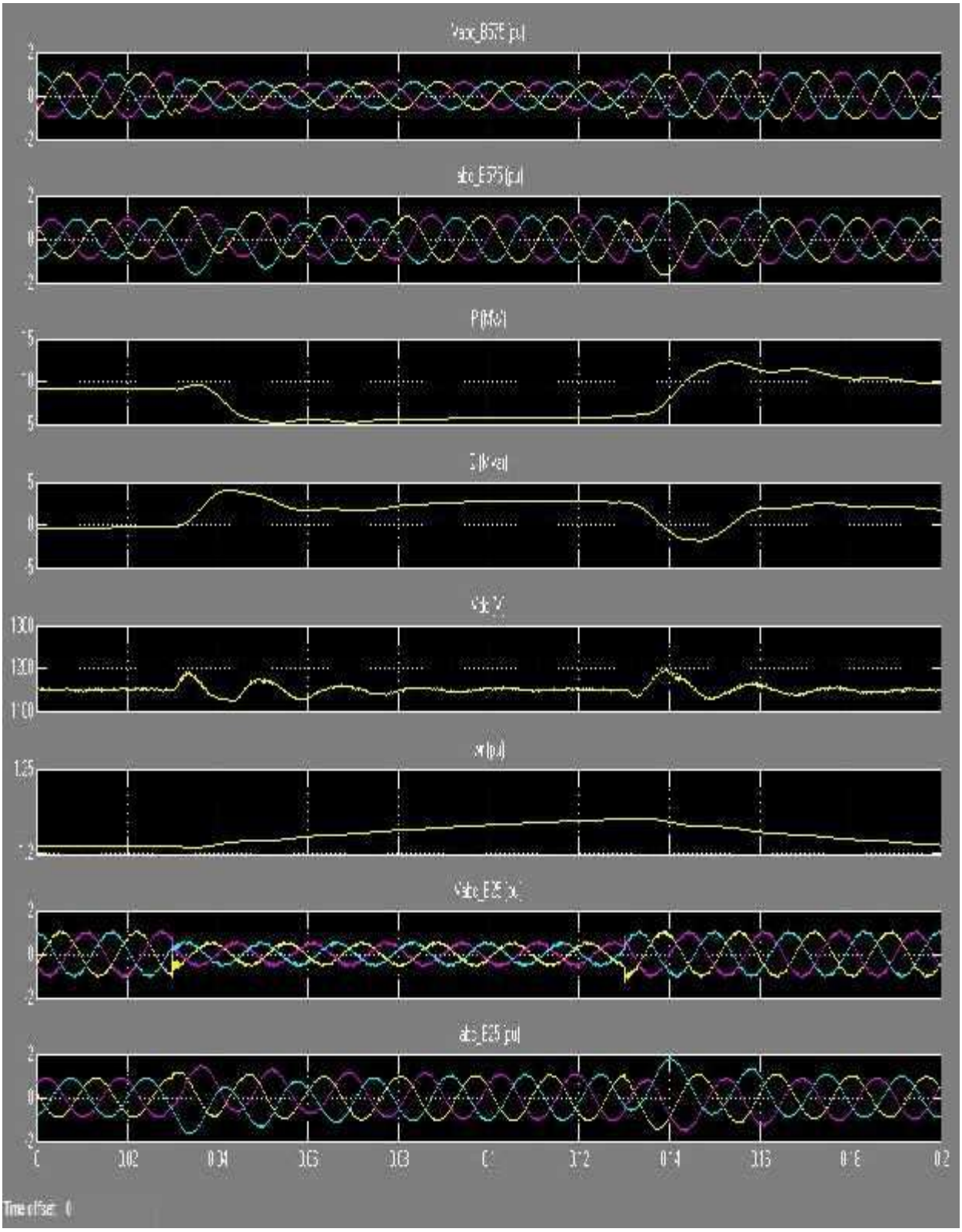

EXPNO:7 **DATE:**

STUDY OF VARIABLE SPEED WIND ENERGY CONVERSION SYSTEM-PMSG

AIM:

To study of variable speed wind energy conversion system using Permenant magnet synchrouns generator

THEORY:

Sustainability is the main aspect that forces the renewable energy sources to be implemented for electric energy generation instead of fossil ones. Wind energy is quite attractive among other sources because of its commercial potential [72 TW] that is five times higher than world energy demand in all forms. However, the installed capacity in 2009 was only 159GW. Large turbines play a main role on the market, but there is also demand for small turbines in the power range up to 11 kW as the power source for micro generators. Micro generator is an electrical energy source that includes all interface units and operates in parallel with the distribution network.

Current rating of such devices is limited up to 16 A per phase. Some energy sources can be connected directly to the distribution network, but in the case of DC power sources or variable speed wind turbine (VSWT) systems it is necessary to use a power converter that interfaces the source and the grid.VSWT based micro generators consist of a wind turbine, a generator and an inverter. Wind turbines capture wind energy and convert it to rotational mechanical energy. Variable speed operation of the wind turbine allows extraction of higher energy from wind than constant speed systems. The generator converts mechanical energy into electricity. Different types of generators can be used in wind energy conversion systems (WECS), but permanent magnet synchronous generators (PMSG) play a main role on the market. The main advantage of PMSG is the possibility of multipole design that offers slow speed operation and the possibility of gearless WECS construction. Another advantage is maintenance free operation since there are no brushes. The main drawback of PMSG is the dependence of its output voltage on the rotation speed. The difference between the minimum and the maximum voltage can reach four times in VSWT applications.

This drawback can be easily overcome with the help of an appropriate interfacing converter.The interfacing converter rectifies the input AC with variable voltage and frequency, adjusts voltage levels and inverts DC voltage into AC with grid voltage and frequency. Additionally, it should have maximum power point tracking (MPPT) functionality to extract more power from wind.The new topology of the interfacing converter with the HF isolation transformer for PMSG based VSWT system is presented in this paper. The topology presented has good voltage regulation capabilities at a relatively simple power circuit.

DIFFERENT TOPOLOGIES INTERFACING CONVERTER FOR WIND TURBINE.

Basically they can be divided into two groups: topologies without galvanic isolation (Fig. 1a) and those with isolation. Line frequency (LF) transformers (Fig. 1b) were widely used for galvanic isolation in last decades.Main drawbacks of LF transformer are high weight and high price. For these reasons topologies with HF isolation (Fig. 1c) have became popular especially for photovoltaic applications and wind power applications.

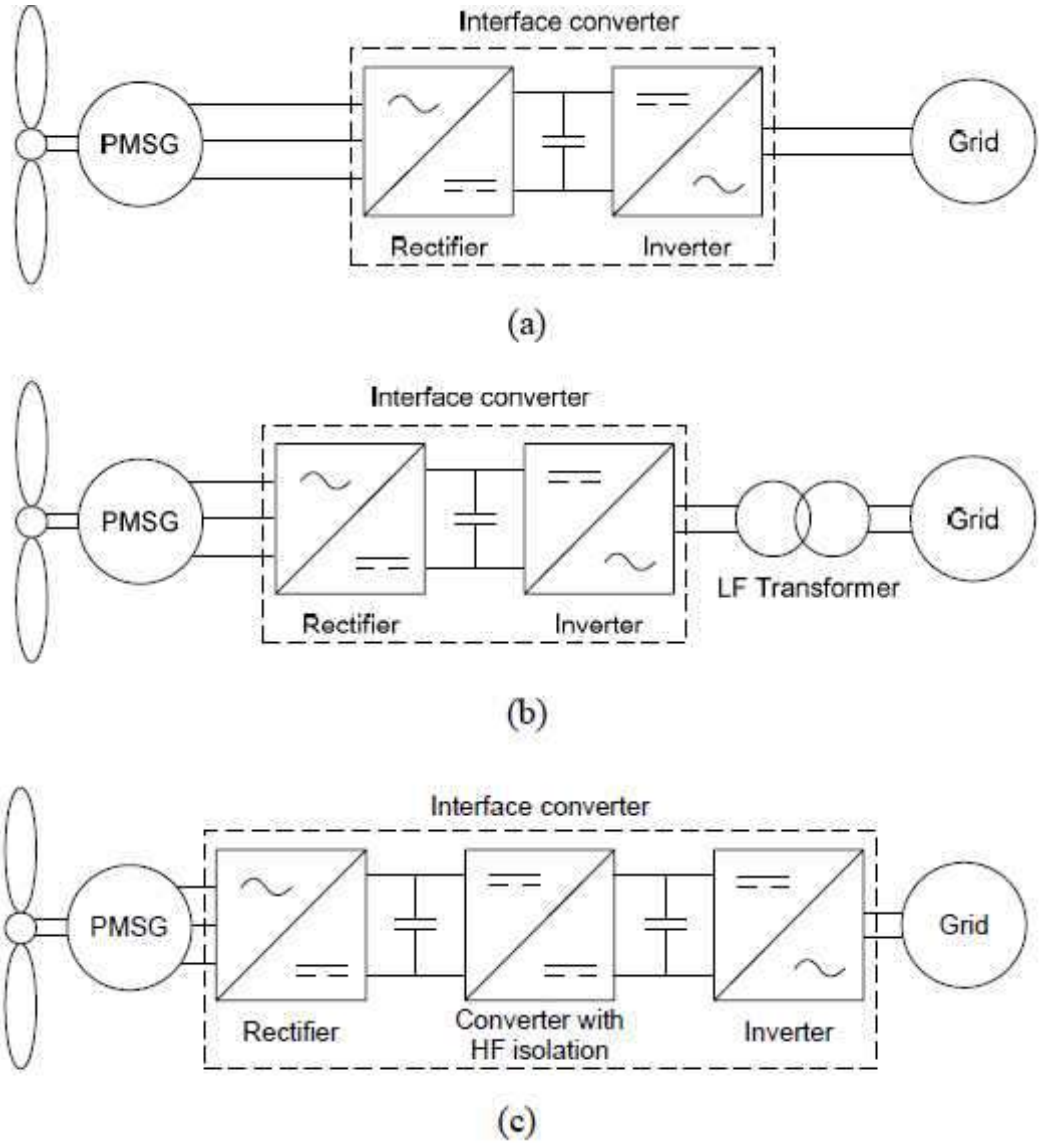

Fig 1:Block diagram of interfacing converters

CHALLENGES OF PMSG BASED VSWT

This section introduces the concept of wind energy,properties of wind energy, emphasizing wind energy extraction by means of PMSG based VSWT. Operation modes of VSWT with fixed blades are analyzed and generator characteristics are given.

ENERGY FROM THE WIND

Wind is simple air in motion. It is caused by the uneven heating of the earth's surface by the sun. Since the earth's surface is made of very different types of land and water, it absorbs the sun's heat at

different rates. During the day, the air above the land heats up more quickly than the air over water. The warm air over the land expands and rises, and the heavier, cooler air rushes in to take its place, creating winds. At night, the winds are reversed because the air cools more rapidly over land than over water. In the same way, the large atmospheric winds that circle the earth are created because the land near the earth's equator is heated more by the sun than the land near the North and South Poles. Today, wind energy is mainly used to generate electricity. Wind is called a renewable energy source because the wind will blow as long as the sun shines.

THE HISTORY OF WIND

Since ancient times, people have harnessed the winds energy. Over 5,000 years ago, the ancient Egyptians used wind to sail ships on the Nile River. Later, people built windmills to grind wheat and other grains. The earliest known windmills were in Persia (Iran). These early windmills looked like large paddle wheels. Centuries later, the people of Holland improved the basic design of the windmill. They gave it propeller-type blades, still made with sails. Holland is famous for its windmills.American colonists used windmills to grind wheat and corn, to pump water, and to cut wood at sawmills. As late as the 1920s, Americans used small windmills to generate electricity in rural areas without electric service. When power lines began to transport electricity to rural areas in the 1930s, local windmills were used less and less, though they can still be seen on some Western ranches. The oil shortages of the 1970s changed the energy picture for the country and the world. It created an interest in alternative energy sources, paving the way for the re-entry of the windmill to generate electricity. In the early 1980s wind energy really took off in California, partly because of state policies that encouraged renewable energy sources. Support for wind development has since spread to other states, but California still produces more than twice as much wind energy as any other state. The first offshore wind park in the United States is planned for an area off the coast of Cape Cod, Massachusetts.

HOW THE WIND MACHINES WORK

Like old fashioned windmills, today’s wind machines use blades to collect the wind’s kinetic energy. Windmills work because they slow down the speed of the wind. The wind flows over the airfoil shaped blades causing lift, like the effect on airplane wings, causing them to turn. The blades are connected to a drive shaft that turns an electric generator to produce electricity. With the new wind

machines, there is still the problem of what to do when the wind isn't blowing. At those times, other types of power plants must be used to make electricity

TYPES OF WIND MACHINES

There are two types of wind machines (turbines) used today based on the direction of the rotating shaft (axis): horizontal–axis wind machines and vertical-axis wind machines. The size of wind machines varies widely. Small turbines used to power a single home or business may have a capacity of less than 100 kilowatts. Some large commercial sized turbines may have a capacity of 5 million watts, or 5 megawatts. Larger turbines are often grouped together into wind farms that provide power to the electrical grid.

HORIZONTAL AXIS WIND MACHINE

Most wind machines being used today are the horizontal-axis type. Horizontal-axis wind machines have blades like airplane propellers. A typical horizontal wind machine stands as tall as a 20-story building and has three blades that span 200 feet across. The largest wind machines in the world have blades longer than a football field! Wind machines stand tall and wide to capture more wind.

VERTICAL AXIS WIND MACHINE

Vertical–axis wind machines have blades that go from top to bottom and the most common type (Darrieus wind turbine) looks like a giant two-bladed egg beaters. The type of vertical wind machine typically stands 100 feet tall and 50 feet wide. Vertical-axis wind machines make up only a very small percent of the wind machines used today.

The Wind Amplified Rotor Platform (WARP) is a different kind of wind system that is designed to be more efficient and use less land than wind machines in use today. The WARP does not use large blades; instead, it looks like a stack of wheel rims. Each module has a pair of small, high capacity turbines mounted to both of its concave wind amplifier module channel surfaces. The concave surfaces channel wind toward the turbines, amplifying wind speeds by 50 percent or more. Eneco, the company that designed WARP, plans to market the technology to power offshore oil platforms and wireless telecommunications systems.

WIND POWER PLANTS.

Wind power plants, or wind farms as they are sometimes called, are clusters of wind machines used to produce electricity. A wind farm usually has dozens of wind machines scattered over a large area. The world's largest wind farm, the Horse Hollow Wind Energy Center in Texas, has 421 wind turbines that generate enough electricity to power 220,000 homes per year. Unlike power plants, many wind plants are not owned by public utility companies. Instead they are owned and operated by business people who sell the electricity produced on the wind farm to electric utilities. These private companies are known as Independent Power Producers. Operating a wind power plant is not as simple as just building a windmill in a windy place. Wind plant owners must carefully plan where to locate their machines. One important thing to consider is how fast and how much the wind blows. As a rule, wind speed increases with altitude and over open areas with no windbreaks. Good sites for wind plants are the tops of smooth, rounded hills, open plains or shorelines, and mountain gaps that produce wind funneling. Wind speed varies throughout the country. It also varies from season to season. In Tehachapi, California, the wind blows more from April through October than it does in the winter. This is because of the extreme heating of the Mojave Desert during the summer months. The hot air over the desert rises, and the cooler, denser air above the Pacific Ocean rushes through the Tehachapi mountain pass to take its place. In a state like Montana, on the other hand, the wind blows more during the winter. Fortunately, these seasonal variations are a good match for the electricity demands of the regions. In California, people use more electricity during the summer for air conditioners. In Montana, people use more electricity during the winter months for heating.

COMPONENTS OF THE WIND TURBINE

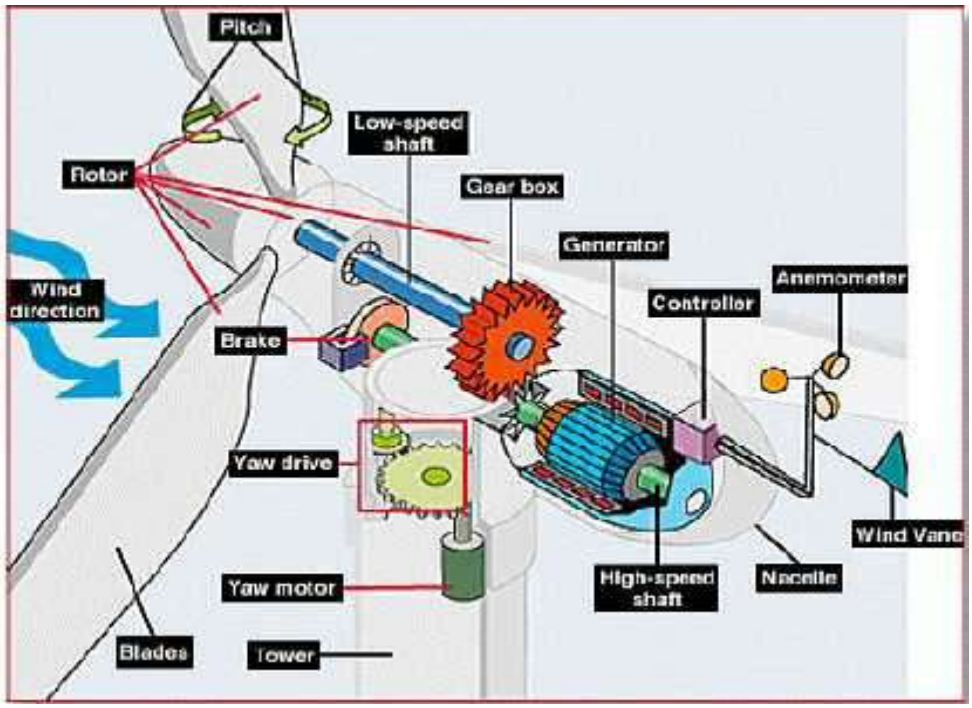

Fig 2: Wind turbine components

Anemometer:

Measures the wind speed and transmits wind speed data to the controller.

Blades:

Most turbines have either two or three blades. Wind blowing over the blades causes the blades to "lift" and rotate.

Brake:

A disc brake, which can be applied mechanically, electrically, or hydraulically to stop the rotor in emergencies.

Controller:

The controller starts up the machine at wind speeds of about 8 to 16 miles per hour (mph) and shuts off the machine at about 55 mph. Turbines do not operate at wind speeds above about 55 mph because they might be damaged by the high winds.

Gear box:

Gears connect the low-speed shaft to the high-speed shaft and increase the rotational speeds from about 30 to 60 rotations per minute (rpm) to about 1000 to 1800 rpm, the rotational speed required by most generators to produce electricity. The gear box is a costly (and heavy) part of the wind turbine and engineers are exploring "direct-drive" generators that operate at lower rotational speeds and don't need gear boxes.

Generator:

Usually an off-the-shelf induction generator that produces 60-cycle AC electricity.

High-speed shaft:

Drives the generator.

Low-speed shaft:

The rotor turns the low-speed shaft at about 30 to 60 rotations per minute.

Nacelle:

The nacelle sits atop the tower and contains the gear box, low- and high-speed shafts, generator, controller, and brake. Some nacelles are large enough for a helicopter to land on.

Pitch:

Blades are turned, or pitched, out of the wind to control the rotor speed and keep the rotor from turning in winds that are too high or too low to produce electricity.

Rotor:

The blades and the hub together are called the rotor.

Tower:

Towers are made from tubular steel (shown here), concrete, or steel lattice. Because wind speed increases with height, taller towers enable turbines to capture more energy and generate more electricity.

Wind direction:

This is an "upwind" turbine, so-called because it operates facing into the wind. Other turbines are designed to run "downwind," facing away from the wind.

Wind vane:

Measures wind direction and communicates with the yaw drive to orient the turbine properly with respect to the wind.

Yaw drive:

Upwind turbines face into the wind; the yaw drive is used to keep the rotor facing into the wind as the wind direction changes. Downwind turbines don't require a yaw drive, the wind blows the rotor downwind.

Yaw motor:

Powers the yaw drive.

WIND TURBINE CHARACTERACTICS

Equation (1) gives the total power available in the wind,where A is the rotor area, ρ is the air density and v is the wind velocity.

$$P_{WIND} = 0.5A\rho v^3 \quad \ldots\ldots\ldots\ldots\ldots \quad (1)$$

Only a part of the total wind energy can be extracted. The available energy part in wind is described by the power coefficient C_p. The theoretical maximum value of this coefficient is 0.59 and it is called the Betz limit.

$$P_{turbine} = 0.5C_p\, Av^3 \quad \ldots\ldots\ldots\ldots \quad (2)$$

The practical values of Cp lie between 0.4 and 0.5 for industrial wind turbines.This power coefficient is a function of the tip-speed ratio λ. An example of this function is shown in Fig. 2. The tip-speed ratio shows the relation between the circumferential velocity of the blade tips and the wind velocity:

$$\lambda = \frac{r\Omega}{v} \quad \ldots\ldots\ldots\ldots\ldots\ldots..(3)$$

where *r* is the rotor radius and *Ω* is the angular rotor speed.

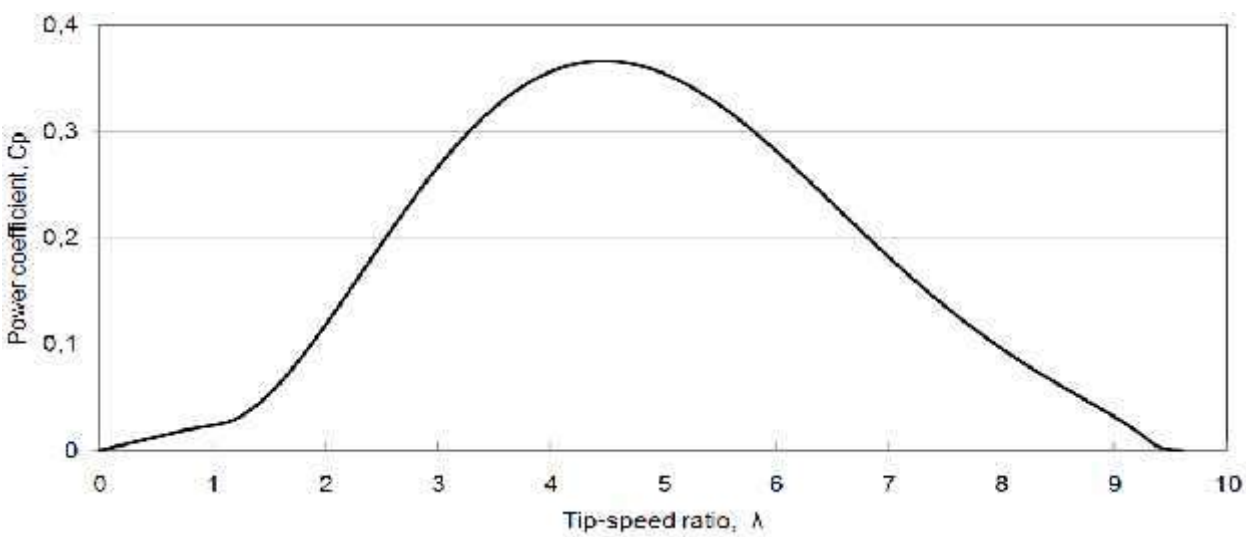

Fig. 3. Power coefficient C_p vs. tip-speed ratio.

Rotors are usually designed so that power coefficient C_p has the maximum values at the-speed ratio in the range from 4 to 8.Since the coefficient C_p is the function of the tip-speed ratio the power

extracted by the wind turbine depends on the wind velocity and the rotational speed. Power curves at different wind velocities for turbines with fixed blade position shown in Fig. 3.

Fig. 4 indicates that the maximal power can be captured from wind turbines only if they are of a variable speed type. This figure illustrates also another feature of variable speed turbines: generator's speed is four times lower at the cut-in wind speed than at the rated velocity. The wind velocity determines the rotational speed of the wind turbine and the generator.

Since it as direct impact on power converter operation modes, an example of wind velocity distribution at 10 meter height is shown in Fig. 5, but the corresponding energy yield in Fig. 6. Three distinct operating modes of the variable speed wind turbine generator can be emphasized: slow speed, rated speed and high speed. Slow speed occurs when the wind velocity lies in the range from 3m/s till 7m/s, rated speed - 7...8m/s and high speed mode is at higher velocities. This division of modes is made according to the normalized energy yield (Fig. 6). The rated speed corresponds to wind velocity with maximum energy distributions are characteristic of Baltic coastal regions and so can be used as reference for interface converter design. The distribution of wind velocity per wind turbine modes is presented in Table I. It shows that the wind turbine is silent one quarter of the time and half of the time works at low speed.

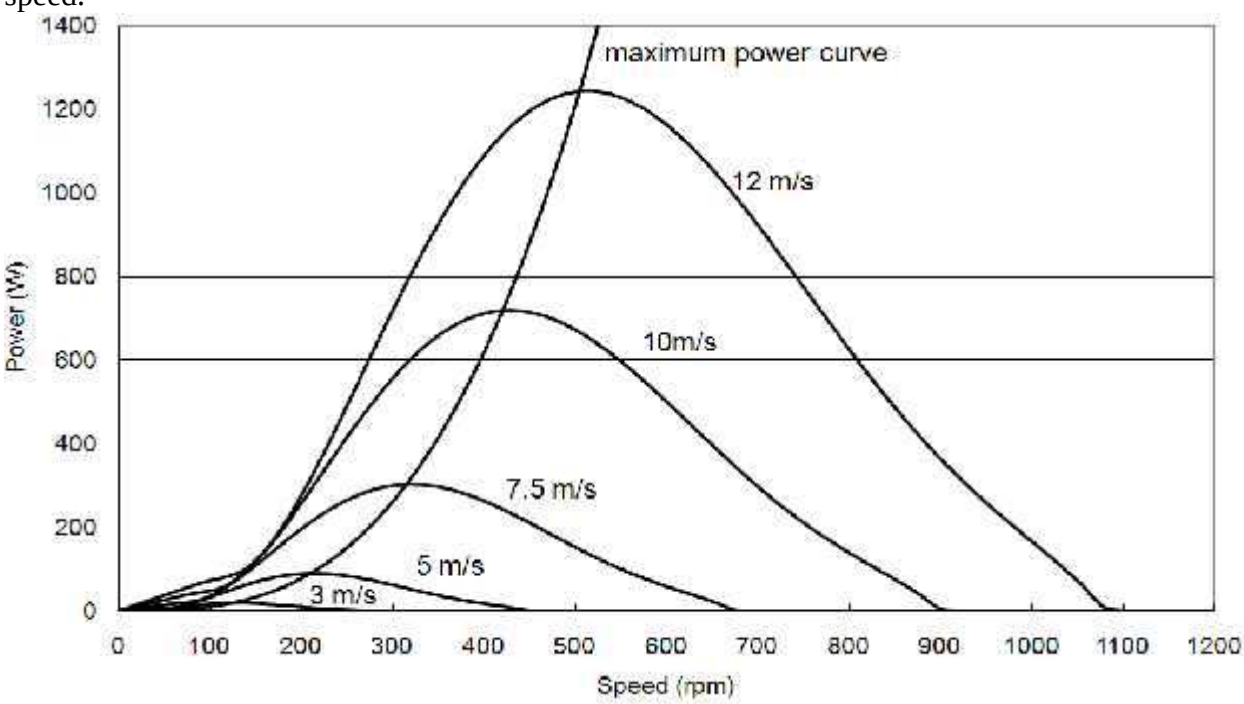

Fig. 4. VSWT power vs. rotation speed of turbine at different wind velocities.

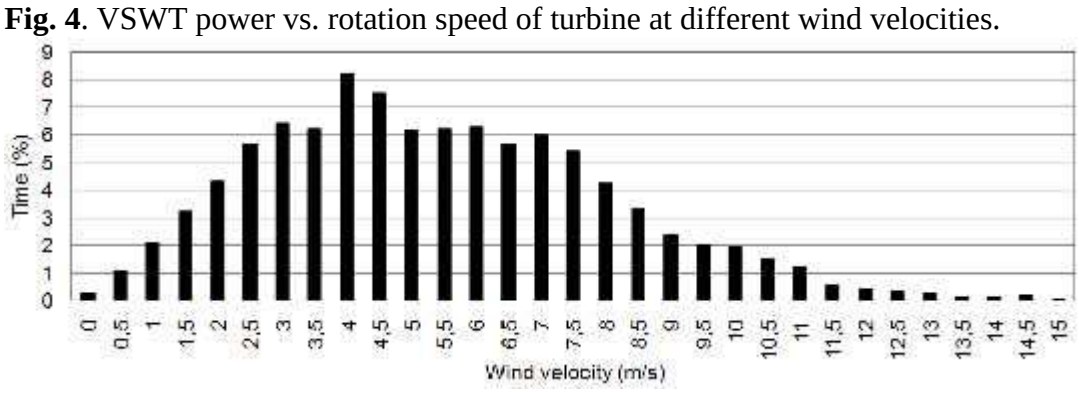

Fig. 5. An example of wind velocity distribution.

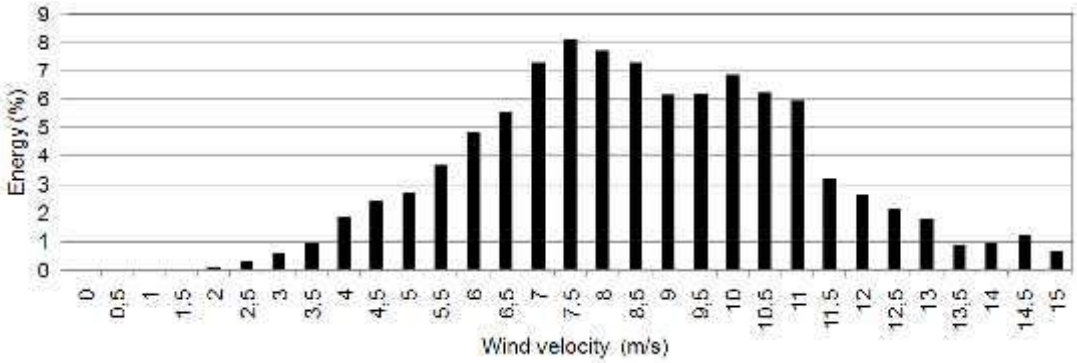

Fig. 6. An example of normalized energy yield.

TABLE I
WIND TURBINE MODES

	No speed	Slow speed	Rated speed	High speed
Wind velocity range	0-3	3.5-6.5	7-8	8.5-25
Time	23%	46%	16%	15%
Energy	0%	22%	24%	54%

NEED OF PERMANENT MAGNET SYNCHRONOUS GENERATOR IN WIND TURBINE GRID SYSTEM

Optimum wind energy extraction is achieved by running the wind turbine generator (WTG) in variable-speed variable- frequency mode. The rotor speed is allowed to vary in sympathy with the wind speed by maintaining the tip speed ratio to the value that maximizes aerodynamic efficiency. In order to achieve this ratio, the permanent-magnet synchronous generator (PMSG) load line should be matched very closely to the maximum power line of the wind turbine generator. In such a case, a good matching exists between the generator and the load for the best performance of the system, as well as the maximum utilization of the wind driven PMSG. However, the recent advancements in power electronics and control strategies have made it possible to regulate the voltage of the PMSG in many different ways. When the generator torque line can be controlled, the generator loading of the turbine can be made to follow the desired locus such as the optimum shaft power locus.

PMSG MODEL

The PMSG dynamic equations are expressed in the " reference" frame. The model of electrical dynamics in terms of voltage and current can be given by the following equations

$$v_q = -(R + pL_q)i_q - \omega_r L_d i_d + \omega_r \lambda_m$$
$$v_d = -(R + pL_d)i_d + \omega_r L_q i_q \qquad \text{.....(4)}$$

where R and L are the machine resistance and inductance per phase, and are the two-axis machine voltages, and i_d and $i_q$are the two-axis machine currents. λ_m is the amplitude of the flux linkages established by the permanent magnet, and $p = d/dt$

The above equations are derived assuming that the q -axis is aligned with the stator terminal voltage phasor (i.e.v_d=0,). The expression for the electromagnetic (EM) torque in the rotor is written as

$$T_e = \left(\frac{3}{2}\right)\left(\frac{P}{2}\right)\left[(L_d - L_q)i_q i_d - \lambda_m i_q\right] \quad \text{.....(5)}$$

Where P is the number of poles of the PMSG, and T_e is the electrical torque from the generator.

The relationship between the angular frequency of the stator voltage and the mechanical angular velocity of the rotor may be expressed as

$$\omega_r = \frac{P}{2}\omega_m. \quad \text{.....(6)}$$

PMSG BASED WIND TURBINE.

PMSG based VSWTs have three distinct operation modes: silent mode, variable speed operation mode and constant speed mode. A turbine is silent in two cases: wind speed is below a cut-in level or above the cut-off speed. If the speed is below its cut-in level it produces insufficient torque to move the turbine. At the same time winds above the cut-off level may damage the turbine that must be stopped at such conditions. A turbine usually starts to operate at 3 m/s and it should be stopped at the wind speed above 25 m/s.Turbines operate at variable speed in the wind velocity range from cut-in to rated wind speed. Rated wind speed differs by turbine types, but often has the value of 12 meters per second. Constant speed mode takes palace above the rated wind speed. Turbine output power remains constant at this mode (Fig. 7).PMSGs with 8 pole pairs are considered as a power source in this research. Its line voltage is 140V at 375 rpm, but it can operate up to 510 rpm. This speed is considered as the maximum power operational point for the turbine and the generator. Generator power reaches 1250W at this point, but the output voltage is 183V.

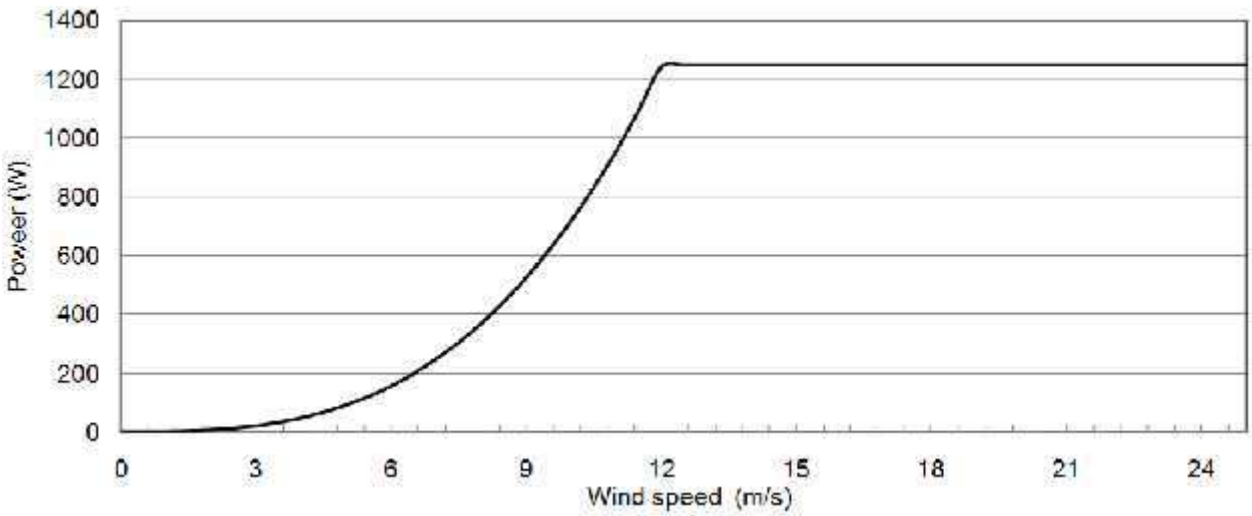

Fig. **7**. Output power of VSWT.

Cut-in speed for a turbine is 125 rpm and it can produce 20W, but the generator voltage is only 48V at this point. So this is the lowest input voltage for a converter. Generator speed and voltage characteristics are shown in Fig. 7.

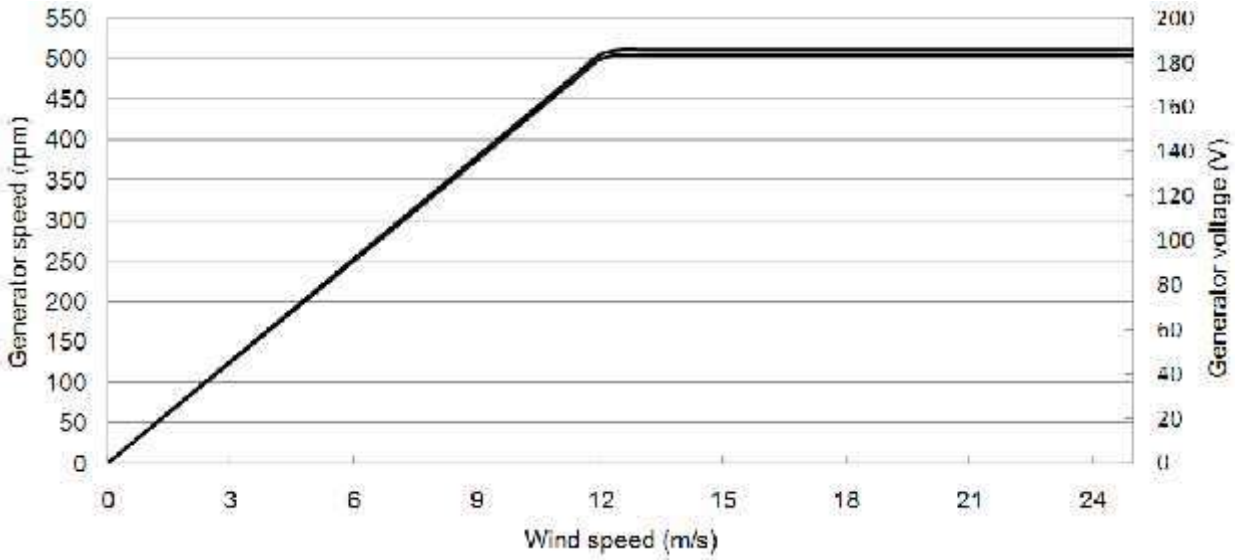

Fig. 8. Generator speed and voltage vs. wind speed.

TOPOLOGIES OF INTERFACE CONVERTERS FOR PMSG BASED VSWT

Interface converter for a PMSG based VSWT can have different topologies. Topologies with HF isolation for VSWT application already known are studied in this section to evaluate their pros and cons in the context of the described PMSG utilization in such systems and a new interface converter topology with qZS DC/DC converter based HF isolation is offered.

3.1.1 TRADITIONAL TOPOLOGIES.

There are only few converter topologies with high frequency isolation for small wind applications studied in the literature. In old technologies proposed a buck type isolated DC/DC converter (Fig. 9a). Variable generator voltage is rectified with a three-phase diode bridge firstly into proportional DC voltage. Stabilization of the second DC link voltage is obtained with the buck type isolated DC/DC converter by means of duty cycle variation. The main drawback of this solution is high currents in the transformer's primary winding at rated wind speeds that will reduce converter efficiency at this operating point. In the second concept of inverter topologies have proposed a one-phase soft-switched dual LCL DC/AC converter (Fig. 9b). This converter utilizes a controlled rectifier for generator voltage rectification and DC link voltage stabilization. The soft-switched dual LCL DC/AC converter needs stable DC link voltage, so generator voltage should be boost up to its maximum voltage amplitude value in the whole input voltage range that will reduce the efficiency of the controlled rectifier at low generator speed.

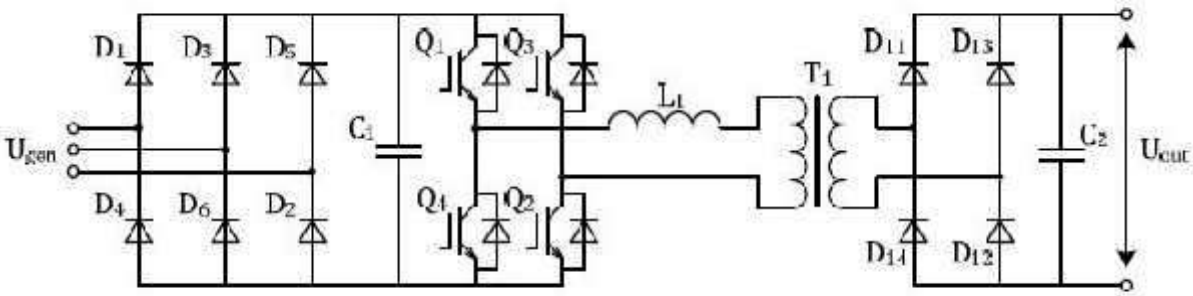

(a)

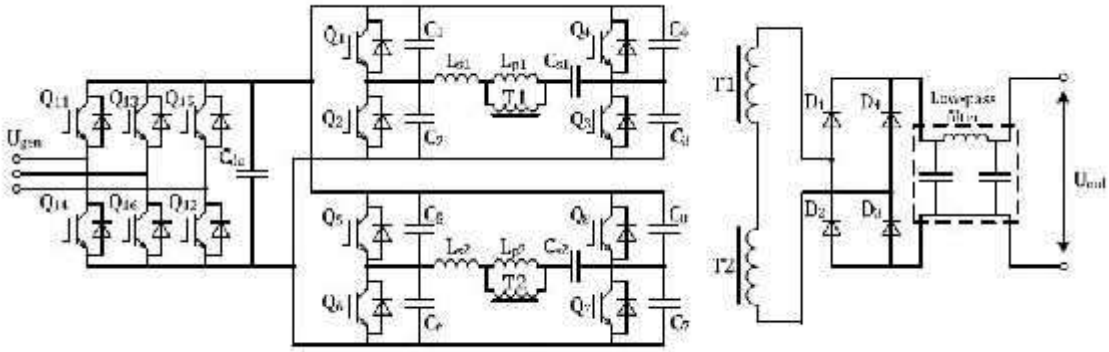

(b)

Fig. 9. Interfacing converter topologies: a) with a buck type isolated DC/DC converter, b) one-phase LCL DC/AC converter

NEW PROPOSED TOPOLOGY

To improve the efficiency of the PMSG based VSWT system a new converter topology is introduced, presented in Fig. 10. It consists of a three-phase full bridge controlled rectifier (generator side inverter) with PFC functionality and a quasi-Z-source (qZS) DC/DC converter with an HF transformer for galvanic isolation. Grid side inverters with Output filters are not discussed here.

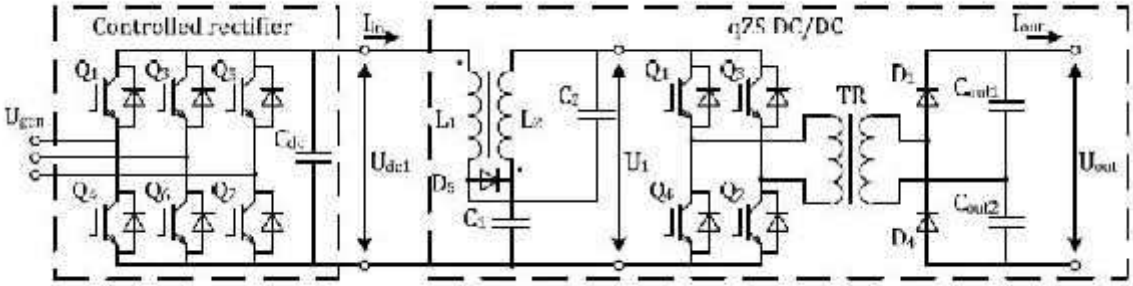

Fig 10. proposed interface converter with qZS DC/DC.

A PFC inverter converts the variable voltage with variable frequency Ugen from the PMSG into a stabilized DC voltage U_{dc1}. The qZS DC/DC converter offers galvanic isolation and voltage level adjustment by means of the transformation coefficient. The unique qZS impedance network and appropriate control offer an additional voltage regulation capability at high efficiency. Stabilized DC link voltage Uout can be inverted into the grid current by an appropriate inverter.

QZS BASED STEP-UP DC/DC CONVERTER WITH HF ISOLATION

The central idea implemented in the proposed converter is to keep the intermediate DC link voltage (U_{DC}) constant despite the variation of the generator side DC link voltage U_{DC1}. By keeping the U_{DC} constant the inverter could be operated with a fixed duty cycle, thus ensuring constant volt-second and flux swing of the isolation transformer.

The main advantage of the implemented quasi-Z-source (qZS) based step-up DC/DC converter is that it can boost the input voltage during special shoot-through op erating states of the inverter. During the shoot-through states the primary winding of the isolation transformer is shorted through all switches of both phase legs of the inverter (Fig. 11*a*). The passive qZS-network makes the shoot-through states possible, effectively protecting the circuit from damage. Moreover, the shoot-through states are used to boost the magnetic energy stored in the inductors L_1 and L_2 without short-circuiting capacitors C_2 and C_3. This increase in the magnetic energy in turn provides the boost of voltage seen on the inverter output during the active states of the inverter (Figs. 11*b* and 11*c*). Thus, by adjusting the shoot-through duty cycle *DS* of the inverter twitches $T_7 \ldots T_{10}$ the U_{DC} could be pre regulated to the desired 250 V despite the variation of U_{DC1} with different wind speeds from 150 V to 250 V (Fig.12).After the preregulation of U_{DC} the isolation transformer TR is being supplied from the inverter with a voltage of constant amplitude (250 V) and duty cycle (*DA*=0.4).

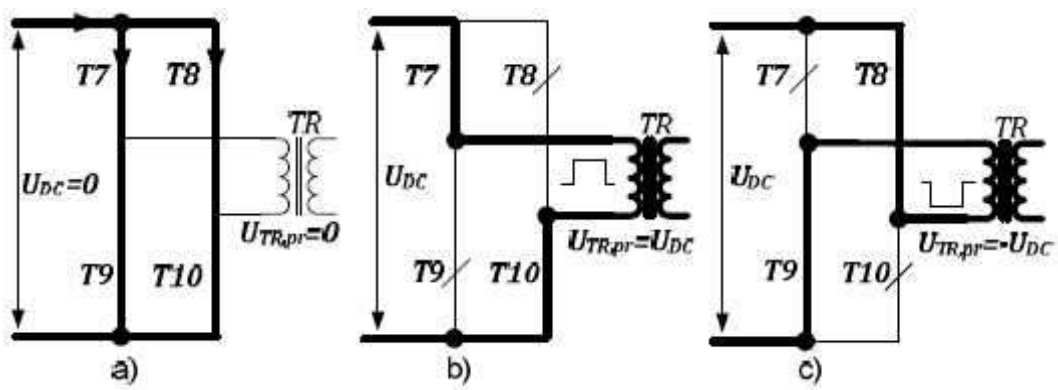

Fig 11. Inverter equivalent scheme during the shoot-through state (a) and during active states: positive (b) and negative (c) half-cycles.

To reduce the turns ratio of the isolation transformer a voltage doubler rectifier (VDR) was implemented on the secondary side of the converter. In contrast to the traditional full-bridge rectifier, two diodes of one leg in the VDR topology were replaced by the capacitors. The operation principle of the VDR is explained in Figs.12. During the positive half cycle, the capacitor C_4 is charged through the diode D_2 to the peak secondary voltage of the isolation transformer (Fig. 12*a*). During the negative half cycle the capacitor C_5 is charged through diode *D3* (Fig. 12*b*). At every time instant the output voltage (U_{DC2})

from this circuit will be the sum of the two capacitor voltages ,or twice the peak voltage ($U_{TR,sec}$) of the secondary winding of the isolation transformer.

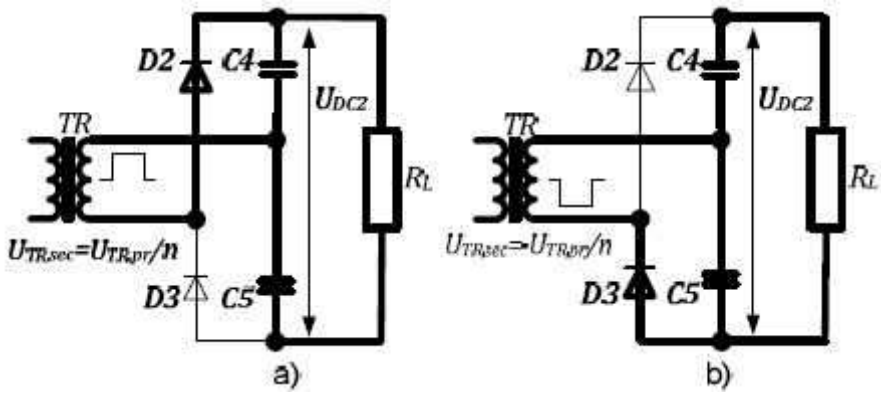

Fig 12. Operation principle of VDR: positive (a) and negative (b) half cycles.

OPERATING MODES OF NEW INTERFACING CONVERTER

This research attempts to prove the ability of the proposed topology to ensure stable grid side DC link voltage U_{out}. For this reason only the operating studied in more detail. The power circuit of the qZS based DC/DC converter is shown in Fig. 10, but operation modes in Fig. 13.

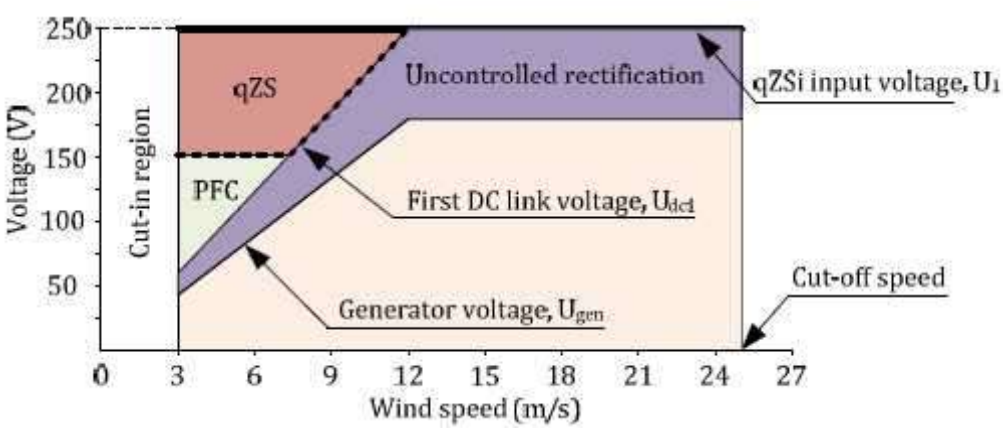

Fig 13.operating modes of converter

The voltage boost necessary is obtained by two steps. The PFC rectifier stabilizes the first DC link voltage U_{dc1} to a 150V level when the generator voltage is below 112V

The controlled rectifier works as a usual rectifier when the generator voltage U_{gen} is above 112V. In this mode the DC link voltage is changed proportionally to the generator voltage, at the range from 150V in rated speed conditions up to 250V at the maximal speed.

The qZS based HF isolation converter is stabilizing the HF inverter input voltage U_1 to 250V despite the voltage variations on the first DC link. The stabilized input voltage U_1 ensures inverter operation with the fixed duty cycle, thus ensuring constant volt second balance of the isolation transformer. The input voltage U_1 regulation is obtained by changing the shoot-through duty cycle

PERMANENT MAGNET SYNCHRONOUS MACHINE

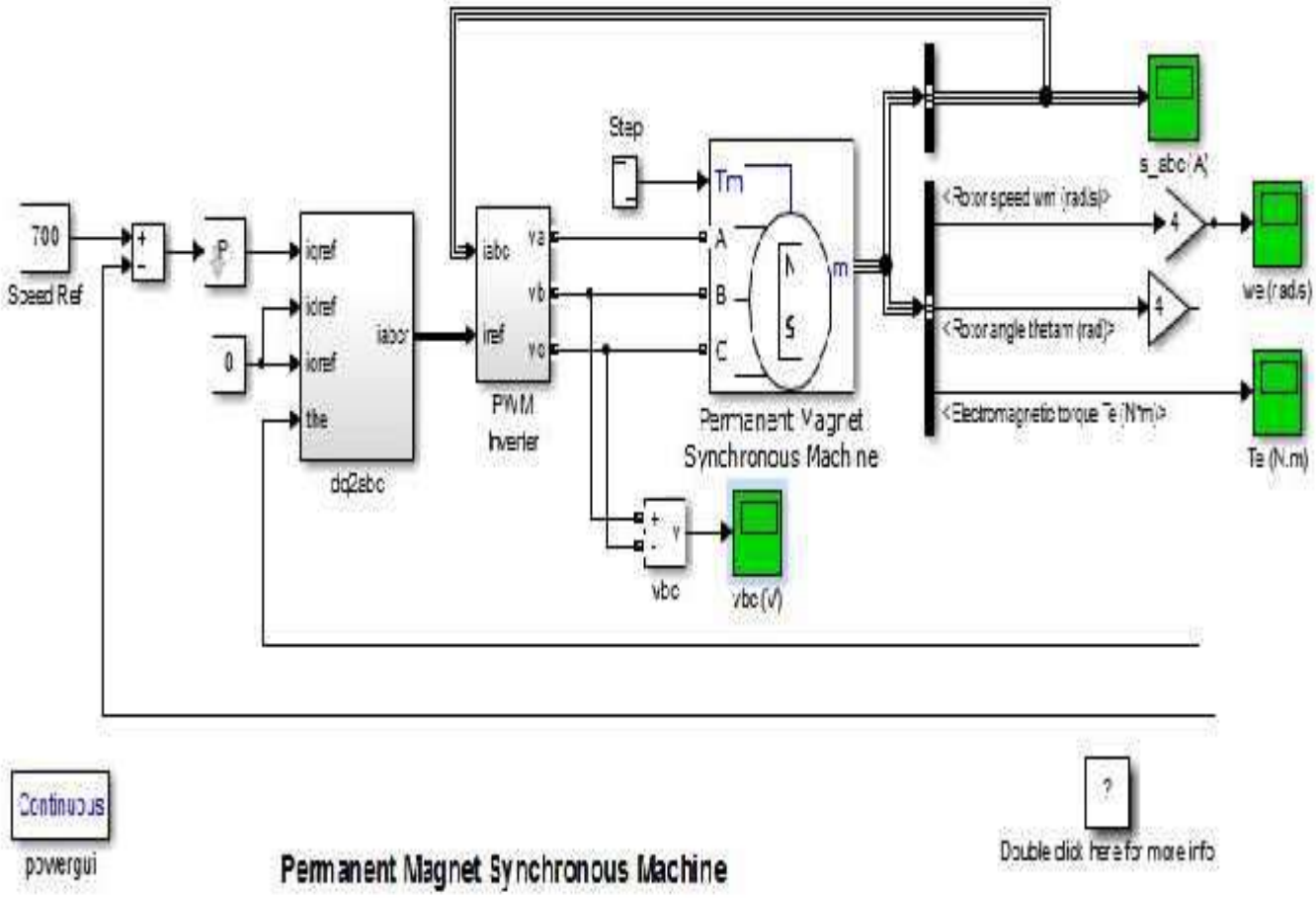

OUTPUT:

(1) is_abc(A)

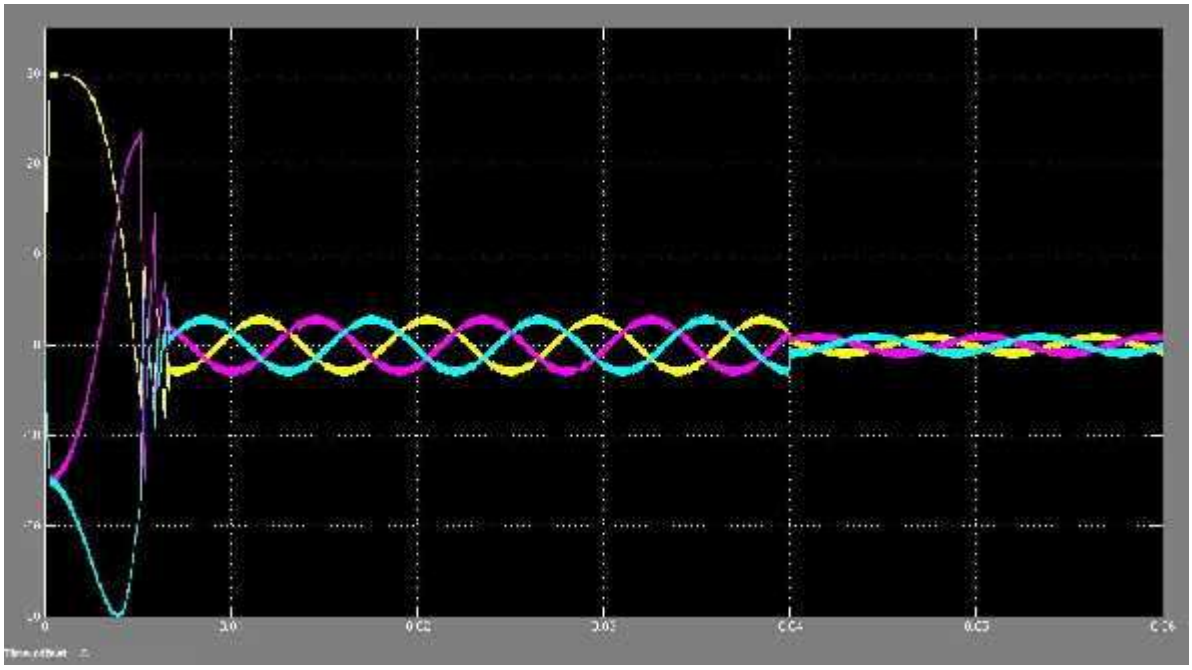

(2) we(rad/s)

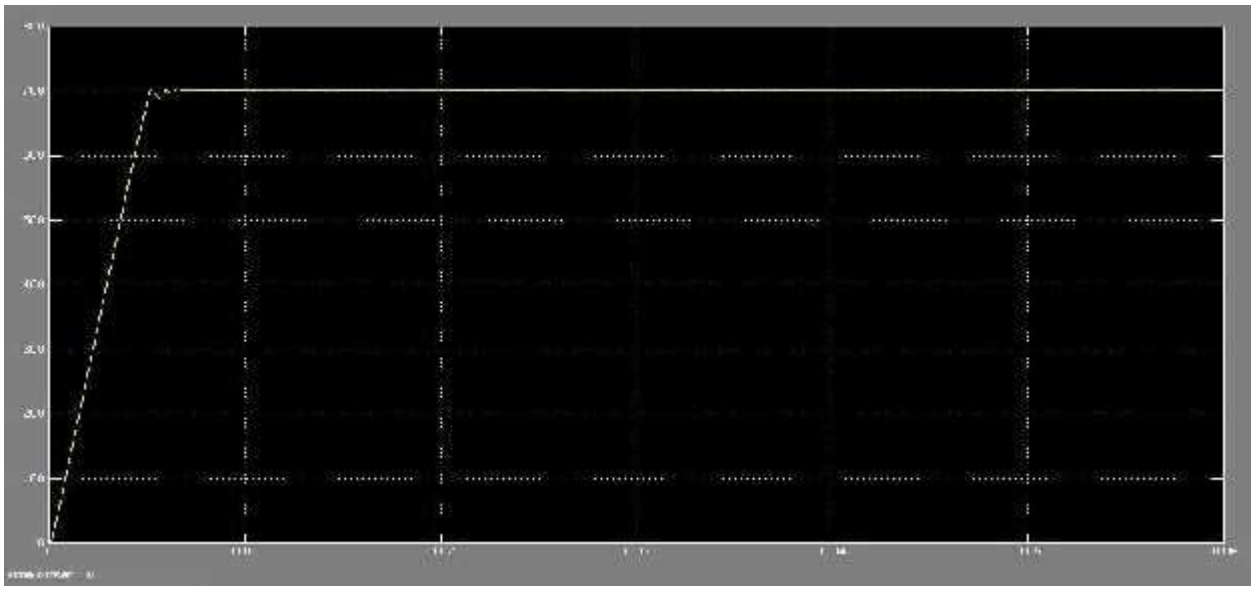

(3)Te(Nm)

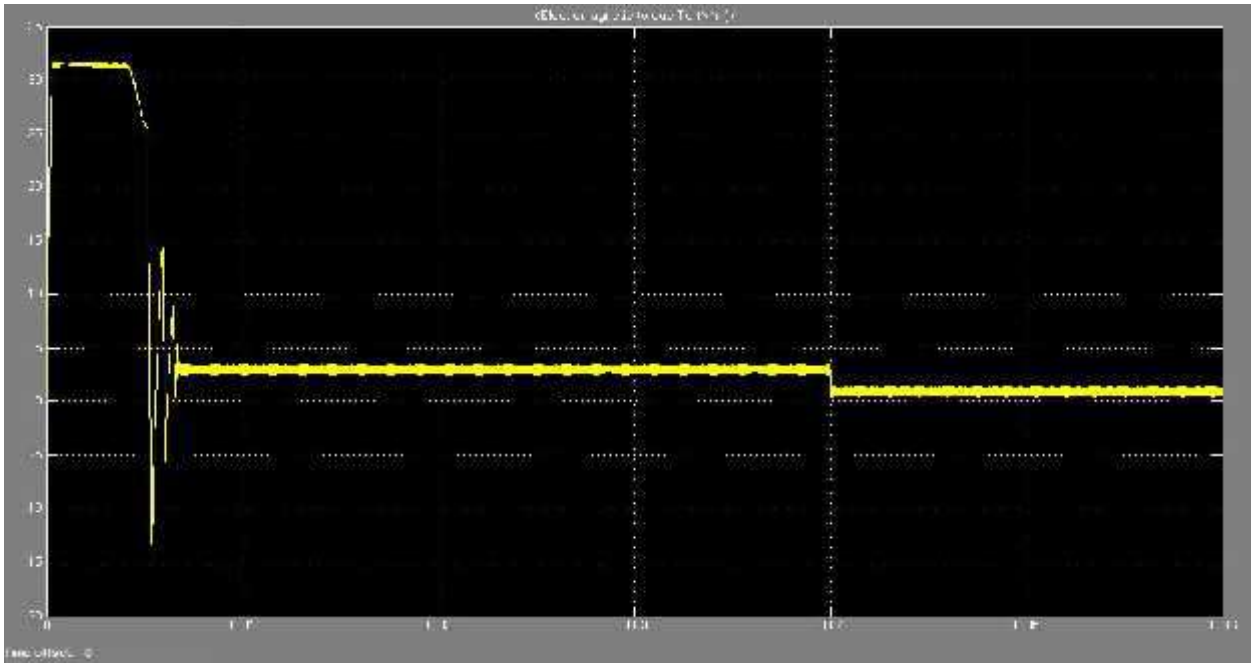

RESULT:

EXPNO:8 **DATE:**

COMPUTATION OF HARMONIC INDICES GENERATED BY A RECTIFIER FEEDING A R-L LOAD

AIM:

To perform the harmonic analysis of single phase full bridge converter with R-L load using Matlab (Simulink).

SOFTWARE REQUIRED:

Power system module of MATLAB

THEORY

HARMONICS:

There are certain loads on the system that produce harmonic currents. These currents result in distorted voltages and currents that can adversely impact the system performance in different ways. Generally this load is called as non linear load. The current wave shape on a non-linear load is not the same as the voltage as shown in fig2.

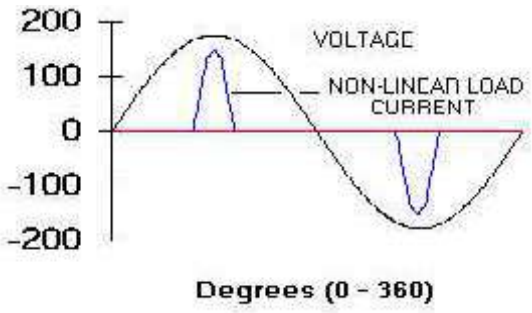

Fig 1:-Voltage and Current waveforms for non-linear loads

Typical examples of non-linear loads include rectifiers (power supplies, UPS units, discharge lighting), adjustable speed motor drives, ferromagnetic devices, DC motor drives and arcing equipment. The current drawn by non-linear loads is not sinusoidal but it is periodic, meaning that the current wave looks the same from cycle to cycle. Periodic waveforms can be described mathematically as a series of sinusoidal waveforms that have been summed together as shown in fig 3.

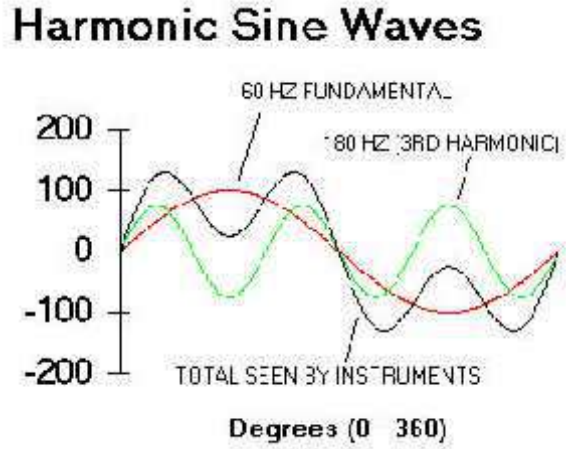

Fig 2:-Waveform with symmetrical harmonic components

The sinusoidal components are integer multiples of the fundamental where the fundamental. The only way to measure a voltage or current that contains harmonics is to use true-RMS reading meter. If an averaging meter is used, which is the most common type, the error can be significant.

HARMONIC ANALYSIS:

Harmonic analysis is the branch of mathematics that studies the representation of functions or signals as the superposition of basic waves. It investigates and generalizes the notions of Fourier series and Fourier transforms. The basic waves are called "harmonics", hence the name "harmonic analysis".

RECTIFIER:

DEFINITION: Converting AC (from mains or other AC source) to DC power by using power diodes or by controlling the firing angles of thyristors /controllable switches.

BASIC BLOCK DIAGRAM:

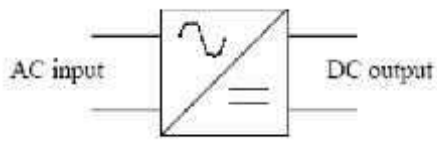

•Input can be single or multi-phase (e.g. 3-phase).

•Output can be made fixed or variable.

EXERCISE:

A single phase AC source of 230V, 50Hz supplying to a RL branch through a full bridge converter connected using IGBT. The pulse trigger given to the IGBT is of amplitude 2 for a period 0.02 seconds with a period of 50% period. Deign a harmonic filter for 2 cycles and obtain the necessary wave form.

ALGORITHM:

Step1: Start.
Step2: Obtain various blocks from simulink library and construct the block diagram of the converter.
Step3: Perform FFT analysis for the above.

Step4: Extract the harmonics.
Step5: Stop.

FLOW CHART:

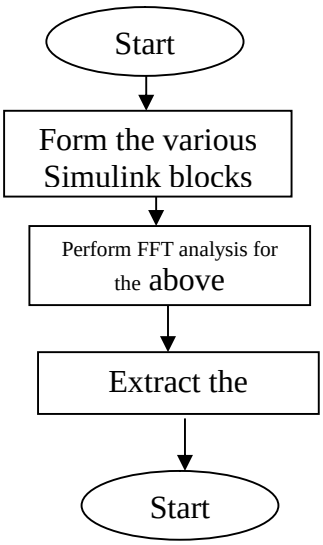

Simulation diagram for THD voltage:

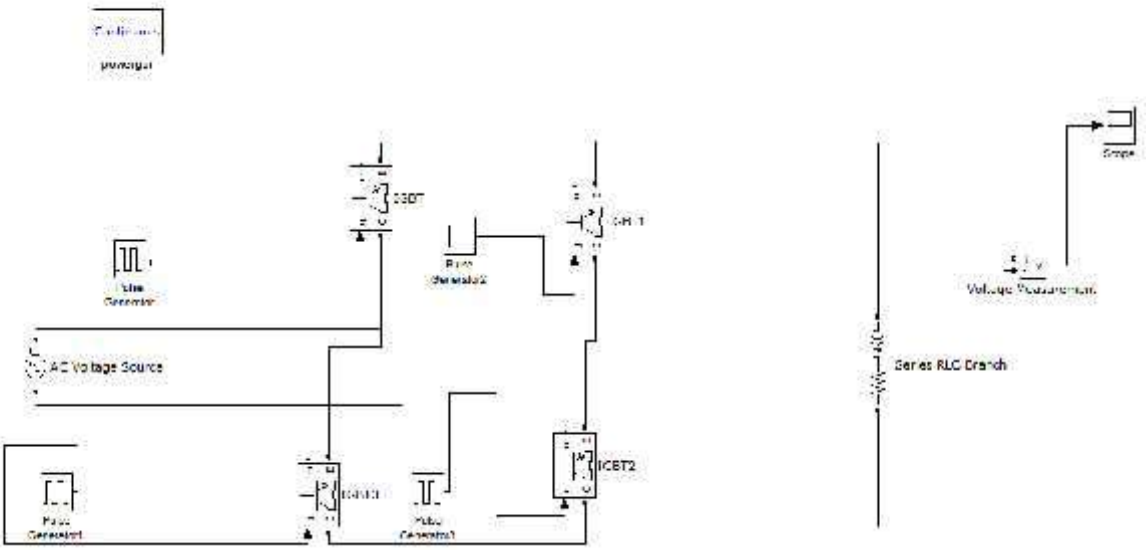

OUTPUT:

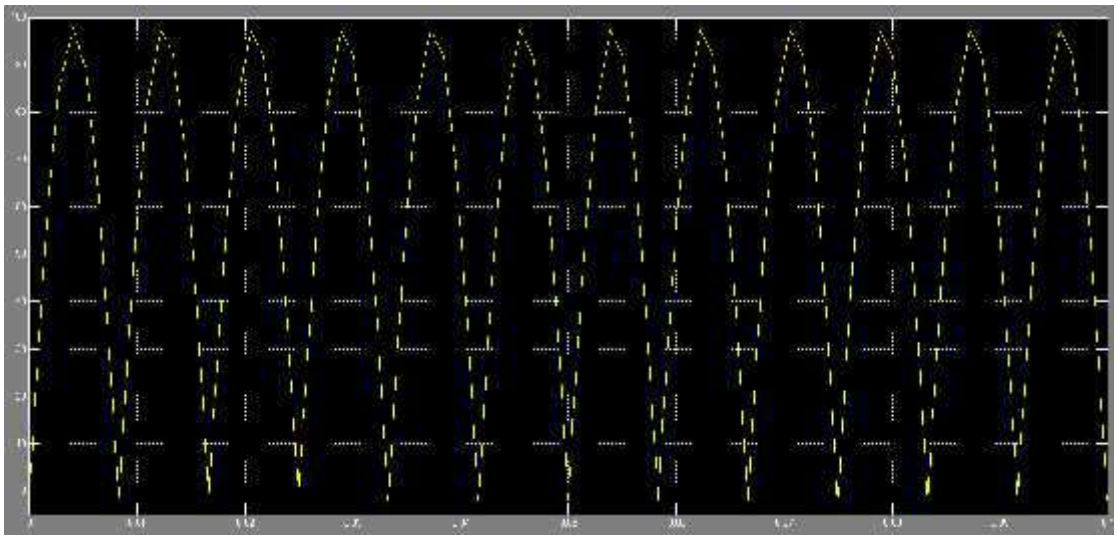

FFT Analysis:

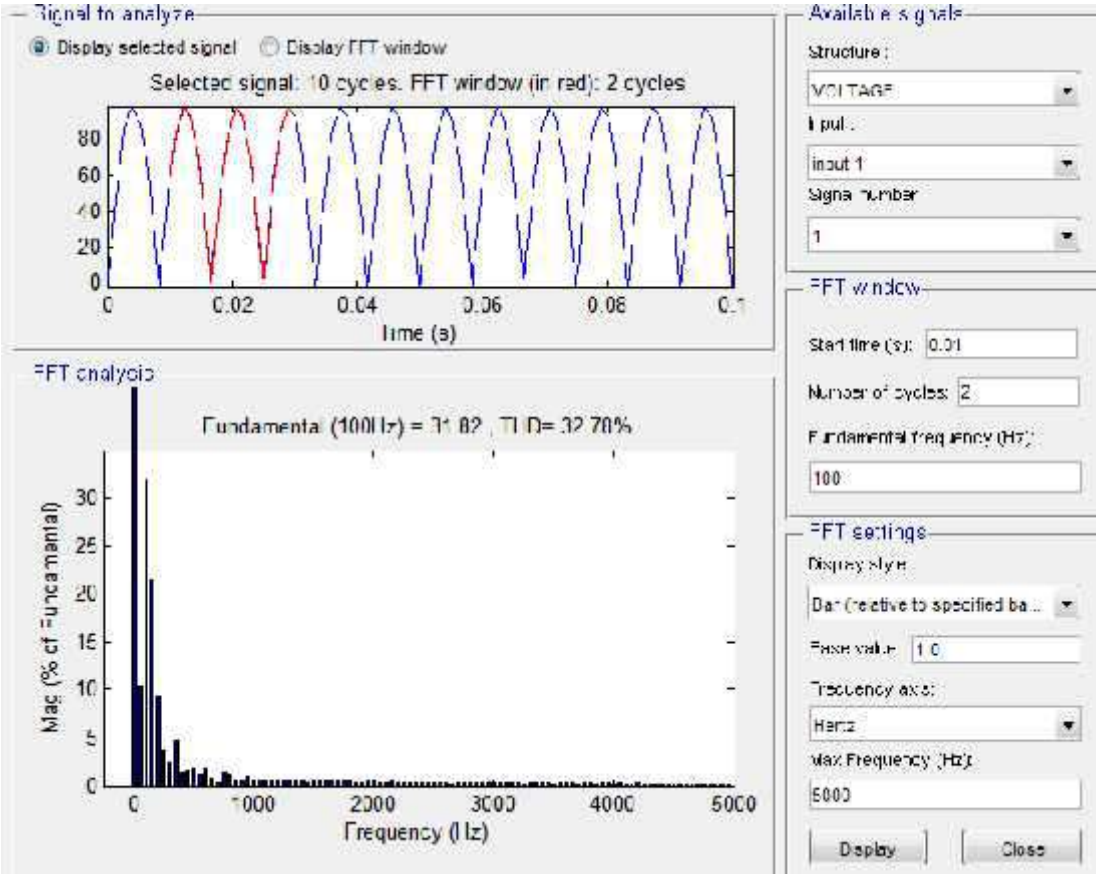

RESULT:

Hence the harmonic analysis of a single phase full bridge converter using a RL branch is simulated and its 3rd and 5th harmonics are extrated.

EX.NO:9 **DATE:**

DESIGN OF ACTIVE FILTER FOR MITIGATING HARMONICS

AIM:

To Design the active filter to improve power quality by mitigation harmonics

THEORY:

As the development of modern power electronics technology and the wider application of various nonlinear devices, the current distortion makes increasingly serious pollution to the grid. Therefore, harmonic current compensation has been drawn great attention.Active power filter is a new type of power electronic device using for dynamic suppressing harmonics and compensating reactive power. It can compensate harmonics with varying amplitude and frequency, and can overcome the shortage of passive filter effectively. It is a harmonics suppression device with prospect .

In 1980's, with the self turn-off power semiconductor appeared, PWM control technology and the instantaneous reactive power theory for three-phase system put into use, study on active power filter become fast.Because of extensive use for three-phase four-wire in power system, such as industry, official and business, many people pay more attention to the trouble which is caused by harmonics and unbalance of three-phase. Therefore, it is important to compensate harmonics and reactive power in three-phase four-wire system This paper introduces a shunt active power filter for three-phase four-wire system. It presents the principles and structure. And the design and performance of a 3KW experimental prototype is proposed.

PRINCIPLE AND STRUCTURE:

The structure of a shunt active power filter used for three-phase four-wire is shown in Fig. 1. In this system, the load may product harmonics and unbalance current in three-phase, and current is flown in neutral wire.

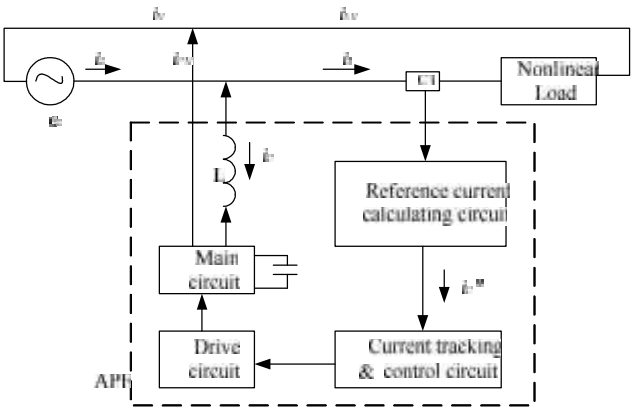

Fig. 1: The structure of active power filter for three-phase four-wire system

The shunt active power filter is a voltage source inverter controlled as a current source by means of pulse width modulation signals. As it can be seen in Fig. 1, the filter is connected in paralleled with the nonlinear load. Harmonic current compensation is achieved by injecting equal but opposite

harmonic current components at the point of connection, therefore canceling the original distortion and improving the power quality . In most cases, the load also needs reactive power, which can also be generated by the same current source. In three-phase unbalanced and nonlinear loads, it is also possible to redistribute power and to keep the system balance. The active power filter is composed of the reference current calculating circuit, current tracking circuit, driving circuit and the main circuit. While, the generation circuit of compensating current is composed of the last three parts Three-phase four-wire system is different from three-phase three-wire system because of the neutral wire. Thus, handling zero-sequence components of three-phase current is the key point. Reference current calculating circuit should product the reference current correctly and fast in three-phase four-wire system. That means it should detect the harmonics, fundamental negative-sequence current components and zero-sequence current components of the compensating . The generation circuit of compensating current should product compensating current correctly according to the reference current signals.

Because the sum of three-phase current is not zero in three-phase four-wire system, the detection method based on instantaneous reactive power theory should be modified. The way is to calculate the zero-sequence current components, then subtract them from three-phase current. Finally three-phase current without zero-sequence components can be detected by the method based on instantaneous reactive power theory. The compensating current signals of the neutral wire can be also calculated by turning the polarity of the neutral wire current over . The principle of reference current calculating circuit is shown in Fig. 2. In which, i_a, i_b, i_c are load currents. The zero-sequence component of three-phase current i_n is calculated as:

$$i_n = \frac{1}{3}(i_a + i_b + i_c) \qquad (1)$$

Then zero-sequence components can be subtracted from three-phase current:

$$\begin{aligned} i_a^{'} &= i_a - i_n \\ i_b^{'} &= i_b - i_n \\ i_c^{'} &= i_c - i_n \end{aligned} \qquad (2)$$

Eventually the three-phase currents without zero-sequence component $i_a^{'}, i_b^{'}, i_c^{'}$ will comply with:

$$i_a^{'} + i_b^{'} + i_c^{'} = 0 \qquad (3)$$

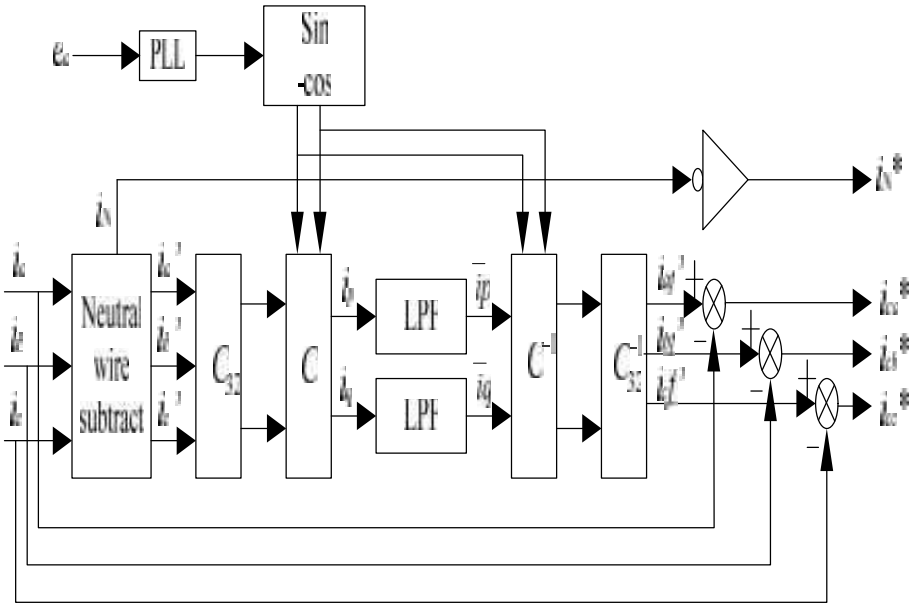

Fig. 2: The principle diagram of reference current calculating circuit

Afterward, as shown in Fig. 2, the three-phase currents without zero-sequence components $i_a^{'}, i_b^{'}, i_c^{'}$ are coordinately transformed and achieve corresponding active power current component i_p and reactive power current component i_q, then it can acquire dc component $\overline{i_p}, \overline{i_q}$ through the low pass filters. Fundamental positive-sequence components $i_{af}^{'}, i_{bf}^{'}, i_{cf}^{'}$ can be calculated by inverse coordinate transformation. When the positive-sequence components are subtracted from load current i_a,i_b,i_c, there will be reference current i_{ca}^{*},i_{cb}^{*},i_{cc}^{*}. After the compensating currents generated by the reference signals offset the harmonics, the currents flowing into source which are equal to fundamental positive-sequence components are sinusoid and balanced

DESIGN OF SHUNT ACTIVE POWER FILTER

Active power filter is an advanced power electronic device, which can be used for integrated compensating harmonics, reactive currents and negative-sequence currents. Because of the characteristics of real time and accurate compensation, it is possible to take full advantage of digital signal processing and many other technologies. If so, the performance of active power filters can be improved significantly.

Control circuit

The control circuit consists of current control and voltage control. The principle is shown in Fig. 3. The current controller uses the current error between reference current i_c^{*} and compensating current i_c filtered by a proportional-integral regulator as the modulating signal. The current control circuit uses a tracking PWM current control and timing comparing. The comparator is judged at each clock-cycle, so the PWM control signals change once at least one clock cycle. The clock-cycle limits the highest frequency of switching devices in the main circuit, thus damages to the devices due to over-high switching frequency may be avoided. The shortcoming of this control method is that the tracking error of compensating current is unfixed .

For voltage control, it mainly means controlling of DC-link voltage. There are two control techniques: PI control and fuzzy control. PI control is similar to the current control, but there is some difference. When the supply voltage is unbalanced or distorted, the input of the voltage controller is not the actual supply voltage but a unitary sinusoidal waveform in phase with the supply voltage . Therefore, the active power filter will have good performance even under the condition of unbalanced or distorted source voltage. In other words, PI control uses the voltage error between DC-link voltage and its reference filtered by a proportional-integral regulator multiplied by the unitary sinusoidal waveform in phase with the supply voltage to obtain the reference current.

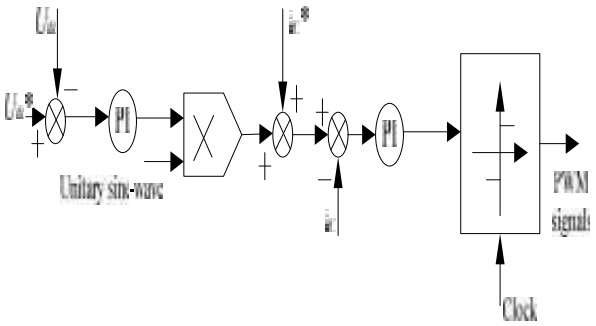

fig. 3: The principle diagram of control circuit

Fuzzy control can be also applied to DC-link voltage control. The input of the controller is the error voltage and its incremental variation. And the output is the incremental variation of the amplitude of the active current injected into active power filter. Compared with PI control, fuzzy control has better dynamic response and can keep the DC-link voltage stability well. However, fuzzy control makes the controller complicated. This paper adopts PI control as control method.

Main circuit

In three-phase four-wire system, active power filter not only compensates the harmonics of three-phase current, but also suppresses the current of neutral wire to get rid of the neutral wire current of the source. There are many methods to suppress the neutral current. Generally, four-leg converter and three-leg converter are commonly used . The structures of their main circuit are shown respectively in Fig. 4 and Fig. 5.For four-leg structure, to compensate the neutral current is provided through the forth leg which products the compensating current of the neutral wire, which offset the neutral current of the source side. The compensating principle of this method is easy, but it makes the circuit more complicated and the cost is high. In this paper, the main circuit uses three-leg converter. Through reference current calculating circuit, it can acquire reference current signals of compensating three-phase currents and the neutral current. The compensating current of three-phase currents is equal to the sum of harmonics, fundamental negative-sequence and zero-sequence components in load current which offsets the load current. So the supply current flowing into the source which is equal to the fundamental positive-sequence components becomes sinusoidal and balanced. For three-leg structure, to keep the DC-link voltage balance is to control the neutral current to be zero . From the point of active power filter, the sum of harmonics and fundamental negative-sequence components of three-phase current without zero-sequence components is aero. The sum of zero-sequence components of three-phase current is equal to the compensating neutral current which is regulated through DC-link control.

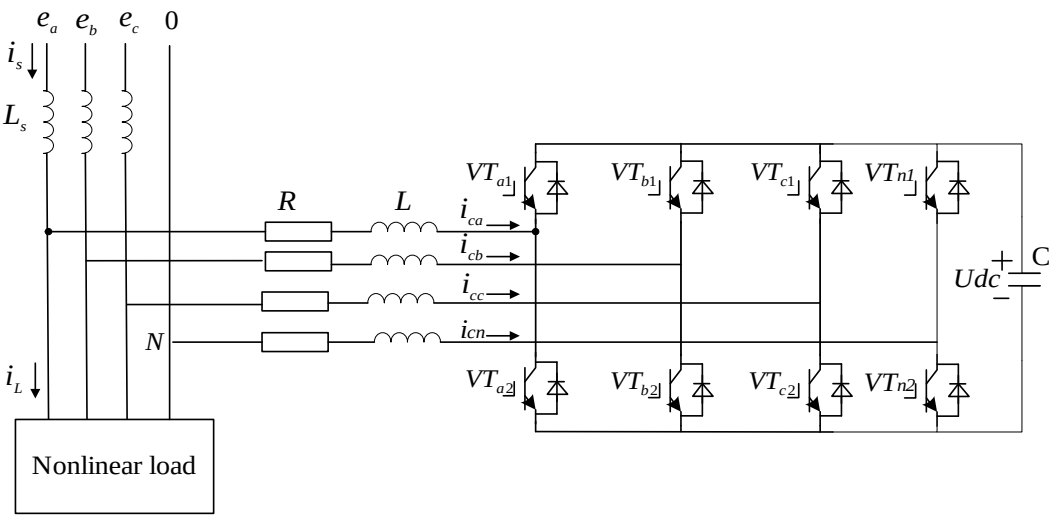

Fig. 4: The four-leg structure of main circuit

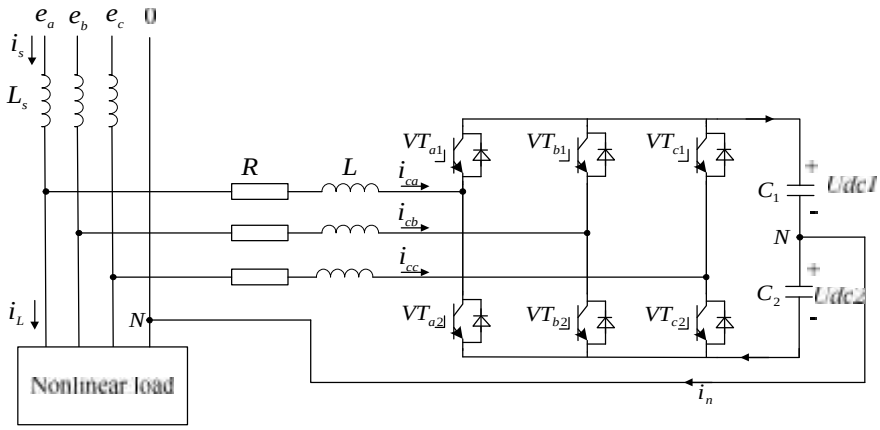

Fig. 5: The three-leg structure of main circuit

After compensation of active power filter, the three-phase supply current will be sinusoidal and balanced, the neutral current of the source will be zero.

A 3kW shunt three-phase four-wire active power filter experimental prototype is constructed. Firstly, the minimum DC-link voltage U_c should be greater than the value three times of AC phase peak voltage E_m. If DC-link voltage is too small, compensation current can not track instruction current as requests, and the compensation effect will be unsatisfied. On this basis, the greater Uc is, the faster i_c changes, the higher voltage the devices should endure . Secondly, the smaller inductance L is, the faster i_c changes. Thirdly, the longer current controlling cycle t_c is, the greater ripple current tracking error has. The value of t_c also determines the highest time of harmonic which the active power filter can compensate and the frequency demands for switching devices.

The work process of active power filter is also the process of capacitor charging and discharging. The fluctuation of DC-link voltage can be explained by the changes of the stored charges volume, and the volume can be obtained from the integral of current to time. According to the parameters design method for capacitance in and , the capacitor C under ideal condition can be calculated by equation (4) ,where C is capacitor value; Q is the electric charges stored on capacitor; u is reference capacitor

voltage; Q_1 is the maximal charge, $\Delta u \backslash u$ is the maximal voltage fluctuation; i_a^* is compensating current of phase a; i is fundamental active current; I_d is load current.

$$\begin{cases} C = \dfrac{Q}{u} \\ Q = Q_1 * \dfrac{u}{\Delta u} \\ Q_1 = \dfrac{1}{\mu} \displaystyle\int_{®/3}^{2®/3} i_a^* d\mu t \\ i = \dfrac{3\sqrt{6}}{®^2} i_d \\ i_a^* = i_d - \sqrt{2} * i \sin(\mu t + ® / 6) \end{cases}$$

C. Driving circuit

IGBT is used as switching device in this system. The IGBT driving circuit uses the driving block M57962L produced by MITSUBISHI company in Japan. This drive block is a mix integrated circuit. Because of gathering the drive and over-current protecting circuit, it can satisfy the needs perfectly.

EXPERIMENT RESULTS

According to the design described above, a 3 KW experimental prototype of shunt active power filter for three-phase four-wire system is developed. The experiment results are given in Fig. 6 and Fig. 7. The nonlinear load is composed of the inductance three-phase transistor rectifier bridge. Fig. 6 is the waveform of the supply current before using the active power filter. It is three-phase unbalanced and distorted current source. Fig. 7 is the waveform of the supply current after compensation, and it is three-phase balanced and sinusoidal current. This indicates that the proposed active power filter has a good performance and the design method is basically correct.

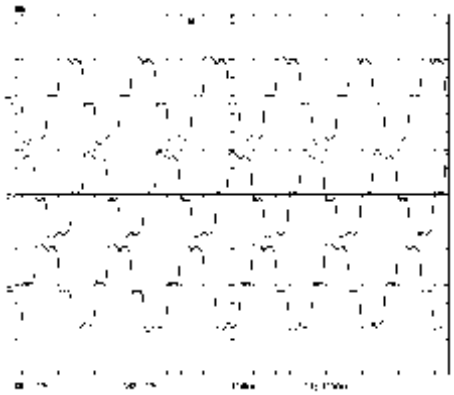

Fig. 6: Three-phase currents before compensation

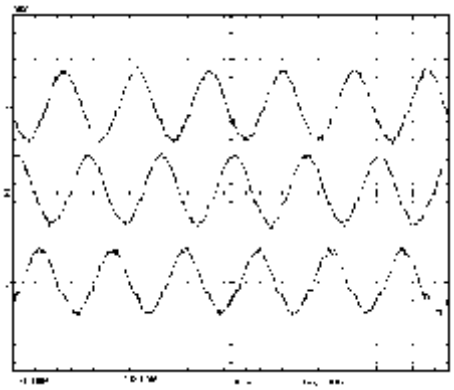

Fig. 7: Three-phase currents after compensation

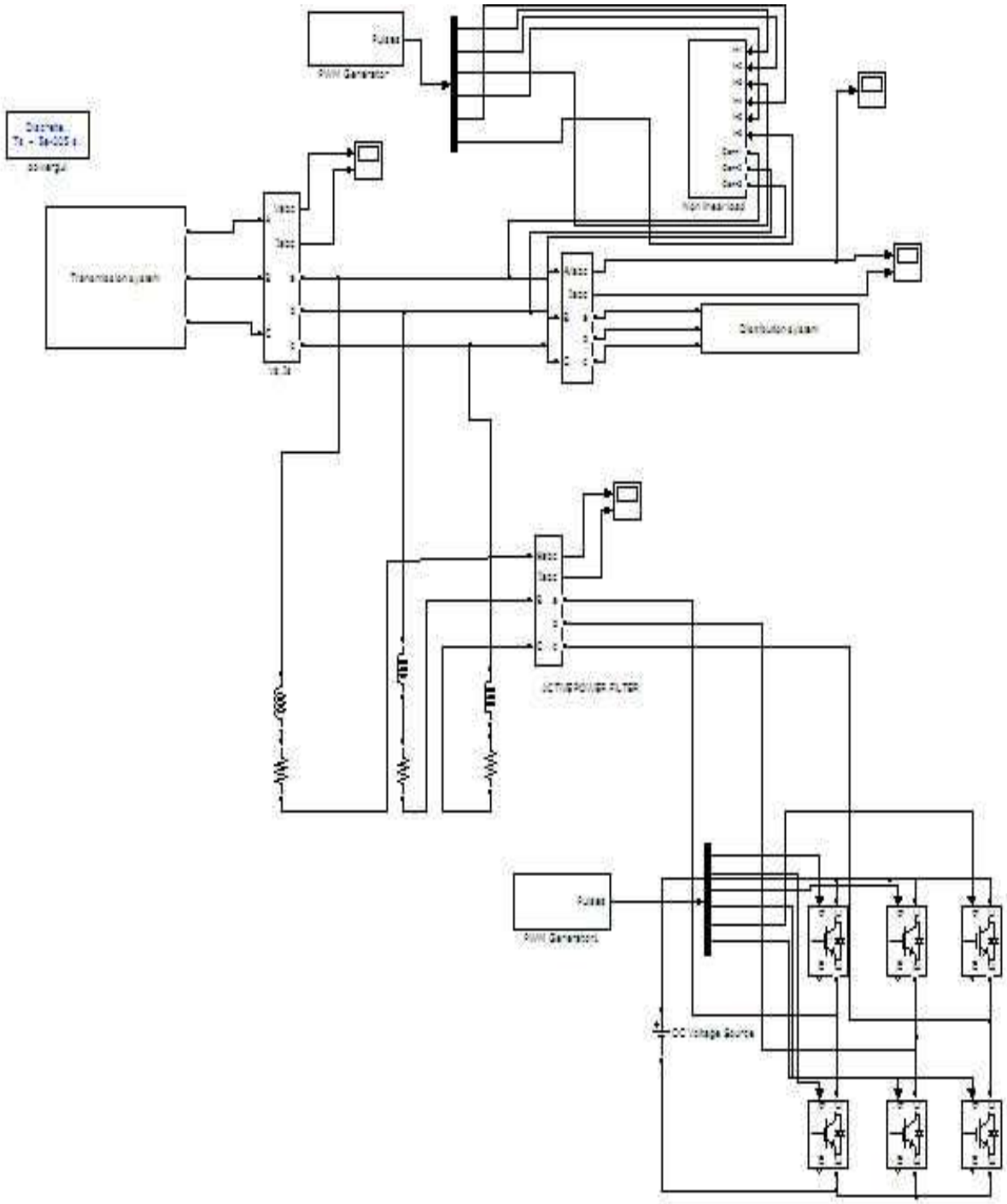
Pulses
PWM Generator
Transmission system
Distribution system
Pulses
PWM Generator
DC Voltage Source

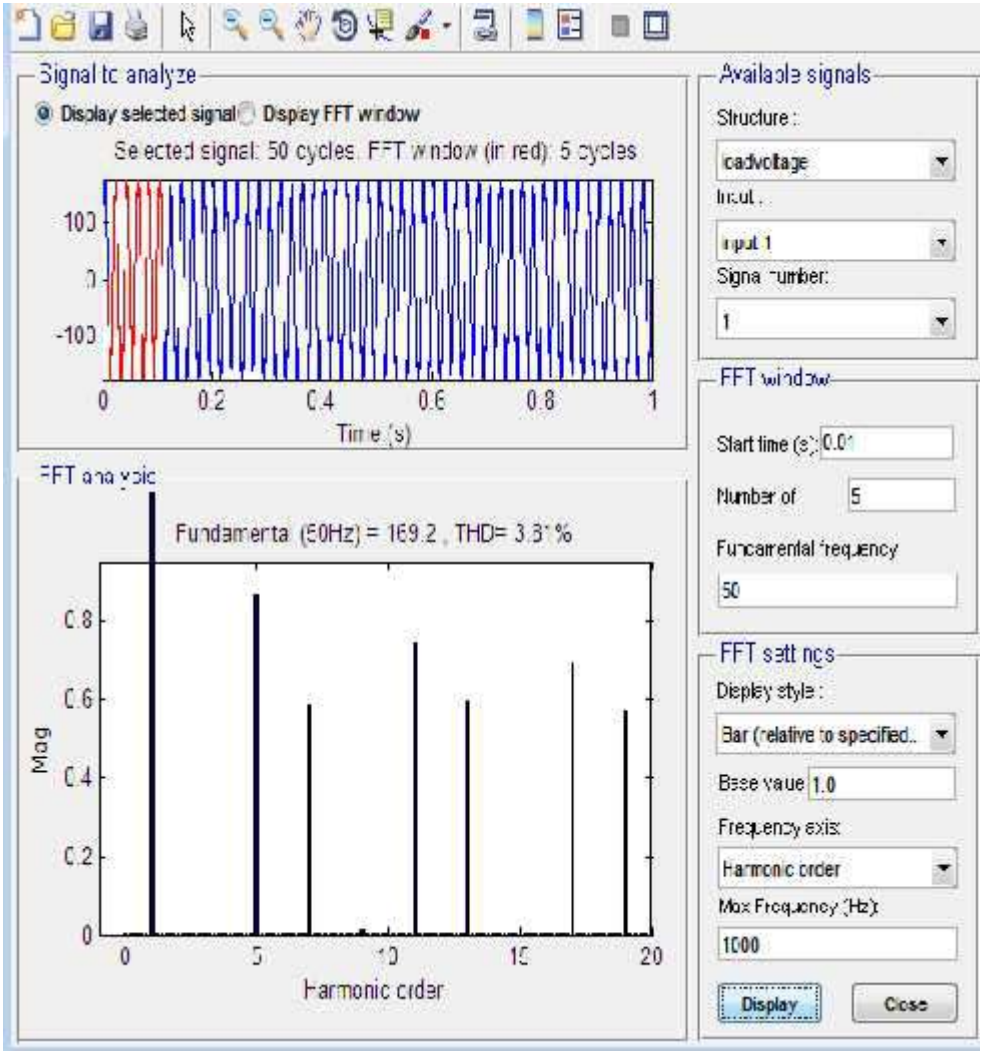

RESULT: Thus the active filter for mitigation harmonics was designed

EXP NO:10 **DATE:**

TESTING LOW-IMPEDANCE BIASED CURRENT DIFFERENTIAL PROTECTION WITH SIMULATION OF EXCITATION FAILURE OF GENERATION IN PSCAD/EMTDC

Aim:

To study about testing of the low-impedance biased current differential protection with simulation of excitation failure of generation in PSCAD/EMTDC

Theory:

Step 1: Prepare the System Model:

Define the power system model: Create a detailed representation of the power system in PSCAD/EMTDC. Include generators, transformers, transmission lines, loads, and the low-impedance biased current differential protection scheme.

Step 2: Generator Excitation Failure Model:

Introduce the excitation failure scenario: Model the excitation system of the generator and simulate the failure of the excitation system. The generator will lose voltage regulation, leading to a loss of synchronous operation.

Step 3: Low-Impedance Biased Current Differential Protection:

Model the low-impedance biased current differential protection scheme in PSCAD/EMTDC. This protection scheme typically includes current transformers (CTs), relays, and communication channels.

Configure the relay settings for sensitivity, pickup, and time delay parameters based on your protection requirements. Ensure the scheme is designed to detect faults accurately and minimize unnecessary tripping.

Step 4: Fault Scenario Setup:

Introduce a fault in the power system. The fault can be a three-phase fault, phase-to-phase fault, or other types of fault scenarios. The fault location should be within the protected zone.

Step 5: Simulation and Testing:

Run the simulation in PSCAD/EMTDC and monitor the response of the low-impedance biased current differential protection scheme.

Analyze the relay's operation during normal system conditions and when a fault occurs.

Verify that the protection scheme operates correctly, initiates a trip signal when a fault is detected, and does not trip for external faults outside the protected zone or for transient system disturbances.

Assess the performance of the protection scheme under various operating conditions, such as load variations and generator excitation system failures.

Step 6: Data Collection and Analysis:

Collect and analyze data generated during the simulation, including relay operation, fault clearance times, and system response.

Evaluate the performance of the protection scheme against your specified protection goals, such as selectivity, speed, and reliability.

Step 7: Troubleshooting and Optimization:

If the protection scheme does not perform as expected, troubleshoot the issues and make necessary adjustments to the relay settings or the system model.

Optimize the settings and parameters to improve the protection's performance.

Step 8: Reporting and Documentation:

Prepare a comprehensive report summarizing the simulation setup, results, and any recommended changes or improvements to the protection scheme.

Include diagrams, waveforms, and other relevant data to illustrate the performance of the low-impedance biased current differential protection under excitation failure scenarios.

Testing low-impedance biased current differential protection with the simulation of excitation failure is a critical aspect of ensuring the reliability of protection systems in power generation. It's important to thoroughly analyze and validate the protection scheme to avoid unnecessary trips and ensure that it operates correctly under various operating conditions and fault scenarios.

Result:

EXP NO: 11 **DATE**:

TRANSIENT STABILITY ANALYSIS: SINGLE MACHINE INFINITE BUS SYSTEM USING CLASSICAL MODEL

AIM

To become familiar with various aspects of the transient stability analysis of Single Machine Infinite Bus (SMIB) system.

OBJECTIVE

To understand modeling and analysis of transient stability of a SMIB power system.

SOFTWARE REQUIRED

TRANSIENT - SMIB module of AU Power lab or equivalent.

THEORY

Stability

Stability problem is concerned with the behavior of power system when it is subjected to disturbances and is classified into small signal stability problem if the disturbances are small and transient stability problem when the disturbances are large.

Transient Stability

When a power system is under steady state, the load plus transmission loss equals to the generation in the system. The generating units run at synchronous speed and system frequency, voltage, current and power flows are steady. When a large disturbance such as three phase fault, loss of load, loss of generation etc., occurs the power balance is upset and the generating units rotors experience either acceleration or deceleration. The system may come back to a steady state condition maintaining synchronism or it may break into subsystems or one or more machines may pull out of synchronism. In the former case the system is said to be stable and in the later case it is said to be unstable.

SINGLE MACHINE- INFINITE BUS SYSTEM

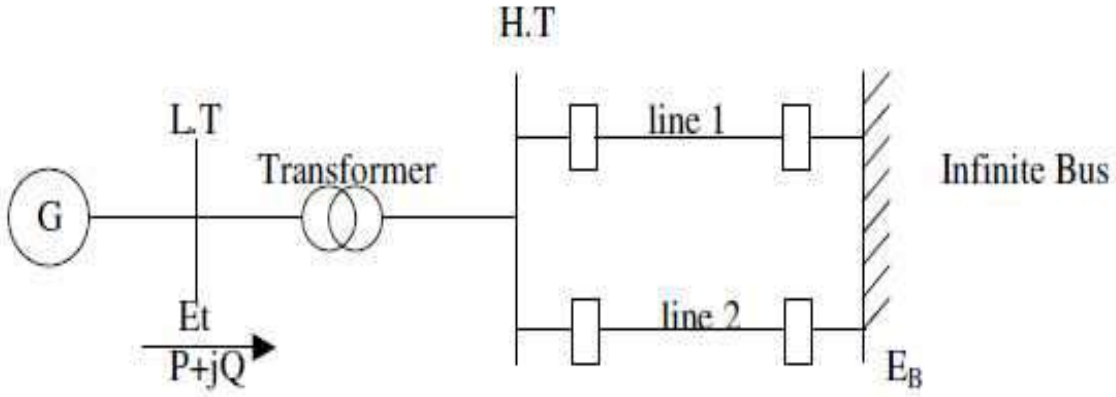

OUTPUT

Case 1: Opening & Closing of Circuit Breaker at line-2

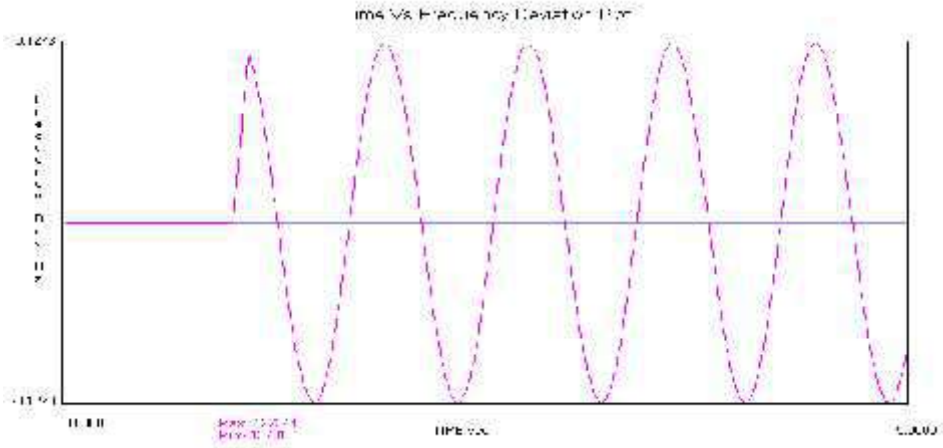

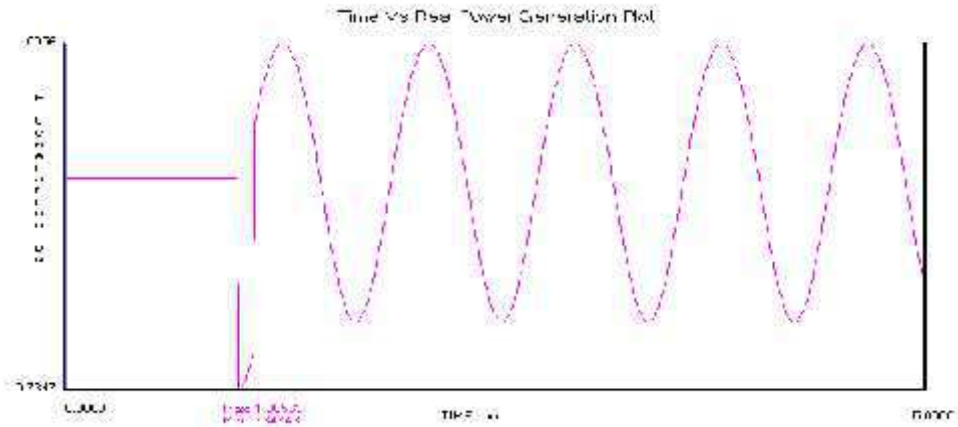

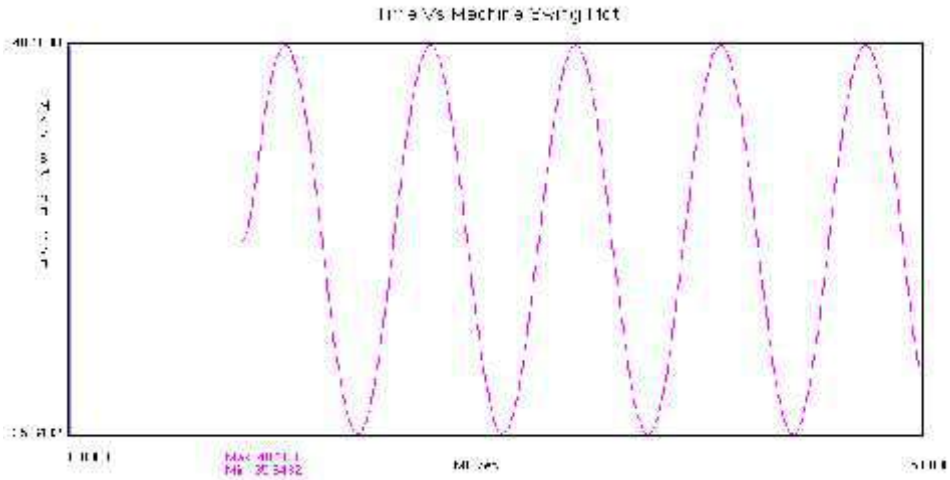

Case 2: Three-phase to ground fault at the mid point of line-2

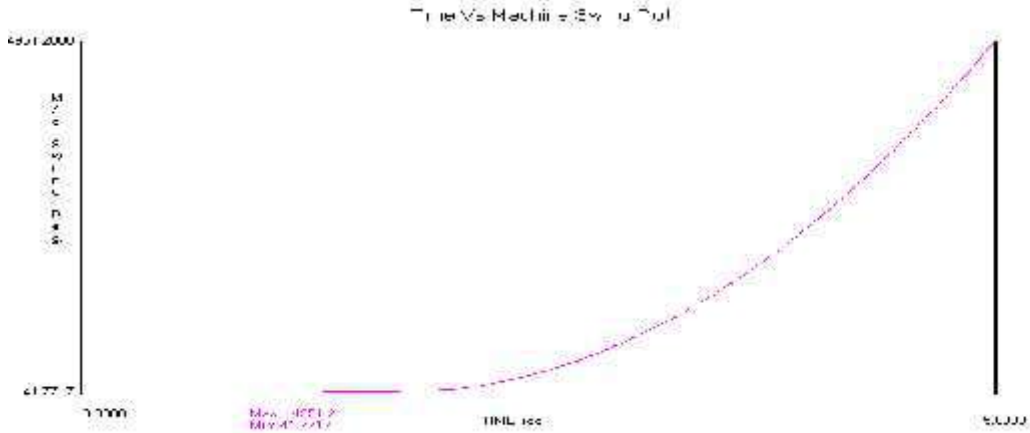

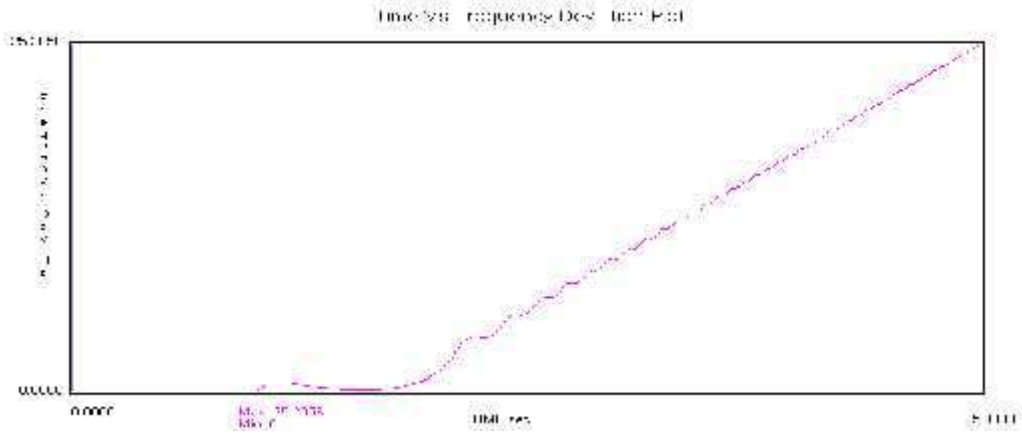

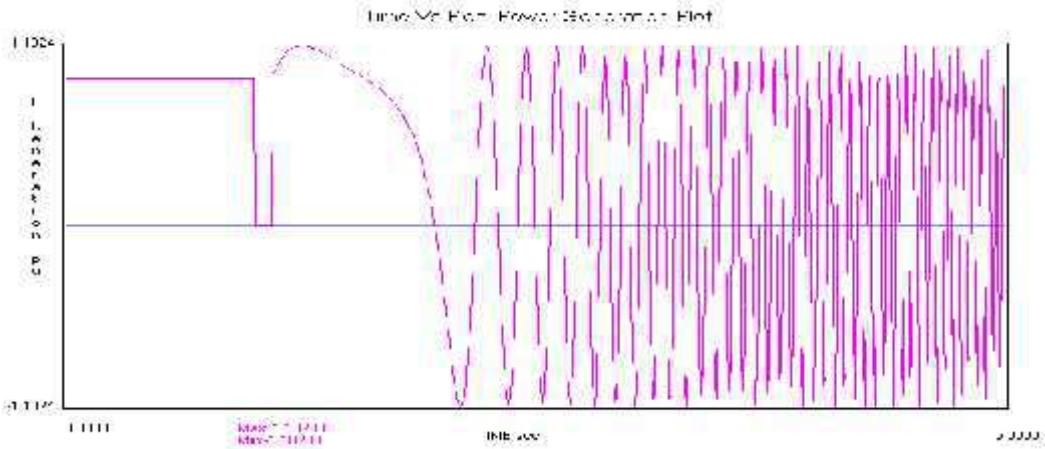

Case 3: Three-phase to ground fault at the end of line-2

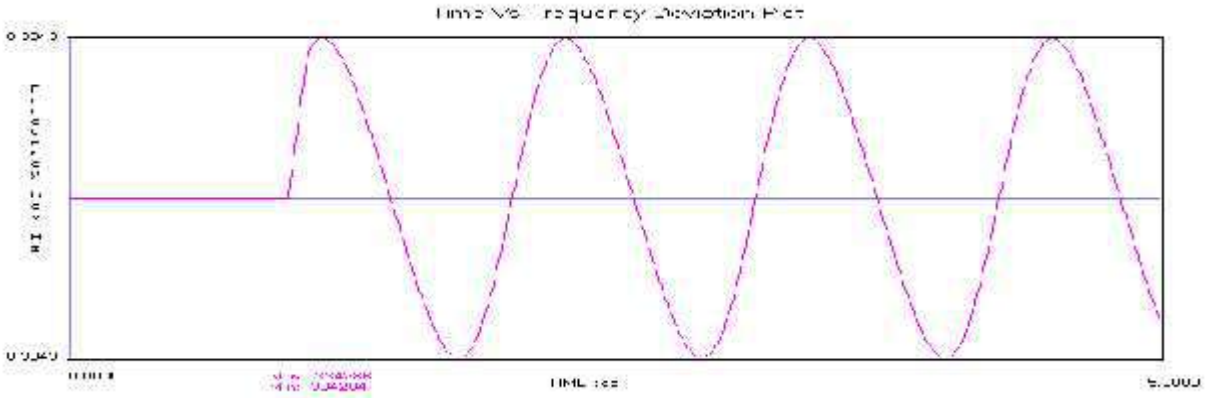

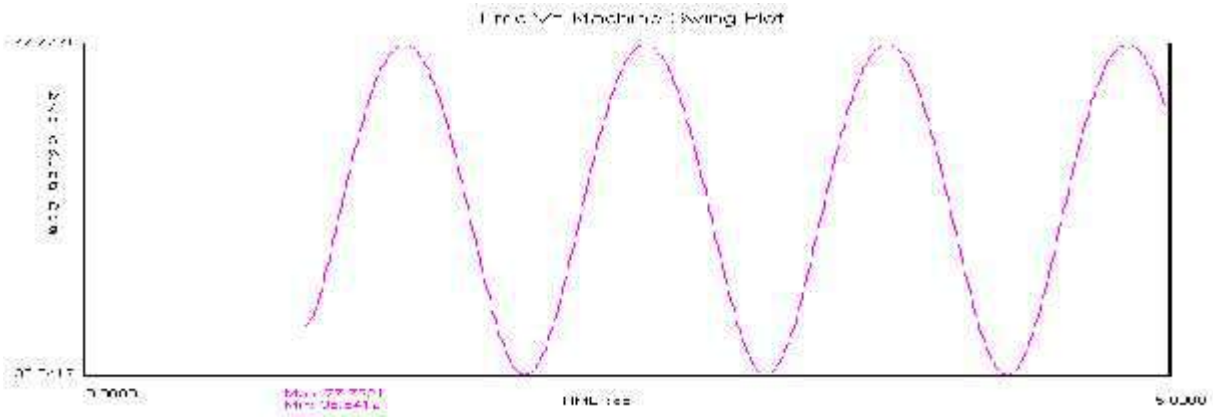

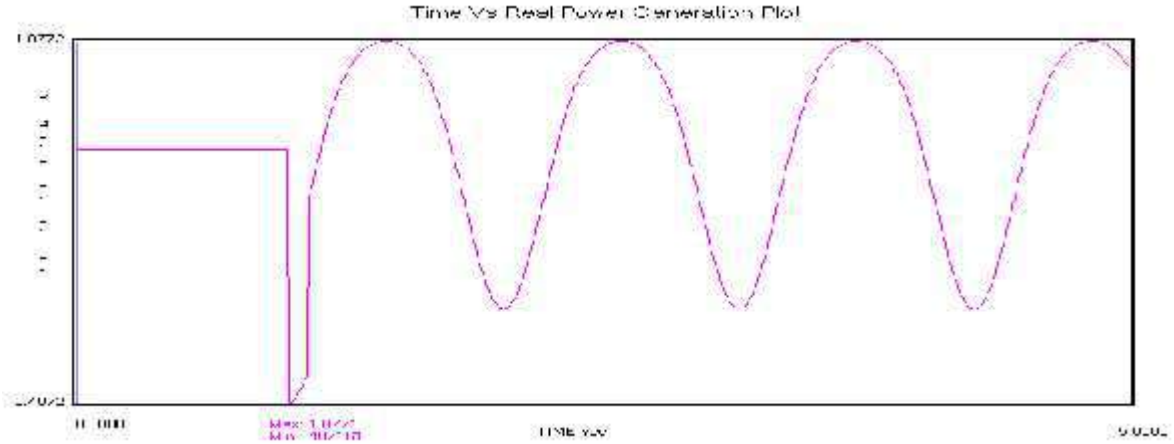
Time Vs Real Power Generation Plot

RESULT:

Thus the transient stability of a Single-Machine Infinite Bus(SMIB) System was analyzed & output graphs for different cases were obtained.

EXP NO: 12 **DATE**:

SMALL SIGNAL STABILITY ANALYSIS OF A SINGLE MACHINE INFINITE BUS SYSTEM WITH FIELD CIRCUIT, EXCITER AND POWER SYSTEM STABILIZER

AIM:

To write a MATLAB program for analyzing the small signal stability of a single machine infinite bus system with field circuit, exciter and power system stabilizer.

SOFTWARE REQUIRED:

Power system module of MATLAB.

THEORY:

Effect of Synchronous Machine Field Circuit Dynamics:

We now consider the system performance including the effect of field flux variations. The amortisseur effects will be neglected and the field voltage will be assumed constant (manual excitation control).

Synchronous machine equations:

As in the case of the classical generator model, the acceleration equations are

$$p\Delta\omega_r = \frac{1}{2H}\left(T_m - T_e - K_D\Delta\omega_r\right) \quad (1)$$

$$p\delta = \omega_0\Delta\omega_r$$

where

Network equations:

The machine terminal and infinite bus voltages in terms of the d and q components are

$$\overset{0}{E}_t = e_d + je_q \quad (2)$$

$$\overset{0}{E}_B = E_{Bd} + jE_{Bq} \quad (3)$$

The network constraint equation for the system

$$\overset{0}{E}_t = \overset{0}{E}_B + \left(R_E + jX_E\right)\overset{0}{I}_t \quad (4)$$

$$\left(e_d + je_q\right) = \left(E_{Bd} + jE_{Bq}\right) + \left(R_E + jX_E\right)\left(i_d + ji_q\right) \quad (5)$$

Resolving into d and q components gives

$$e_d = R_E i_d - X_E i_q + E_{Bd} \quad (6)$$

$$e_q = R_E i_q + X_E i_d + E_{Bq} \quad (7)$$

Where,

$$E_{Bd} = E_B \sin\delta \quad (8)$$

$$E_{Bq} = E_B \cos\delta \quad (9)$$

The expressions for i_d and i_q in terms of the state variables ψ_{fd} and δ is given by

$$i_d = \frac{X_{Tq}\left[\psi_{fd}\left(\frac{L_{ads}}{L_{ads} + L_{fd}}\right) - E_B\cos\delta\right] - R_T E_B \sin\delta}{D} \quad (10)$$

$$i_q = \frac{R_T\left[\psi_{fd}\left(\frac{L_{ads}}{L_{ads}+L_{fd}}\right) - E_B\cos\delta\right] + X_{Td}E_B\sin\delta}{D} \quad (11)$$

$$R_T = R_a + R_E \quad (12)$$

$$X_{Tq} = X_E + \left(L_{aqs} + L_l\right) = X_E + X_{qs} \quad (13)$$

$$X_{Tqd} = X_E + \left(L'_{ads} + L_l\right) = X_E + X'_{ds} \quad (14)$$

$$D = R_T^2 + X_{Tq}X_{Td} \quad (15)$$

The reactance's L_{ads} and L_{aqs} are saturated values. In per unit they are equal to the corresponding inductances.
These equations are nonlinear and have to be linearized for small signal analysis.

Linearized system equations

Expressing equations (11) and (13) in terms of perturbed values, we may write

$$\Delta i_d = m_1\Delta\delta + m_2\Delta\psi_{fd} \quad (16)$$

$$\Delta i_q = n_1\Delta\delta + n_2\Delta\psi_{fd} \quad (17)$$

$$m_1 = \frac{E_B\left(X_{Tq}\sin\delta_0 - R_T\cos\delta_0\right)}{D} \quad (18)$$

$$n_1 = \frac{E_B\left(R_T\sin\delta_0 + X_{Td}\cos\delta_0\right)}{D} \quad (19)$$

$$m_2 = \frac{X_{T¶q}}{D}\frac{L_{ads}}{\left(L_{ads}+L_{fd}\right)} \quad (20)$$

$$n_2 = \frac{R_T}{D}\frac{L_{ads}}{\left(L_{ads}+L_{fd}\right)} \quad (21)$$

By linearizing ψ_{ad} and ψ_{aq}, and substituting them in the above expressions and , we get

$$\Delta\psi_{ad} = L'_{ads}\left(-\Delta i_d + \frac{\Delta\psi_{fd}}{L_{fd}}\right) \quad (22)$$

$$= \left(\frac{1}{L_{fd}} - m_2\right)L'_{ads}\Delta\psi_{fd} - m_1L'_{ads}\Delta\delta \quad (23)$$

$$\Delta\psi_{aq} = -L_{aqs}\Delta i_q \quad (24)$$

$$= -n_2L_{aqs}\Delta\psi_{fd} - n_1L_{aqs}\Delta\delta \quad (25)$$

Linearizing i_{fd} and substituting for $\Delta\psi_{ad}$ from equation (19) gives

$$\Delta i_{fd} = \frac{\Delta\psi_{fd} - \Delta\psi_{ad}}{L_{fd}} \tag{26}$$

$$= \frac{1}{L_{fd}}\left(1 - \frac{L'_{ads}}{L_{fd}} + L'_{ads}\right)\Delta\psi_{fd} + \frac{1}{L_{fd}} m_1 L'_{ads}\Delta\delta \tag{27}$$

The linearized form of air gap torque T_e is given by

$$\Delta T_e = \psi_{ad0}\Delta i_q + i_{q0}\Delta\psi_{ad} - \psi_{aq0}\Delta i_d - i_{d0}\Delta\psi_{aq} \tag{28}$$

$$\Delta T_e = K_1\Delta\delta + K_2\Delta\psi_{fd} \tag{29}$$

$$K_1 = n_1\left(\psi_{ad0} + L_{aqs} i_{d0}\right) - m_1\left(\psi_{aq0} + L'_{ads} i_{q0}\right) \tag{30}$$

$$K_2 = n_2\left(\psi_{ad0} + L_{aqs} i_{d0}\right) - m_2\left(\psi_{aq0} + L'_{ads} i_{q0}\right) + \frac{L'_{ads}}{L_{fd}} i_{q0} \tag{31}$$

The system equation in the desired final form :

$$\begin{bmatrix} \Delta\dot{\omega}_r \\ \Delta\dot{\delta} \\ \Delta\dot{\psi}_{fd} \end{bmatrix} = \begin{bmatrix} a_{11} & a_{12} & a_{13} \\ a_{21} & 0 & 0 \\ 0 & a_{32} & a_{33} \end{bmatrix} \begin{bmatrix} \Delta\omega_r \\ \Delta\delta \\ \Delta\psi_{fd} \end{bmatrix} \tag{32}$$

Where,

$$a_{11} = -\frac{K_D}{2H} \tag{33}$$

$$a_{12} = -\frac{K_1}{2H} \tag{34}$$

$$a_{13} = -\frac{K_2}{2H} \tag{35}$$

$$a_{21} = \omega_0 = 2\pi f_0 \tag{36}$$

$$a_{32} = \frac{\omega_0 R_{fd}}{L_{fd}} m_1 L'_{ads} \tag{37}$$

$$a_{33} = -\frac{\omega_0 R_{fd}}{L_{fd}}\left[1 - \frac{L'_{ads}}{L_{fd}} + m_2 L'_{ads}\right] \tag{38}$$

$$b_{11} = \frac{1}{2H} \tag{39}$$

$$b_{32} = \frac{\omega_0 R_{fd}}{L_{adu}}$$

and ΔT_m and ΔE_{fd} depend on prime mover and excitation controls. With constant mechanical input torque, ΔT_m =0; with constant exciter output voltage, ΔE_{fd} =0.

Summary of procedure for formulating the state matrix

(a)The following steady state operating conditions , machine parameters and network parameters are given below:

$\mathbf{P_t \;\; Q_t \;\; E_t \;\; R_E \;\; X_E}$

$\mathbf{L_d \;\; L_q \;\; L_l \;\; R_a \;\; L_{fd} \;\; A_{sat} \;\; B_{sat} \;\; \Psi_{Tl}}$

Alternatively E_B may be specified instead of Q_t or E_t

(b)The first step is to compute the initial steady state values of system variables:

I_t , power factor angle ,Total saturation factors K_{sd} and K_{sq} .

$$\mathbf{X_{ds} = L_{ds} = K_{sd}L_{adu} + L_l} \quad \textbf{(40)}$$

$$\mathbf{X_{qs} = L_{qs} = K_{sq}L_{aqu} + L_l} \quad \textbf{(41)}$$

$$\mathbf{\delta_i = \tan^{-1}\left(\frac{I_tX_{qs}\cos j - I_tR_a\sin j}{E_t + I_tR_a\cos j + I_tX_{qs}\sin j}\right)} \quad \textbf{(42)}$$

$$\mathbf{e_{d0} = E_t\sin\delta_i} \quad \textbf{(43)}$$

$$\mathbf{e_{q0} = E_t\cos\delta_i} \quad \textbf{(44)}$$

$$\mathbf{i_{d0} = I_t\sin(\delta_i + j)} \quad \textbf{(45)}$$

$$\mathbf{i_{q0} = I_t\cos(\delta_i + j)} \quad \textbf{(46)}$$

$$\mathbf{E_{Bd0} = e_{d0} - R_Ei_{d0} + X_Ei_{q0}} \quad \textbf{(47)}$$

$$\mathbf{a_{32} = \frac{\omega_0R_{fd}}{L_{fd}}m_1L'_{ads}} \quad \textbf{(48)}$$

$$\mathbf{\delta_0 = \tan^{-1}\left(\frac{E_{Bdo}}{E_{Bq0}}\right)} \quad \textbf{(49)}$$

$$\mathbf{E_B = \left(E_{Bdo}^2 + E_{Bqo}^2\right)^{1/2}} \quad \textbf{(50)}$$

$$\mathbf{i_{fd0} = \frac{e_{q0} + R_ai_{q0}L_{ds}i_{d0}}{L_{ads}},} \quad \textbf{(51)}$$

$$\mathbf{E_{fd0} = L_{adu}i_{fd0}} \quad \textbf{(52)}$$

$$\mathbf{\psi_{ad0} = L_{ads}(-i_{d0} + i_{fd0})} \quad \textbf{(53)}$$

$$\mathbf{\psi_{aq0} = -L_{aqs}i_{q0}} \quad \textbf{(54)}$$

(c)The next step is to compute incremental saturation factors and the corresponding saturated values of L_{ads} ,L_{aqs} ,L'_{ads} , and then

$\mathbf{R_T, X_{Tq}, X_{Td}, D}$

$\mathbf{m_1, m_2, n_1, n_2}$

$\mathbf{K_1, K_2}$

is calculated from the equations (11) and (14).

(d) Finally, compute the elements of matrix A.

Block diagram representation

Fig.1 shows the block diagram representation of the small signal performance of the system .In this representation, the dynamic characteristics of the system are expressed in terms of the so called K constants. The basis for the block diagram and the expressions for the associated constant are developed .

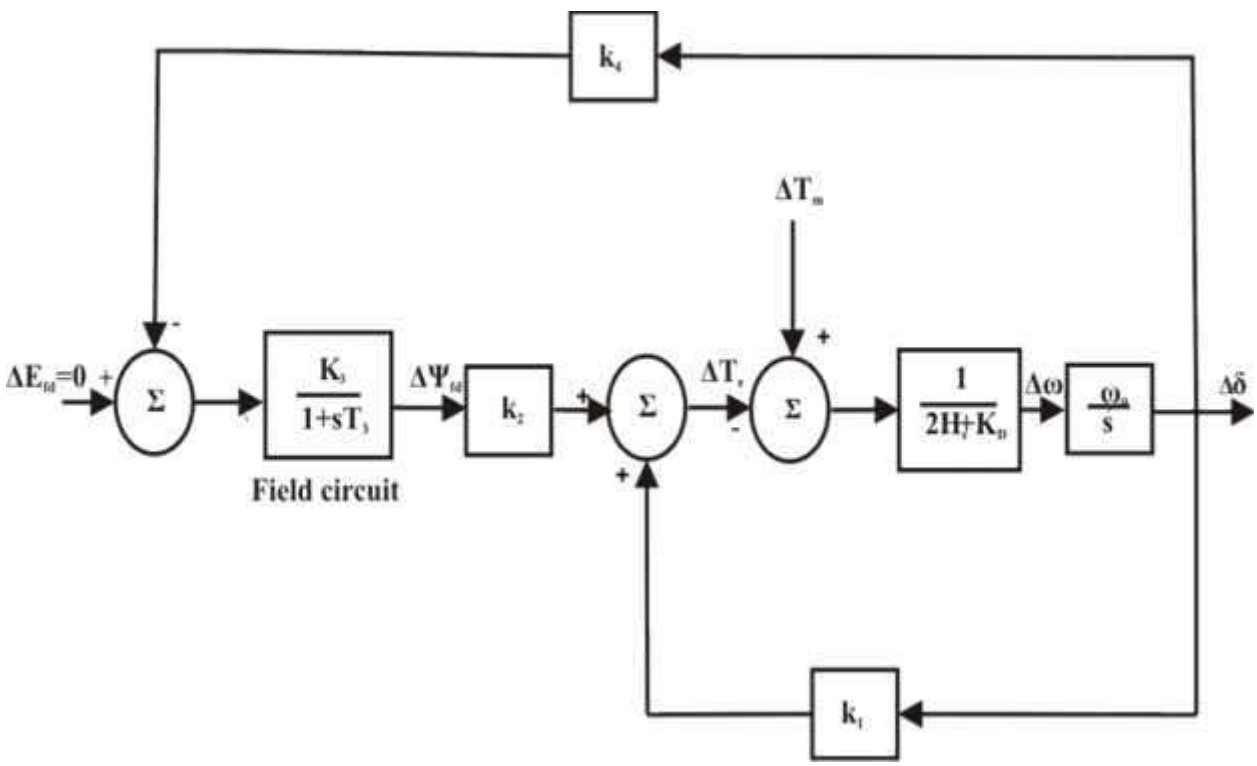

Fig.1-BLOCK DIAGRAM REPRESENTATION WITH CONSTANT E_{fd}

EFFECTS OF EXCITATION SYSTEM:

We will examine the effect of the excitation system on the small signal stability performance of the single machine infinite bus system.

The input control signal to the excitation system is normally the generator terminal voltage E_t. In the generator model E_t is not a state variable. Therefore, E_t has to be expressed in terms of the state variables $\Delta\omega_r$, $\Delta\delta$, and $\Delta\psi_{fd}$.

$\tilde{E}$ May be expressed in complex form:

$$\mathbf{E_t^0 = e_d + je_q} \qquad \textbf{(55)}$$

Hence,

$$\mathbf{E_t^2 = e_d^2 + e_q^2} \qquad \textbf{(56)}$$

Applying a small perturbation, we may write

$$\mathbf{(E_{t0} + \Delta E_t)^2 = (e_{d0} + \Delta e_d)^2 + (e_{q0} + \Delta e_q)^2} \qquad \textbf{(57)}$$

By neglecting second order terms involving perturbed values , the above equation reduces to

$$\mathbf{E_{t0}\Delta E_t = e_{d0}\Delta e_d + e_{q0}\Delta e_q} \qquad \textbf{(58)}$$

Therefore,

$$\mathbf{\Delta E_t = \frac{e_{d0}}{E_{t0}}\Delta e_d + \frac{e_{q0}}{E_{t0}}\Delta e_q} \qquad \textbf{(59)}$$

In terms of the perturbed values, Equations

$$\mathbf{\Delta e_d = -R_a\Delta i_d + L_l\Delta i_q - \Delta\psi_{aq}}$$
$$\mathbf{\Delta e_q = -R_a\Delta i_q + L_l\Delta i_d - \Delta\psi_{ad}} \qquad \textbf{(60)}$$

Use of Equations to eliminate $\Delta i_d, \Delta i_q, \Delta\psi_{ad}$ and $\Delta\psi_{aq}$ from the above equations in terms of the state variables and substitution of the resulting expressions for Δe_d and Δe_q in equation yield

$$\mathbf{\Delta E_t = K_5\Delta\delta + K_6\Delta\psi_{fd}} \qquad \textbf{(61)}$$

Where

$$\mathbf{K_5 = \frac{e_{d0}}{E_{t0}}[-R_a m_1 + L_l n_1 + L_{aqs} n_1] + \frac{e_{q0}}{E_{t0}}[-R_a n_1 - L_l m_1 - L'_{ads} m_1]} \qquad \textbf{(62)}$$

$$\mathbf{K_6 = \frac{e_{d0}}{E_{t0}}[-R_a m_2 + L_l n_2 + L_{aqs} n_2] + \frac{e_{q0}}{E_{t0}}[-R_a n_2 - L_l m_2 + L'_{ads}(\frac{1}{L_{fd}} - m_2)]} \qquad \textbf{(63)}$$

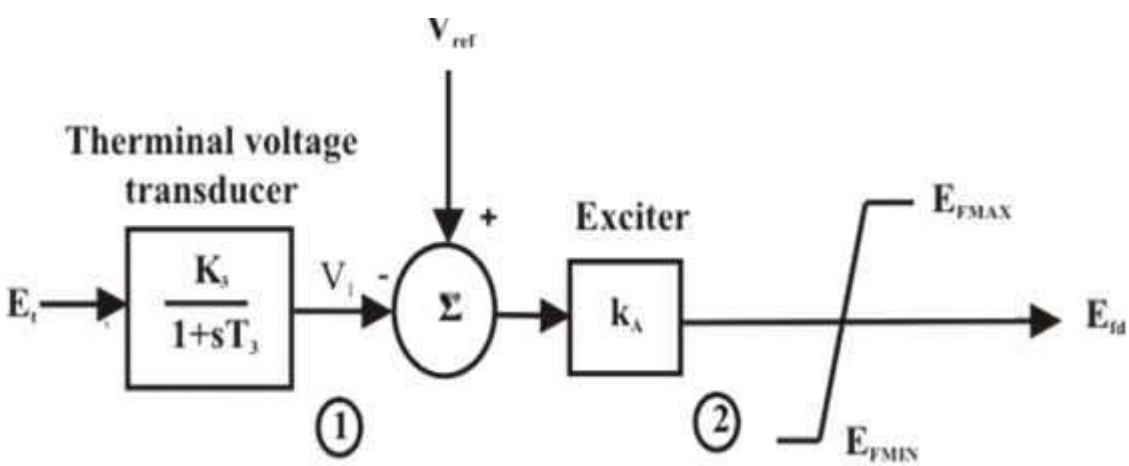

Fig.2 THYRISTOR EXCITATION SYSTEM WITH AVR

$$a_{34} = -b_{32}K_A$$
$$a_{41} = 0$$
$$a_{42} = \frac{K_5}{T_R} \qquad (64)$$
$$a_{43} = \frac{K_6}{T_R}$$
$$a_{44} = -\frac{1}{T_R}$$

The complete state space model for the power system , including the excitation system is given by

$$\begin{bmatrix} \Delta\dot{\omega}_r \\ \Delta\dot{\delta} \\ \Delta\dot{\psi}_{fd} \\ \Delta\dot{v}_1 \end{bmatrix} = \begin{bmatrix} a_{11} & a_{12} & a_{13} & 0 \\ a_{21} & 0 & 0 & 0 \\ 0 & a_{32} & a_{33} & a_{34} \\ 0 & a_{42} & a_{43} & a_{44} \end{bmatrix} \begin{bmatrix} \Delta\omega_r \\ \Delta\delta \\ \Delta\psi_{fd} \\ \Delta v_1 \end{bmatrix} + \begin{bmatrix} b_1 \\ 0 \\ 0 \\ 0 \end{bmatrix} \Delta T_m \qquad (65)$$

<u>Block diagram including the excitation system:</u>

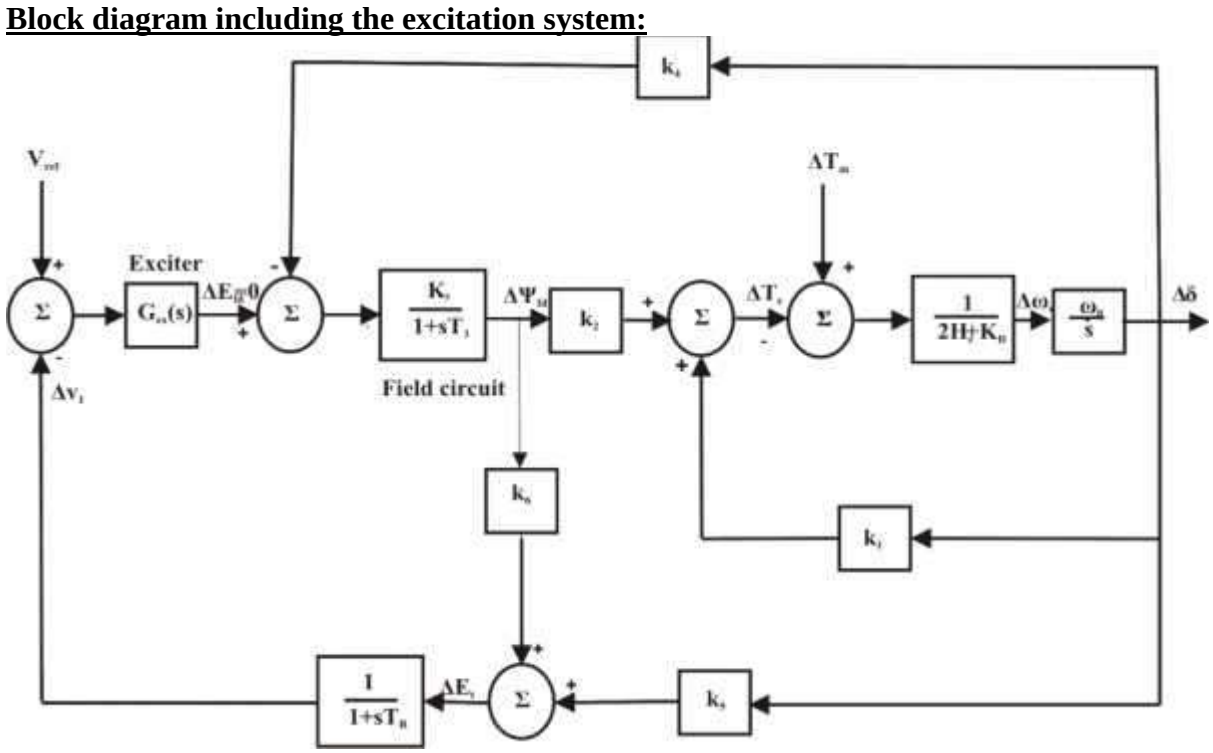

Fig 3- BLOCK DIAGRAM REPRESENTATION WITH EXCITER AND AVR

POWER SYTEM STABILIZER:

The basic function of a power system stabilizer (PSS) is to add damping to the generator rotor oscillations by controlling its excitation using auxiliary stabilizing signal(s). To provide damping, the stabilizer must produce a component of electrical torque in phase with the rotor speed deviations.

The theoretical basis for a PSS may be illustrated with the aid of the block diagram shown below.

Since the purpose of a PSS is to introduce a damping torque component, a logical signal to use for controlling generator excitation is the speed deviation $\Delta_{\omega r}$.

If the exciter transfer function $G_{ex}(s)$ and the generator transfer function between ΔE_{fd} and Δ_{Te} were pure gains, a direct feedback of $\Delta_{\omega r}$ would result in a damping torque component. However, in practice both the generator and the exciter (depending on its type) exhibit frequency dependent gain and phase characteristics. Therefore, the PSS transfer function, GPSS(s), should have appropriate phase compensation circuits to compensate for the phase lag between the exciter input and the electrical torque. In the ideal case, with the phase characteristics of GPSS(S) being an exact inverse of the exciter and generator phase characteristics to be compensated, the PSS would result in a pure damping torque at all oscillating frequencies.

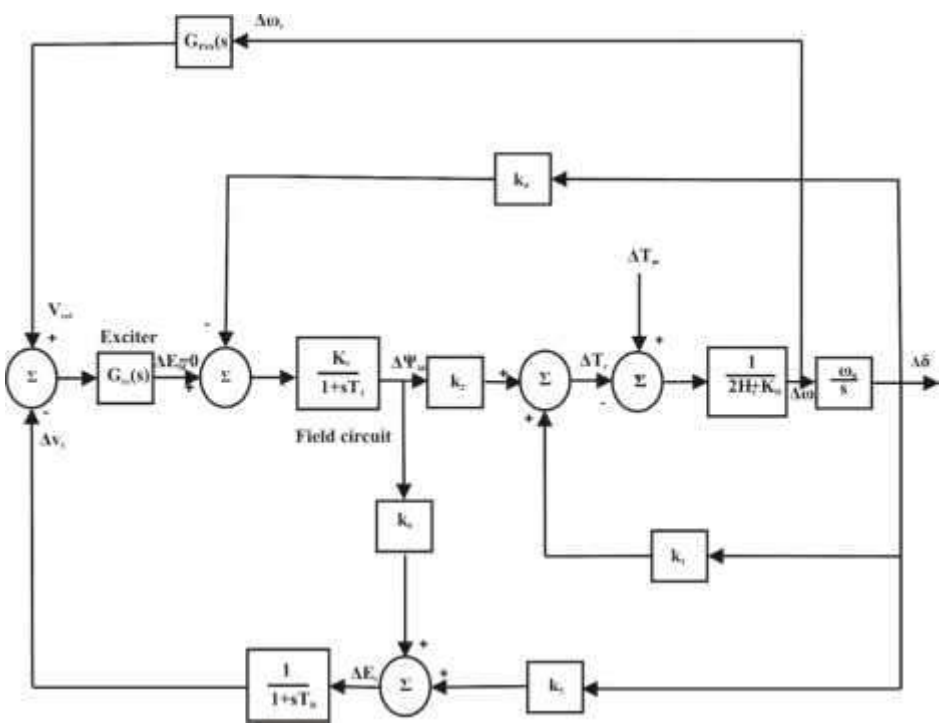

Fig 4- BLOCK DIAGRAM REPRESENTATION WITH AVR AND PSS.

The PSS representation in figure shown below consists of three blocks: a phase compensation block, a signal washout block, and a gain block.

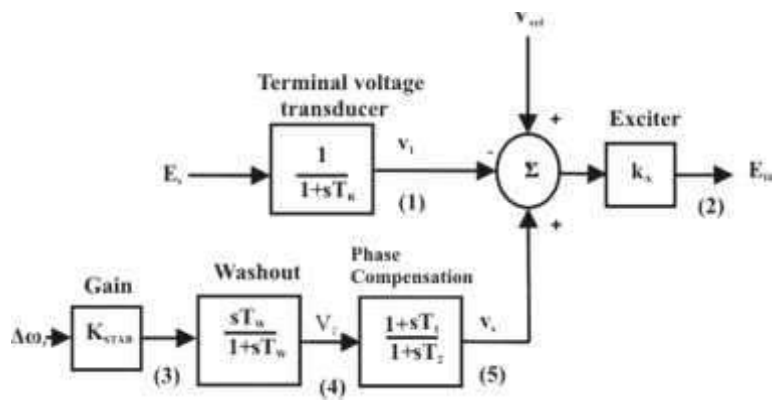

Fig 5- THYRISTOR EXCITATION SYSTEM WITH AVR AND PSS

<u>System state matrix including PSS</u>

$$\mathbf{a_{51} = K_{STAB} a_{11}}$$

$$\mathbf{a_{52} = K_{STAB} a_{12}}$$

$$\mathbf{a_{53} = K_{STAB} a_{13}}$$

$$\mathbf{a_{55} = -\frac{1}{T_w}}$$

$$\mathbf{a_{61} = \frac{T_1}{T_2} a_{51}}$$

$$\mathbf{a_{62} = \frac{T_1}{T_2} a_{52}}$$

$$\mathbf{a_{63} = \frac{T_1}{T_2} a_{53}}$$

$$\mathbf{a_{65} = \frac{T_1}{T_2} a_{55} + \frac{T_1}{T_2}}$$

$$\mathbf{a_{36} = \frac{\omega_0 R_{fd}}{L_{adu}} K_A} \qquad \textbf{(66)}$$

The complete state space model, including the PSS, has the following form

$$\begin{bmatrix} \Delta\dot{\omega}_r \\ \Delta\dot{\delta} \\ \Delta\dot{\psi}_{fd} \\ \Delta\dot{v}_1 \\ \Delta\dot{v}_2 \\ \Delta\dot{v}_s \end{bmatrix} = \begin{bmatrix} a_{11} & a_{12} & a_{13} & 0 & 0 & 0 \\ a_{21} & 0 & 0 & 0 & 0 & 0 \\ 0 & a_{32} & a_{33} & a_{34} & 0 & a_{36} \\ 0 & a_{42} & a_{43} & a_{44} & 0 & 0 \\ a_{51} & a_{52} & a_{53} & 0 & a_{55} & 0 \\ a_{61} & a_{62} & a_{63} & 0 & a_{65} & a_{66} \end{bmatrix} \begin{bmatrix} \Delta\omega_r \\ \Delta\delta \\ \Delta\psi_{fd} \\ \Delta v_1 \\ \Delta v_2 \\ \Delta v_s \end{bmatrix} \quad \textbf{(67)}$$

RESULT:

A MATLAB program was written to analyze the small signal stability of single machine infinite bus system with field circuit, exciter and power system stabilizer.

PROGRAM FOR SMALL SIGNAL STABILITY ANALYSIS OF SINGLE MACHINE INFINITE BUS SYSTEM

1. WITH FIELD CIRCUIT

```
p=0.9;q=0.3;Et=1;h=3.5;xd=1.81;xq=1.76;xdp=0.3;x1=0.16;Ra=0.003;Tdop=8;Ladu=1.65;Laqu
=1.60;L1=0.16;Rfd=0.0006;
Xtr=0.15;x1=0.5;ksd=0.8491;ksq=0.8491;x2=0.93;Re=0;Lfd=0.153;kd=0;fo=60;
Xe=Xtr+x1;
s=p+q*i;
It=s'/Et';
phi=atan(q/p);
Lds=(ksd*Ladu)+L1;
Lqs=(ksq*Laqu)+L1;
Xqs=Lqs;
Xds=Lds;
a=(abs(It)*Xqs*cos(phi)-abs(It)*Ra*sin(phi));
b=(Et+(abs(It)*Ra*cos(phi))+(abs(It)*Xqs*sin(phi)));
deli=atan(a/b);
edo=Et*sin(deli);
eqo=Et*cos(deli);
ido=abs(It)*sin(deli+phi);
iqo=abs(It)*cos(deli+phi);
Ebdo=edo-(Re*ido)+(Xe*iqo);
Ebqo=eqo-(Re*iqo)-(Xe*ido);
delo=atan(Ebdo/Ebqo);
Ep=sqrt(Ebdo^2+Ebqo^2);
Lads=Lds-L1;
Laqs=Lqs-L1;
ifdo=(eqo+(Ra*iqo)+(Lds*ido))/Lads;
Efdo=Ladu*ifdo;
siado=Lads*(-ido+ifdo);
siaqo=-Laqs*iqo;
Rt=Ra+Re;
Xtq=Xe+(Laqs+L1);
Ladsp=1/(inv(Lads)+inv(Lfd));
Xtd=Xe+(Ladsp+L1);
D=(Rt^2)+(Xtq*Xtd);
m1=(Ep*(Xtq*sin(delo))-(Rt*cos(delo)))/D;
n1=(Ep*(Rt*sin(delo))+(Xtd*cos(delo)))/D;
m2=(Xtq*Lads)/(D*(Lads+Lfd));
n2=(Rt*Lads)/(D*(Lads+Lfd));
k1=n1*(siado+(Lads*ido))-m1*(siaqo+(Ladsp*iqo));
```

```
k2=n2*(siado+(Laqs*ido))-m2*(siaqo+(Ladsp*iqo))+((Ladsp/Lfd)*iqo);
a11=-kd/(2*h);
a12=-k1/(2*h);
a13=-k2/(2*h);
wo=2*pi*fo;
a21=wo;a22=0;a23=0;a31=0;
a32=(-wo*Rfd*m1*Ladsp)/Lfd;
a33=((-wo*Rfd)/Lfd)*(1-(Ladsp/Lfd)+(m2*Ladsp));
A=[a11 a12 a13;a21 a22 a23;a31 a32 a33];
lamda=eig(A);
c(1)=real(lamda(1));
d(1)=imag(lamda(1));
zeta=-c(1)/(sqrt(c(1)*c(1)+d(1)*d(1)));
ks=abs(Ep)*abs(Ep)*cos(delo)/(Xe+xdp);
wn=sqrt(-det(A));
wnhz=wn/(2*pi)
wd=wn*sqrt(1-zeta*zeta);
theta=acos(zeta);
Dd0=5*pi/180;
t=0:0.01:30;
Dd=Dd0/sqrt(1-zeta*zeta)*exp(-zeta*wn*t).*sin(wd*t+theta);
d=(delo+Dd)*180/pi;
plot(t,d)
xlabel('t sec'),ylabel('delta degrees')
```

OUTPUT:

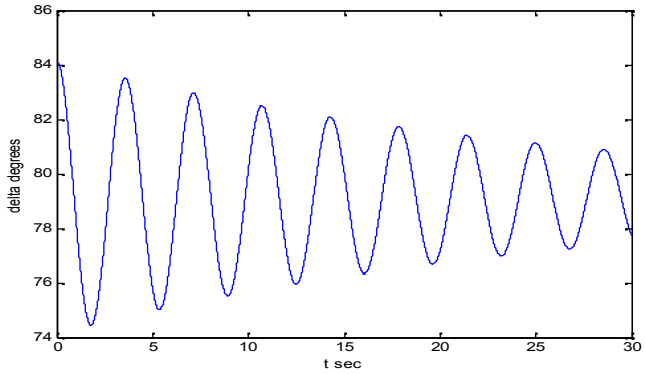

2.WITH EXCITER

```
p=0.9;q=0.3;Et=1;h=3.5;xd=1.81;xq=1.76;xdp=0.3;x1=0.16;Ra=0.003;Tdop=8;Ladu=1.65;Laqu
=1.60;L1=0.16;Rfd=0.0006;
Xtr=0.15;x1=0.5;ksd=0.8491;ksq=0.8491;x2=0.93;Re=0;Lfd=0.153;kd=0;fo=60;Tr=.02;ka=0;
Xe=Xtr+x1;
s=p+q*i;
It=s'/Et';
phi=atan(q/p);
Ep=Et+xdp*It*i;
Lds=(ksd*Ladu)+L1;
Lqs=(ksq*Laqu)+L1;
Xqs=Lqs;
Xds=Lds;
a=(abs(It)*Xqs*cos(phi)-abs(It)*Ra*sin(phi));
b=(Et+(abs(It)*Ra*cos(phi))+(abs(It)*Xqs*sin(phi)));
deli=atan(a/b);
edo=Et*sin(deli);
eqo=Et*cos(deli);
ido=abs(It)*sin(deli+phi);
iqo=abs(It)*cos(deli+phi);
Ebdo=edo-(Re*ido)+(Xe*iqo);
Ebqo=eqo-(Re*iqo)-(Xe*ido);
delo=atan(Ebdo/Ebqo);
Ep=sqrt(Ebdo^2+Ebqo^2);
Lads=Lds-L1;
Laqs=Lqs-L1;
ifdo=(eqo+(Ra*iqo)+(Lds*ido))/Lads;
Efdo=Ladu*ifdo;
siado=Lads*(-ido+ifdo);
siaqo=-Laqs*iqo;
Rt=Ra+Re;
Xtq=Xe+(Laqs+L1);
Ladsp=1/(inv(Lads)+inv(Lfd));
Xtd=Xe+(Ladsp+L1);
D=(Rt^2)+(Xtq*Xtd);
m1=(Ep*(Xtq*sin(delo))-(Rt*cos(delo)))/D;
n1=(Ep*(Rt*sin(delo))+(Xtd*cos(delo)))/D;
m2=(Xtq*Lads)/(D*(Lads+Lfd));
n2=(Rt*Lads)/(D*(Lads+Lfd));
Eto=sqrt(edo*edo+eqo*eqo);
k1=n1*(siado+(Lads*ido))-m1*(siaqo+(Ladsp*iqo));
```

```
k2=n2*(siado+(Laqs*ido))-m2*(siaqo+(Ladsp*iqo))+((Ladsp/Lfd)*iqo);
k5=(-Ra*m1+L1*n1+Laqs*n1)*(edo/Eto)+(eqo/Eto)*(-Ra*n1-L1*m1-Ladsp*m1);
k6=(edo/Eto)*(-Ra*m2+L1*n2+Laqs*n2)+(eqo/Eto)*(-Ra*n2-L1*m2+Ladsp*(inv(Lfd)-m2));
a11=-kd/(2*h);
a12=-k1/(2*h);
a13=-k2/(2*h);
a14=0;
wo=2*pi*fo;
a21=wo;a22=0;a23=0;a31=0;a24=0;
a32=(-wo*Rfd*m1*Ladsp)/Lfd;
a33=((-wo*Rfd)/Lfd)*(1-(Ladsp/Lfd)+(m2*Ladsp));
a34=-wo*Rfd*ka*inv(Ladu);
a41=0;
a42=k5/Tr;
a43=k6/Tr;
a44=-inv(Tr);
A=[a11 a12 a13 a14;a21 a22 a23 a24;a31 a32 a33 a34;a41 a42 a43 a44];
lamda=eig(A);
c=real(lamda(3));
d=imag(lamda(3));
zeta=-c/(sqrt(c*c+d*d));
ks=abs(Ep)*abs(Ep)*cos(delo)/(Xe+xdp);
wn=sqrt(ks*wo/(2*h));
wnhz=wn/(2*pi)
wd=wn*sqrt(1-zeta*zeta);
theta=acos(zeta);
Dd0=5*pi/180;
t=0:0.01:10;
Dd=Dd0/sqrt(1-zeta*zeta)*exp(-zeta*wn*t).*sin(wd*t+theta);
d=(delo+Dd)*180/pi;
plot(t,d)
xlabel('t sec'),ylabel('delta degrees')
```

OUTPUT:

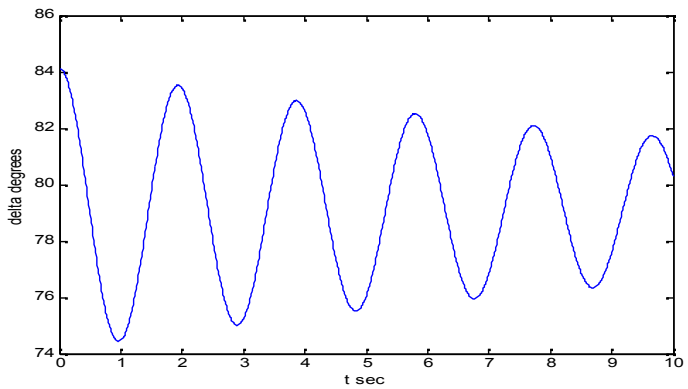

3.WITH POWER SYSTEM STABILIZER

```
p=0.9;q=0.3;Et=1;h=3.5;xd=1.81;xq=1.76;xdp=0.3;x1=0.16;Ra=0.003;Tdop=8;Ladu=1.65;Laqu
=1.60;L1=0.16;Rfd=0.0006;
Xtr=0.15;x1=0.5;ksd=0.8491;ksq=0.8491;x2=0.93;Re=0;Lfd=0.153;kd=0;fo=60;Tr=.02;ka=10;k
stab=48.5;Tw=1.4;T1=0.154;T2=.033;
Xe=Xtr+x1;
s=p+q*i;
It=s'/Et';
phi=atan(q/p);
Ep=Et+xdp*It*i;
Lds=(ksd*Ladu)+L1;
Lqs=(ksq*Laqu)+L1;
Xqs=Lqs;
Xds=Lds;
a=(abs(It)*Xqs*cos(phi)-abs(It)*Ra*sin(phi));
b=(Et+(abs(It)*Ra*cos(phi))+(abs(It)*Xqs*sin(phi)));
deli=atan(a/b);
edo=Et*sin(deli);
eqo=Et*cos(deli);
ido=abs(It)*sin(deli+phi);
iqo=abs(It)*cos(deli+phi);
```

```
Ebdo=edo-(Re*ido)+(Xe*iqo);
Ebqo=eqo-(Re*iqo)-(Xe*ido);
delo=atan(Ebdo^2+Ebqo^2);
Lads=Lds-L1;
Laqs=Lqs-L1;
ifdo=(eqo+(Ra*iqo)+(Lds*ido))/Lads;
Efdo=Ladu*ifdo;
siado=Lads*(-ido+ifdo);
siaqo=-Laqs*iqo;
Rt=Ra+Re;
Xtq=Xe+(Laqs+L1);
Ladsp=1/(inv(Lads)+inv(Lfd));
Xtd=Xe+(Ladsp+L1);
D=(Rt^2)+(Xtq*Xtd);
m1=(Ep*(Xtq*sin(delo))-(Rt*cos(delo)))/D;
n1=(Ep*(Rt*sin(delo))+(Xtd*cos(delo)))/D;
m2=(Xtq*Lads)/(D*(Lads+Lfd));
n2=(Rt*Lads)/(D*(Lads+Lfd));
Eto=sqrt(edo*edo+eqo*eqo);
k1=n1*(siado+(Lads*ido))-m1*(siaqo+(Ladsp*iqo));
k2=n2*(siado+(Laqs*ido))-m2*(siaqo+(Ladsp*iqo))+((Ladsp/Lfd)*iqo);
k5=(-Ra*m1+L1*n1+Laqs*n1)*(edo/Eto)+(eqo/Eto)*(-Ra*n1-L1*m1-Ladsp*m1);
k6=(edo/Eto)*(-Ra*m2+L1*n2+Laqs*n2)+(eqo/Eto)*(-Ra*n2-L1*m2+Ladsp*(inv(Lfd)-m2));
a11=-kd/(2*h);
a12=-k1/(2*h);
a13=-k2/(2*h);
wo=2*pi*fo;
a21=wo;
a32=(-wo*Rfd*m1*Ladsp)/Lfd;
a33=((-wo*Rfd)/Lfd)*(1-(Ladsp/Lfd)+(m2*Ladsp));
a34=-wo*Rfd*ka*inv(Ladu);
a36=wo*Rfd*ka*inv(Ladu);
a42=k5/Tr;
a43=k6/Tr;
a44=-inv(Tr);
a51=kstab*a11;
a52=kstab*a12;
a53=kstab*a13;
a55=-inv(Tw);
a61=T1*a51*inv(T2);
a62=T1*a52*inv(T2);
a63=T1*a53*inv(T2);
a65=T1*a55*inv(T2)+inv(T2);
a66=-inv(T2);
```

```
A=[a11 a12 a13 0 0 0;a21 0 0 0 0 0;0 a32 a33 a34 0 a36;0 a42 a43 a44 0 0;a51 a52 a53 0 a55
0;a61 a62 a63 0 a65 a66];
lamda=eig(A);
c=real(lamda(4));
d=imag(lamda(4));
zeta=-c/(sqrt(c*c+d*d));
ks=abs(Ep)*abs(Ep)*cos(delo)/(Xe+xdp);
wn=sqrt(ks*wo/(2*h));
wnhz=wn/(2*pi)
wd=wn*sqrt(1-zeta*zeta);
theta=acos(zeta);
Dd0=5*pi/180;
t=0:0.01:10;
Dd=Dd0/sqrt(1-zeta*zeta)*exp(-zeta*wn*t).*sin(wd*t+theta);
d=(delo+Dd)*180/pi;
plot(t,d)
xlabel('t sec'),ylabel('delta degrees')
```
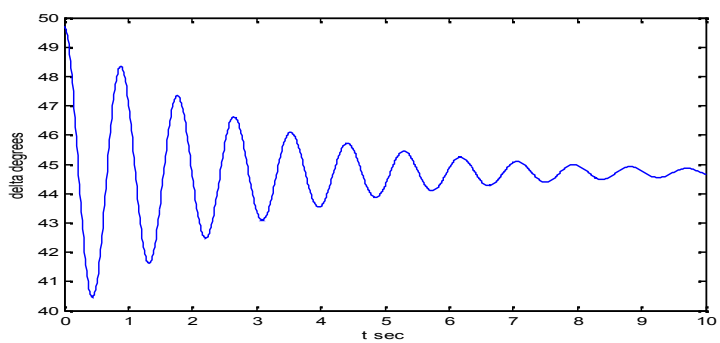
OUTPUT: